FRACTURE TOUGHNESS AND FATIGUE PROPERTIES OF STEEL PLATE BUTT JOINTS WELDED BY SUBMERGED ARC AND ELECTROSLAG WELDING PROCEDURES

MICHIGAN DEPARTMENT OF
STATE HIGHWAYS AND TRANSPORTATION

MAY 1976

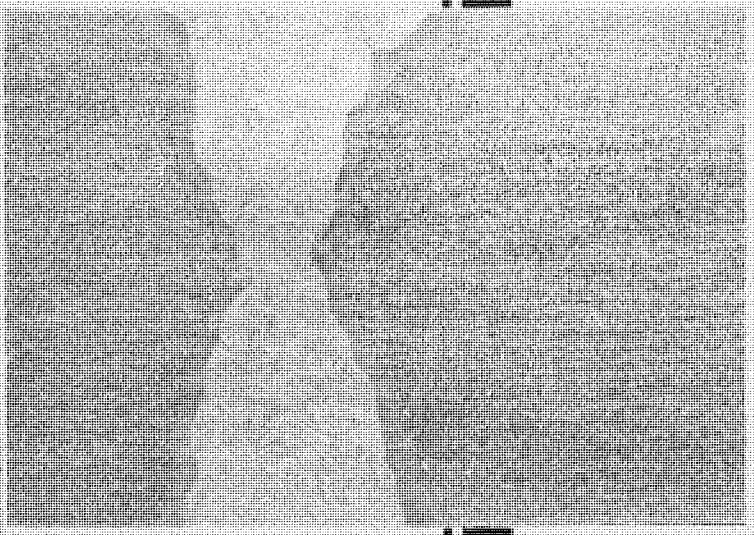

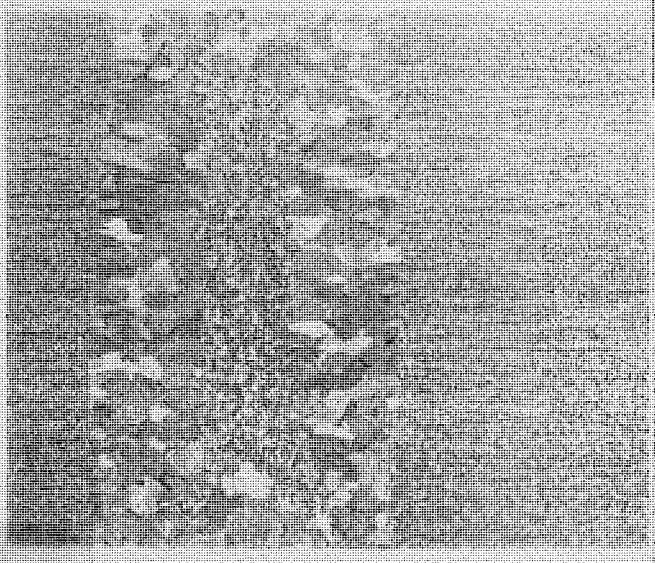

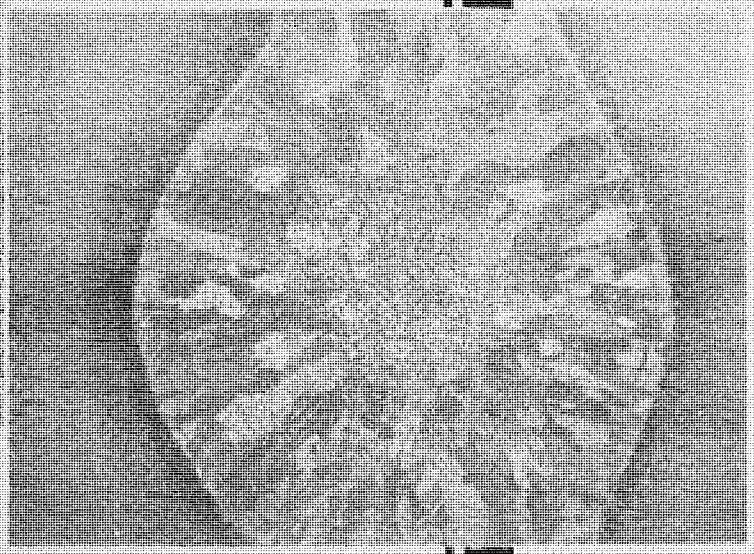

TA492.W4 C8 1976 c. 3
Fracture toughness and
fatigue properties of steel
plate butt joints welded by
submerged arc and

Technical Report Documentation Page

1. Report No.	2. Government Accession No.	3. Recipient's Catalog No.
FHWA-R-1011		

4. Title and Subtitle	5. Report Date
FRACTURE TOUGHNESS AND FATIGUE PROPERTIES OF STEEL PLATE BUTT JOINTS WELDED BY SUBMERGED ARC AND ELECTROSLAG WELDING PROCEDURES	May 1976
	6. Performing Organization Code
7. Author(s)	8. Performing Organization Report No.
James D. Culp	R-1011
9. Performing Organization Name and Address	10. Work Unit No. (TRAIS)
Testing and Research Division Michigan Department of State Highways and Transportation Lansing, Michigan 48904	11. Contract or Grant No. H. P. & R.
	13. Type of Report and Period Covered
12. Sponsoring Agency Name and Address	Final Report (1972 - 1976)
Michigan Department of State Highways and Transportation Lansing, Michigan 48904	14. Sponsoring Agency Code

15. Supplementary Notes

This study was conducted in cooperation with the U. S. Department of Transportation, Federal Highway Administration.

16. Abstract Welded butt joints, typical of those used in the flanges of steel plate girders, were welded by electroslag and submerged arc processes in ASTM A36 and A588 steel plates. The electroslag weldments were made by the consumable guide method using both the water cooled and non-cooled retaining shoes. Complete metallurgical studies were done on the weldments to define and document the various weld metal and heat-affected zones that were present. Chemical compositions of the various weldment zones are presented and discussed. Deficiencies were discovered in the alloy composition of some of the weldments in A588 steel that were approved for use in a bare, unpainted exposure. Control of weld metal chemistry is seen to be very difficult in an electroslag weldment. Tensile tests on the various weldments reveal significant nonhomogeneous and anisotropic behaviors in the electroslag weld metal. Three series of Charpy V-notch impact evaluations were conducted on the weldments. The 1st series evaluated the performance of all the weld metal zones, the heat affected zones, and the base metal at a test temperature of 0 F. These tests revealed the nonhomogeneous nature of the impact toughness in electroslag weld metal and a failure to meet acceptance criteria by some of the weldments. The 2nd series involved impact testing over the temperature range of -40 to +40 F and revealed the temperature-transition characteristics of the weldment zones. The 3rd series of Charpy tests revealed the highly anisotropic nature of the impact toughness of the electroslag weld metal zones. Fatigue crack initiation tests were conducted on small tensile specimens taken from the weldments with crack starter notches machined in them. These tests revealed that the submerged arc weld metal has a significantly longer crack initiation life than the electroslag weld metal and that in some cases the electroslag weld metal was inferior to the base metal. Recommended changes in specifications are also included.

17. Key Words	18. Distribution Statement
arc welding, welded joints, steel alloys, bridge members, weldments, weld metal, base metal, impact tests, metallurgical analysis.	No restrictions. This document is available to the public through the National Technical Information Service, Springfield, Virginia 22161.

19. Security Classif. (of this report)	20. Security Classif. (of this page)	21. No. of Pages	22. Price
unclassified	unclassified	136	

Form DOT F 1700.7 (8-72) Reproduction of completed page authorized

FRACTURE TOUGHNESS AND FATIGUE PROPERTIES OF STEEL PLATE BUTT JOINTS WELDED BY SUBMERGED ARC AND ELECTROSLAG WELDING PROCEDURES

James D. Culp

Final Report on a Highway Planning and Research Investigation Conducted in Cooperation with the U. S. Department of Transportation, Federal Highway Administration

Research Laboratory Section
Testing and Research Division
Research Project 72 F-124
Research Report No. R-1011

Michigan State Highway Commission
Peter B. Fletcher, Chairman; Carl V. Pellonpaa,
Vice-Chairman, Hannes Meyers, Jr., Weston E. Vivian
John P. Woodford, Director
Lansing, May 1976

ACKNOWLEDGEMENTS

The research reported herein was conducted by the Research Laboratory of the Michigan Department of State Highways and Transportation in cooperation with the Federal Highway Administration, U. S. Department of Transportation, under the FHWA's Highway Planning and Research Program. The Research Laboratory is under the general administration of L. T. Oehler, Engineer of Research.

The author wishes to express his appreciation to the following Engineering Professors at Michigan State University for their helpful review of and consultations on the research work; Dr. William N. Sharpe, Jr., Dr. Howard Womochel, Dr. Gary L. Cloud, Dr. Denton D. McGrady and Dr. Robert W. Little. The author wishes to thank Charles Arnold for his general supervision of the project and his careful review of the preliminary draft of this report. Thanks also are due to Gene R. Cudney for his complete review of the preliminary manuscript, and to Gerald J. Hill, Welding Engineer, for coordinating the procurement of the weldments needed for the project.

A special word of commendation is due to Donald Caudell and Gerald Smith for their diligent and precise application of machinist skills in producing the many different test specimens required by this research study. Special thanks are also due to Lawrence Parr and Frederick Cassell for the varied photographic work done in the project and to Ronald Dexter, Vernon Williams, John Caudell, and Anthony Bryhan for their reliable help in the preparation, testing, and evaluation of the various specimens used in the project.

Thanks are due to the following members of the Research Laboratory staff who contributed to the preparation of this report: James Alfredson - Editor; Jack Perrone - Supervisor, Graphic Presentation; Lawrence Parr - Supervisor, Photography; Rebecca Flynn, Cathy Cantrell, Nancy Green, Bill Zakrajsek, Jon Titus, and Dick Morehouse.

ABSTRACT

Welded butt joints, typical of those used in the flanges of steel plate girders, were welded by the electroslag and the submerged arc welding process in ASTM A 36 and A 588 steel plates. The electroslag weldments were made by the consumable guide method using both the water cooled and the non-cooled retaining shoe methods. Complete metallurgical studies were done on the weldments to define and document the various weld metal and heat-affected zones that were present. Chemical compositions of the various weldment zones are presented and discussed. Deficiencies were discovered in the alloy composition of some of the weldments in A 588 steel that were approved for use in a bare, unpainted exposure. Control of weld metal chemistry is seen to be very difficult in an electroslag weldment. Tensile tests on the various weldments reveal significant nonhomogeneous and anisotropic behaviors in the electroslag weld metal. Three series of Charpy V-notch impact evaluations were conducted on the weldments. The first series evaluated the performance of all the weld metal zones, the heat-affected zones, and the base metal at a test temperature of 0 F. These tests revealed the nonhomogeneous nature of the impact toughness in electroslag weld metal and a failure to meet acceptance criteria by some of the weldments. The second series involved impact testing over the temperature range of -40 to +40 F and revealed the temperature-transition characteristics of the weldment zones. The third series of Charpy tests revealed the highly anisotropic nature of the impact toughness of the electroslag weld metal zones. Fatigue crack initiation tests were conducted on small tensile specimens taken from the weldments with crack starter notches machined in them. These tests revealed that the submerged arc weld metal has a significantly longer crack initiation life than the electroslag weld metal and that in some cases the electroslag weld metal was inferior to the base metal. Recommended changes in the welding specifications are included which are based on the findings of this research.

CONTENTS

SUMMARY OF CONCLUSIONS

The results of an investigation into the properties of electroslag and submerged arc butt weldments in A 36 and A 588 steel led to the following conclusions:

1) The electroslag welding process offers about a 50 percent reduction in the welding time required for making steel butt joints as compared to the submerged arc process. (The "cooled shoe" and "dry (non-cooled) shoe" methods of consumable guide electroslag welding were evaluated.)

2) Metallurgical studies show that an electroslag weldment contains either one or two distinct weld metal zones and two large heat-affected zones. The primary disadvantage of the electroslag welding process is the coarse grained "cast" type of structure that results in the weld metal due to the high heat input. The properties of these zones are shown to be controlled by the different metallurgical structures that are present. Submerged arc weldments are shown to contain only one weld metal zone and one small heat-affected zone.

3) The chemical composition of a submerged arc weldment is controlled by the welding wire and flux since dilution with base metal is minimal. Some of the submerged arc weldments had deficiencies that were related to deficiencies in the welding wire used.

4) The chemical composition of an electroslag weldment is greatly influenced by the base metal chemistry since dilution rates run between 40 to 60 percent. This makes control of the chemistry of the weld metal very difficult, and excessive or deficient amounts of the alloy elements are common.

5) In electroslag weldments, the Zone 1 weld metal (occurring in the center of the weld) has a lower yield strength and lower tensile strength than the Zone 2 weld metal around it. Current acceptance testing specifications do not account for this difference. In one type of electroslag weldment the yield strength of both zones failed to meet the minimum strength required.

6) Charpy V-notch impact evaluations of the electroslag weldments show that the Zone 1 weld metal, located in the central core of the joints, has a lower toughness than the Zone 2 weld metal that surrounds it. The Zone 1 weld metal usually fails to meet the acceptance criterion of 15 ft-lb at 0 F. No reduction in base metal toughness was observed in the heat-affected zones of the alloys tested.

7) Two different welding procedures were evaluated in the submerged arc process. One procedure produced poor impact toughness in the resulting weld metal. The other procedure produced good toughness, and these weldments had better overall impact properties than the electroslag weldments. Welding procedures can have a considerable effect on the resulting weld metal properties, even when the filler metal, flux, and base metal used are carefully controlled.

8) Impact energy transition-temperature tests over the temperature range of -40 to +40 F reveal the need for consideration of how the impact energy decreases at temperatures below that used in the acceptance testing. In particular, some of the weldment zones lose toughness rapidly at temperatures that are still above the minimum service temperatures.

9) Impact testing of the electroslag weld metal showed that a drastic reduction in impact strength can occur in both weld metal zones when the fracture crack is oriented in a direction parallel to the primary crystal boundaries. Thus, the performance of an electroslag welded joint will be highly dependent upon the orientation of the crystal structure with respect to the directions of the applied stresses.

10) Electroslag weldments, as produced in this study in the "as welded" condition, cannot be used in ASTM A 588 steel plates if the impact toughness and weld metal chemistry requirements are to be strictly enforced.

11) Fatigue crack initiation testing of the electroslag and submerged arc weldments revealed that the submerged arc weldments had significantly longer crack initiation lives than the electroslag weldments did. In some of the fatigue test series the electroslag weld metal had a lower crack initiation life than the base metal. (These conclusions are subject to the limitations of the small specimen tests conducted, which do not exactly parallel the service conditions of a welded beam.)

12) Specification changes have been implemented by the Michigan Department of State Highways and Transportation to correct the inadequacies of the previous acceptance testing criteria for electroslag weldments. The inadequacies of the previous acceptance testing procedures are primarily due to the lack of recognition of the nonhomogeneous nature of the cast structure produced by the electroslag process.

13) Research Project 75 F-144, "Bridge Girder Butt Welds--Resistance to Brittle Fracture, Fatigue and Corrosion," has been initiated by

the Department's Research Laboratory to further quantify the findings of this study. A linear elastic fracture mechanics approach will be used to study the fracture toughness and fatigue properties of the weldments. Corrosion studies will involve a controlled field exposure of different weld metal chemistries and a field investigation into the performance of existing structures.

Discussion

The stated objectives of this research project were "to identify and evaluate the various metallurgical structures present in electroslag and submerged arc butt weldments and to compare the fracture toughness, fatigue strength and other physical and metallurgical properties of the weldments produced by these two welding methods." The following summary discussions are drawn from the body of this report and within the limitations cited meet the objectives of the Research Proposal.

Submerged Arc and Electroslag Welding Processes

1) Submerged arc and electroslag welding as described and illustrated in the text are two alternate methods used for making butt joints in steel plates. The submerged arc process is a multipass technique and has a long history of successful use in welding steel plate girders for highway bridge applications. The electroslag process is a single pass technique which offers about a 50 percent reduction in the welding time, as compared to the submerged arc process, required to produce a steel butt weld in a typical girder flange plate. The primary disadvantage of the electroslag process is its very high heat input and prolonged thermal cycle which result in a "cast" structure in the weld with two large heat-affected zones in the adjacent base plate. This type of weldment is relatively new in applications involving cyclic, impulsive loading such as that experienced in highway bridges. Questions concerning the fatigue, fracture toughness, and corrosion properties of the "as welded" electroslag butt joint need to be answered before such a weldment can be applied with confidence.

2) Both electroslag and submerged arc weldments were produced by two of Michigan's fabricators for evaluation. Fabricator A used the water cooled shoe, consumable guide method of electroslag welding. Fabricator B used the dry (non-cooled) shoe, consumable guide method of electroslag welding. Weldments were produced in 16-in. wide, 1-3/4 and 3 in. thick plates of ASTM A 36 and A 588 steels. All weldments were made under normal fabrication conditions and are, as nearly as possible, representative of the weldments being put into Michigan's bridge structures. (The

normal fabricating conditions used are detailed in the "Discussion of Results" on pp 17-20, 25-29.) The point of view taken in producing these weldments was not to see how well they could be produced but to determine how they were being produced and put into service.

3) Nondestructive testing of the weldments by X-ray and ultrasonic techniques showed both the electroslag and the submerged arc weldments to be of good quality. The electroslag weldments had a high incidence of edge defects and surface defects in the adjacent plate due to the fixturing and starting and runoff sumps used in the procedure. Some of these defects were eliminated from subsequent fabrication work by using a different fixturing technique. The edge defects at the starting and finishing ends of the weld could not be completely eliminated from the fabrication and required repair after the welding was completed.

Metallurgical Structure and Alloy Composition of Weldments

1) The metallurgical structures present in the submerged arc weldments were defined and illustrated. One weld metal zone was defined which was seen to have a relatively fine grained and homogeneous structure (except for areas of additional grain refinement produced by a welding pass reheating the previous pass). Only one small heat-affected zone (HAZ) is present in a submerged arc weldment. The HAZ is an area of grain refinement as compared to the structure present in the unaffected base metal.

2) The metallurgical structures present in the electroslag weldments were defined and illustrated. Two weld metal zones were defined, Zone 1 being composed of thin columnar crystals oriented in the direction of welding and located in the central core of the weld nugget, and Zone 2 being composed of coarse columnar crystals that begin at the fusion line and grow inward and upward towards the direction of welding. Two large heat-affected zones (denoted as HAZ 1 and HAZ 2) were present in all the electroslag weldments. HAZ 1 was seen to be a zone of grain coarsening of the base metal and HAZ 2 a zone of grain refinement of the base metal. The structure of the electroslag weld metal was that characteristic of a steel casting. The relative proportions of Zone 1 and Zone 2 weld metal occurring was seen to vary between the cooled shoe and the dry shoe electroslag methods.

3) The alloy composition of the various submerged arc weldment zones was determined. Excessive amounts of manganese and silicon were found in some of the weldments in A 588 steel, which could have had a detrimental effect on the notch toughness of the weld metal. The weldments made

by Fabricator B were deficient in nickel, chromium, and copper, all of which are needed to give the weld metal the enhanced corrosion resistance needed in bare, unpainted exposures of A 588 steel. The submerged arc weldments in A 36 steel were also found to have excessive levels of manganese and in one case silicon. The weld metal composition in a submerged arc weldment is seen to be mainly a function of the chemistry present in the welding wire and flux, since dilution with base metal is a minimum, (except in the pass immediately adjacent to the fusion line).

4) The alloy chemistry of the various electroslag weldment zones was determined. Due to the large amount of dilution of the weld metal with the base metal (normally about 50 percent) the weld metal chemistry is highly dependent upon the base metal chemistry. This was seen as the cause for all of the electroslag weldments exceeding the 0.12 maximum limit on carbon content. The weldments placed in A 588 steel were also seen to have deficiencies in nickel, chromium, and copper due to deficiencies in the welding wire and the high dilution rates. These deficiencies will adversely affect the enhanced corrosion resistance needed by the welds for unpainted exposures. The electroslag weldments were also seen to be low in silicon. Apparently they were not picking up silicon from the flux in the manner experienced in submerged arc weldments. Silicon is also one of the major corrosion inhibitors in the weld metal. The two electroslag weld metal zones in a weldment had identical alloy compositions as tested on the macroscopic scale, but micro-segregation within the structures is known to occur and needs to be carefully assessed.

Tensile Properties of Electroslag Weldments

1) In the standard "all weld metal tension test" the electroslag weldments were shown to possess a lower yield point and tensile strength in Zone 1 weld metal than in Zone 2 weld metal. In one case both zones were below the 50,000 psi minimum yield point required (A 588 steel). The ductility of Zone 1 weld metal was greater than that of the Zone 2 weld metal as measured by both percent elongation and percent reduction in area in the tensile specimen. The percent reduction in area was seen to be quite low in Zone 2 of some of the weldments due to the influence of the large columnar crystals on the failure mode. A possible serious anisotropy in the tensile properties of the electroslag weldments was pointed out but no testing was done to quantify this effect. Two of the electroslag specimens failed the side bend test, even though they had exhibited adequate ductility in the tensile test.

2) It was concluded that any specification on the tensile testing of electroslag weldments should include the testing of all the weld metal zones present. If the welded joint is to be subjected to a biaxial or triaxial loading condition, a complete testing program is needed to evaluate the anisotropic nature of the tensile properties.

Charpy Impact Evaluation of Weldments

1) Charpy V-notch impact tests were run on all the electroslag weld metal and heat-affected zones at 0 F for comparison with the acceptance criterion of 15 ft-lb minimum at 0 F. Zone 1 weld metal was shown to have a considerably lower impact strength than Zone 2 weld metal and (except in one case) failed to meet the 15 ft-lb minimum at 0 F. It was pointed out that the current method required by specifications (1, 2) for testing electroslag weldments fails to account for this Zone 1 at all and arbitrarily locates the specimens at the quarter thickness of the plate, thus testing the Zone 2 weld metal. The first heat-affected zone, HAZ 1, where grain coarsening occurs, was seen to be greater than or equal to the base metals tested in impact toughness. HAZ 1 is the zone where toughness degradation would be suspected in higher yield point or different alloy steels. The second heat-affected zone, HAZ 2, where the grain structure of the base metal is refined, was greatly enhanced in impact toughness as compared to the base metal. It was also noted that the weldment zones had a lower toughness at the starting end of the electroslag weld than at the finishing end. This fact should be considered in the location of impact testing in procedure qualification specifications on electroslag weldments.

2) Charpy impact tests were run on the various zones of the submerged arc weldments at 0 F for comparison to the acceptance criterion of 20 ft-lb minimum at 0 F. The weldments produced by Fabricator A using his normal welding procedures were seen to have deficient impact strengths in both the A 36 and A 588 steels. This result was attributed to the welding procedure and the resulting high heat input to the weld, which produced a poor microstructure. (The chemical effects previously mentioned were also influential.) The submerged arc weldments made by Fabricator B had (with one exception) good impact properties. The welding procedure used by Fabricator B was more in line with good practice and resulted in a high toughness weld metal. (These submerged arc weldments had better overall impact properties than the electroslag weldments.) The heat-affected zone present in all of the submerged arc weldments produced a higher toughness than the base metal. This was attributed to the refinement that occurs in base metal structures located within the HAZ.

3) At the time of fabrication of these weldments, the current AASHTO Toughness Specifications (3) were not in effect and no minimum toughness requirements existed for A 36 steel. Some of the base plates welded were seen to possess very low impact toughness (e.g., 3 ft-lb at 0 F). It is interesting to note that the HAZ of the submerged arc weldments greatly increased the base metal toughness (up to 10 times) by the recrystallization that occurred. It is important to point out that it has long been recognized that the weld metal in a butt joint needs to possess a higher impact toughness than the base metal being welded. This is due to the severe service conditions placed on a weldment due to the presence of residual stresses and fabrication flaws in the plane where service stresses act, which do escape detection and repair. Also, the stress conditions caused by repairs are sometimes worse than those due to small flaws.

4) A second series of Charpy impact tests was run to develop energy transition-temperature curves over the range of -40 to +40 F for both the electroslag and submerged arc weldments in the 3-in. plates. These curves substantiated the findings of the tests conducted at 0 F and further illustrated that the impact fracture energies of the various zones decrease with temperature. It is shown that the weld metal zones, heat-affected zones, and base metal, transition quite differently as the temperature ranges from +40 to -40 F. This casts considerable doubt on the validity of specifying a minimum required energy at some temperature, such as 0 F, if that temperature is above the minimum service temperature to be experienced. The assumption behind such an approach is that the metals that meet the required minimum will still have adequate toughness at the lowest service temperature experienced. As seen in the energy transition-temperature curves, however, some zones of the weldment maintain toughness and some zones lose toughness rapidly. Further research into this area needs to be done using a "linear elastic fracture mechanics" (3) approach to quantify the influence of these effects on the service performance of such weldments.

5) The anisotropic nature of the electroslag weld metal roughness was determined by taking Charpy specimens from the weldments at various orientations to the grain structures (see Fig. 55, p 103). In the A 588 alloy, it was seen that the Zone 1 weld metal toughness was practically insensitive to specimen orientation but the Zone 2 weld metal toughness was about 40 percent lower in the direction of the long columnar crystals than in the transgranular directions tested. This effect was attributed to the role of the prior austenite grain boundaries in the mode of fracture. In the A 36 alloy, the Zone 1 weld metal toughness was only 1/4 as high along the axis of the fine columnar crystals as it was normal to the crystals. The Zone 2 weld metal toughness in the A 36 alloy was 1/2 to 1/3 as much along the

crystals as it was in any of the transgranular directions tested. It was thus established that the electroslag weld metal structure was very sensitive to directional changes in its impact properties and such effects were even further influenced by the alloy composition present. Careful consideration needs to be given to this point in any application of electroslag welding when biaxial or triaxial loading conditions are to be applied in service.

6) It is the conclusion of this study that electroslag weld metal, as produced by the current procedures and filler wires, cannot be safely used in the "as welded" condition when service conditions require strict adherence to the current minimum toughness requirement. Submerged arc weld metal can be successfully used in the "as welded" condition in such cases but, as was illustrated in this study, an improper submerged arc welding procedure can also produce inferior toughness.

Fatigue-Notch Sensitivity Evaluation

1) A series of constant amplitude axial fatigue tests were run on notched specimens taken from the various electroslag and submerged arc weldment zones. These tests present a qualitative measure of the fatigue crack initiation life of the weldment zones in the presence of a pre-existing flaw or discontinuity. Such flaws are the origins of fatigue failures in actual bridge beam weldments (4). Two different stress ranges and flaw conditions were evaluated in the A 588 and A 36 weldments. Stress range and notch acuity were taken as the most influential variables on the crack initiation life and were selected to give a failure within a certain number of cycles.

2) The conclusions of these tests are too lengthy to reiterate in detail here. The most important conclusions to be noted, however, are as follows:

A 588 Steel Weldments

a) At a 42.5 ksi stress range with a circular crack starter, the electroslag weld metal zones and HAZ 2 had lower cycle lives than the base metal. The cycle lives of the submerged arc weld metal and its HAZ exceeded the life of the base metal and were at least two times greater than the lives of the electroslag weld metal.

b) At a 21 ksi stress range with a double edge notch crack starter, both of the electroslag weld metal zones had cycle lives that were greater than or equal to those of the base metal. In one case the HAZ 2 had a lower

cycle life than the base metal. The submerged arc weld metal and its HAZ had cycle lives greater than or equal to the cycle life of the base metal. The submerged arc weld metal had a significantly higher life than the corresponding electroslag weld metal zones.

c) In both the electroslag and the submerged arc weldments, the cycle lives measured in specimens from the 3-in. thick joints were lower than those measured in specimens from the corresponding 1-3/4-in. thick joints.

A 36 Steel Weldments

a) At a 38 ksi stress range with a circular crack starter, both the electroslag weld metal zones and HAZs exceeded the cycle life of the base metal. Likewise the cycle lives of the submerged arc weld metal and HAZ exceeded that of the base metal. The submerged arc weld metal had a significantly higher cycle life than the corresponding electroslag weld metal.

b) At a 28 ksi stress range using a double edge notch crack starter, both of the electroslag weld metal zones and HAZ 2 have cycle lives less than or equal to base metal. The submerged arc weld metal and its HAZ at this condition are still greater than or equal to base metal in cycle life. The submerged arc weld metal is seen to have a higher cycle life than the corresponding electroslag weld metal.

c) With one exception, the specimens from the 3-in. thick joints are seen to yield lower cycle lives than the specimens from the 1-3/4-in. thick joints for both welding processes.

3) Based on the results of these tests it is concluded that qualitatively the submerged arc weld metal is more resistant to fatigue crack initiation than electroslag weld metal in the presence of a flaw condition. This needs to be qualified within the limitations of the tests conducted. Since the testing conditions do not parallel service loading conditions it cannot be stated that this difference would appear in service.

INTRODUCTION

Welded butt joints in flange plates and cover plates, ranging from 1/2 to 4 in. in thickness, are commonly encountered in the fabrication of steel plate girders and rolled beams used in highway bridges. (A butt joint is "...a joint between two members lying approximately in the same plane" (5).) Butt welding of steel plates was introduced in the fabrication of highway bridge beams by the submerged arc welding process. This process is a multipass welding technique which has a relatively low heat input and a long history of satisfactory service in applications where fatigue strength and fracture toughness are required, such as in the cyclic, dynamic loading that occurs in bridge structures. The electroslag welding process is a single pass procedure which was originally developed in Russia (6) for welding butt joints in thick plates and castings. In contrast to submerged arc welding, it has a very high heat input and a prolonged thermal cycle that gives the deposited weld metal characteristics similar to those of a steel casting. During the period from early 1970 to June 1974 the consumable guide electroslag process was approved for use by the Michigan Department of State Highways and Transportation and gained a dominant role in the fabrication of steel plate girders. Four major fabricators were qualified in its use and two of these used the process almost exclusively. The electroslag process was qualified in accordance with the specifications set forth in the American Welding Society's Specifications for Welded Highway and Railway Bridges, D 2.0-69. This electroslag butt welding was done on ASTM A 36 steel and on unpainted exposures of ASTM A 588 self-weathering steel. The use of the electroslag process on Michigan bridges was suspended in June 1974. This action was taken as a result of the findings reported herein.

Objectives

A proposal was submitted to the Federal Highway Administration to perform research work under a Highway Planning and Research grant. The HP&R project was approved and the following objectives, set forth in the proposal, were to be accomplished.

The objectives of this research work were to identify and evaluate various metallurgical structures present in electroslag and submerged arc butt weldments and to compare the fracture toughness, fatigue strength, and other physical and metallurgical properties of the weldments produced by these two welding processes. Certain minimum values of these properties are required in a weldment subjected to highway bridge loading and no previous research work was available to completely evaluate these types of butt joints.

The specific objectives of this study as outlined in the Project Proposal were as follows:

"1. To determine the grain size patterns of submerged arc and electroslag weldments.

2. To determine the fatigue-notch sensitivity of the various zones of these weldments.

3. To measure the fracture toughness of various locations in these weldments as determined by the Charpy V-notch impact test.

4. To determine the fracture toughness of these weldments by measuring the material parameter K_{IC} over a representative temperature range. (This objective is subject to applicability of method, and to the equipment and time available.)"

Objective 4 of the Project Proposal was not carried out. The goal of this objective was to measure the plane-strain fracture toughness (K_{IC}) of the welded butt joints. A thorough study of the proposed "pop-in" method (7) for measuring K_{IC} led to the conclusion that the existence of the required meta-instability in crack extension at incipient crack growth was highly unlikely in the low yield strength steels being investigated. In addition, this method for measuring the K_{IC} value of a metal is not recognized by the Standard Method of ASTM E-399, "Plane-Strain Fracture Toughness of Metallic Materials." Since the "pop-in" method was deemed not applicable to the weldments being tested, the loading capacity (20,000 lb) of the Research Laboratory's existing equipment was insufficient for testing in accordance with ASTM E-399, for the specimen size required. The "Crack Follower" budgeted as an equipment item for this phase, was not purchased.

Additional fracture toughness testing (using the Charpy impact test) was carried out that was not in the Project Proposal. The additional objectives of this work were:

5. To characterize the temperature transition behavior of the weldments as measured by the Charpy V-notch impact test over the temperature range of -40 to +40 F.

6. To measure the effect on fracture toughness, as measured by the Charpy V-notch impact test, of the anisotropic (characterized by having different values of a property in different directions) grain structures present in electroslag weldments.

Recent work by Barsom (3, 8) has established the validity of a relationship between the fracture toughness of rolled steel as measured by the energy required to break a Charpy V-notch specimen and as measured by the plane-strain fracture toughness, K_{IC}. This relationship exists as long as the strain rate at the crack tip is the same in both tests. Thus, static K_{IC} measurements correlate with static Charpy specimen energies and dynamic K_{IC} measurements correlate with impact Charpy energies when the strain rate is the same. The fracture toughness measured at any particular strain rate is also shown to be related to the toughness at any other strain rate by a uniform shift of the toughness versus temperature curve along the temperature axis, i.e., reducing the strain rate will lower the toughness transition temperature and increasing the strain rate will raise the toughness transition temperature, the shape of the curve remaining constant. These recent findings, which greatly enhance the usefulness of Charpy impact data, motivated the expansion of the Charpy impact testing in this project. These data will hopefully correlate with K_{IC} data in the future, if a similar relationship can be developed for weld metal.

In the Project Proposal the work plan proposed to obtain ". . . a series of welded butt joints in steel plates using both the submerged arc procedure and the electroslag procedure . . . from one of Michigan's structural steel fabricators." After the proposal and budget were approved, we decided to get a series of test weldments of both the electroslag and the submerged arc processes from two fabricators. Because of this, the amount of work undertaken in this study was doubled from that originally proposed and approved. Our motivation for doing this was to include the two variations of the electroslag process that were in use and get two different sets of submerged arc weldments for comparison.

The following report is directed at meeting the stated objectives of this project. The first section describes the electroslag and submerged arc processes as used by the two fabricators involved. General weld quality as evaluated by visual inspection and non-destructive testing are discussed for each weldment type. The next section presents a metallurgical characterization of the various zones present in the electroslag and submerged arc weldments. Included in this characterization are the macrostructures and microstructures present in the weld metal and heat-affected zones and the corresponding chemical composition found in the weldments. Next is reported the standard physical properties as measured by the tensile test, the guided side bend test, and hardness traverses across the weldments. The fracture toughness of the electroslag and submerged arc weldments is then evaluated by the Charpy V-notch impact test. First, a series of "acceptance tests" is conducted to compare the absorbed impact energy of all

the weldment zones with the current acceptance criteria of 15 or 20 ft-lb at 0 F for electroslag and submerged arc, respectively. Second, a series of temperature-transition testing is conducted over the temperature range of -40 to +40 F to determine how the Charpy impact energy varies with temperature. Third, Charpy specimens are removed from the electroslag weldments at various angles and tested at 0 F to determine what variation with direction, or anisotropy, is present in the fracture toughness of electroslag weld metal. The final section reports the findings of two series of fatigue-notch sensitivity tests which give a measure of the "crack initiation" life of the weldments under the influence of a preexisting flaw condition. The results and conclusions of these sections do meet the objectives of the project proposal as stated, within the application and limitations stated in this report. The details of this report have been made as complete as possible in consideration of the large variation in the backgrounds of the prospective readers.

The contents of this report reflect the views of the author, who is responsible for the facts and the accuracy of the data presented herein. The contents do not necessarily reflect the official views or policies of the Federal Highway Administration. This report does not constitute a standard, specification, or regulation.

DISCUSSION OF RESULTS

Submerged Arc Welding Process

Submerged arc welding is defined as ". . . an arc-welding process wherein coalescence is produced by heating with an arc or arcs between a bare metal electrode or electrodes and the work. The arc is shielded by a blanket of granular, fusible material on the work. Pressure is not used and filler metal is obtained from the electrode and sometimes from a supplementary welding rod" (5). As applied to the welding of butt joints, the submerged arc process is a multipass technique. The plates are placed in the flat position and a beveled joint is filled by depositing weld metal in a series of beads (Fig. 1). After each pass the deposited bead is allowed to cool to some prescribed interpass temperature to prevent excessive heat build up in the joint. (Proper control of interpass temperature will maximize the physical properties of the deposited weld metal, especially the Charpy V-notch impact strength.) Each bead must be thoroughly cleaned by chipping and wire brushing before depositing the next bead to assure good fusion and to eliminate slag inclusions. A small layer of reinforcement is built-up beyond the surface of the plates being welded which is later ground off to give a smooth, flat contour to the joint surface.

The submerged arc process results in a uniformly structured weld joint with a fine grained metal structure as compared to the typical base metal used in bridge construction. One advantage of the multipass technique is that the heat generated by the deposition of a weld bead will partially refine the metallurgical structure of the underlying weld metal. Submerged arc butt weldments in flange plates, when properly made, contain no significant nonhomogeneities (i.e., the physical properties are approximately the same at all points in the weld metal) or anisotropies (i.e., directional variations in properties) and only one narrow heat-affected zone (HAZ) in the base metal adjacent to the weld. In the base metals normally used in highway bridge construction, the HAZ present in a submerged arc weldment will usually have properties superior to those of the unaffected base metal, since the thermal cycle experienced refines the grain structure present in the base metal. Submerged arc weldments in bridge beam butt joints have good metallurgical, physical, fatigue and fracture toughness properties and have been proven serviceable for applications involving cyclic and impact loadings through many years of testing and experience (4). The main disadvantages of the submerged arc process as applied to butt jointing plates are the time required to weld a joint and the need for a careful procedure to control the joint distortion that can occur due to shrinkage during the cooling cycle. These disadvantages are not serious, however,

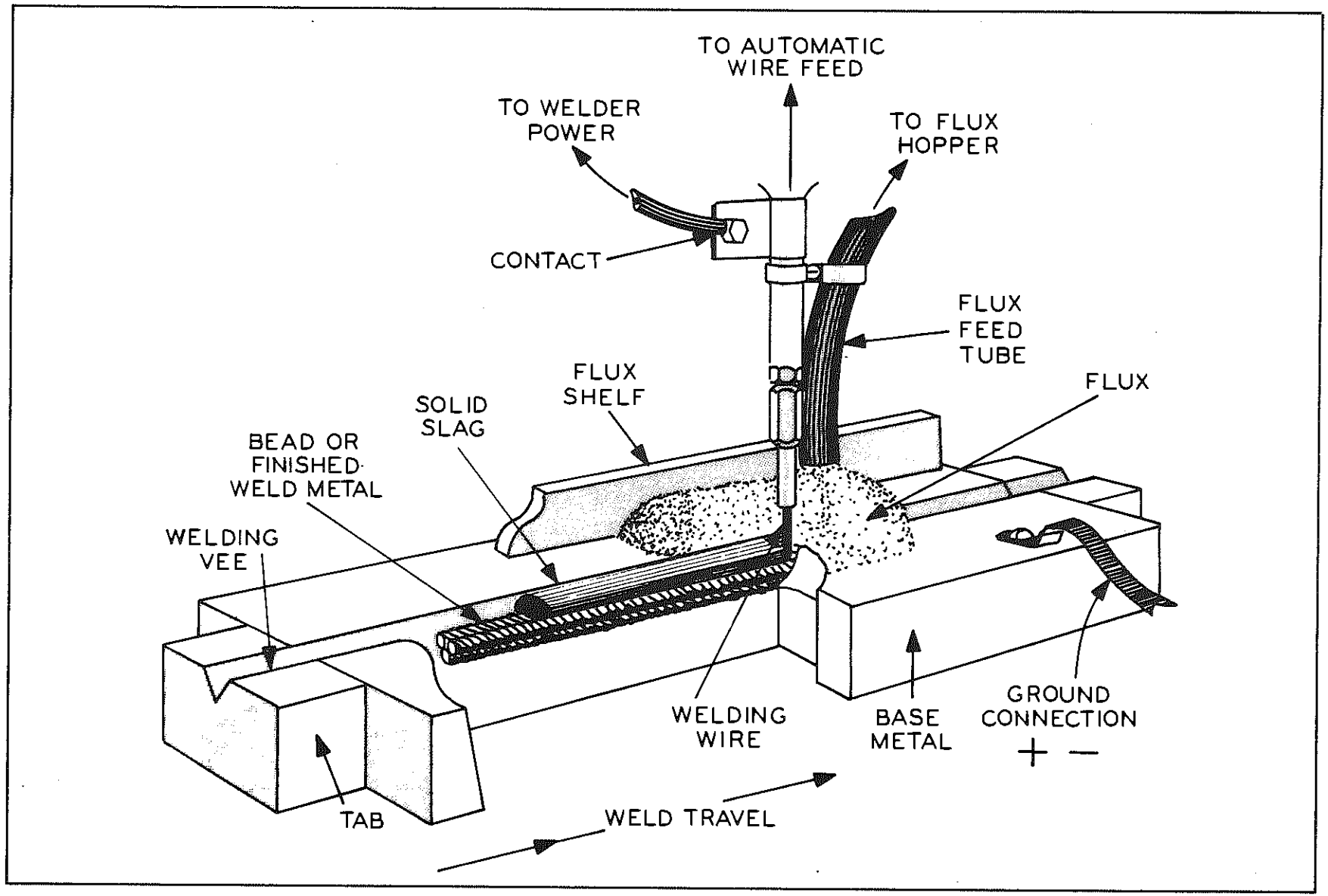

Figure 1. Cutaway view of multiple pass butt welding by the submerged arc welding process.

and a good welding procedure can minimize the problems. Submerged arc welding is also the process used in the fillet welding of built-up plate girders such as in joining the flange plates to the web or cover plates to flange plates. Only the submerged arc butt joints are investigated in this project.

Experimental Weldments - Submerged Arc Process

Weldment specimens for this project were produced by the two structural steel fabricators that were doing a majority of the plate girder work for the Michigan Department of State Highways and Transportation. These fabricators were chosen because they were also our prime users of the electroslag process for butt jointing flange plates. Butt joints were submerged arc welded in 1-3/4 and in 3-in. thick plates of both ASTM A 36 and ASTM A 588 steels. The philosophy applied to the fabrication of these weldments was to produce them exactly as would be done in an actual plate girder fabrication and to not take any special precautions to assure a superior weld unless the same precatuions were routinely observed in production. It was our desire in this project to determine the properties of the weldments that were typical of those being incorporated into our structures, and not the properties that could be obtained under ideal conditions.

Fabricator A selected a procedure that was commonly used by them for submerged arc butt welding (Fig. 2). Joint preparation involved putting a 30-degree bevel on the plate ends with approximately 3/4 to 1 in. of root face left on the bottom edge. The plates were then butted together and fixtured in place, and run-off plates were attached to both ends of the joint. Welding would proceed by depositing between seven to 10 passes in the 60-degree V, then turning the plates over and air carbon-arc gouging a bevel through the root face area until sound weld metal was reached. This bevel was ground and cleaned and weld beads were then deposited until this side of the joint was completed. The plates were then turned over again and the joint was completed. Total number of weld passes ran about 60 on the 3-in. plates and 22 on the 1-3/4-in. plates. A typical macrostructure of the resulting weldments is shown in Figure 3. Interpass temperature was not controlled during the welding of these joints since the operators claimed that they would not normally do so during production. The maximum interpass temperature actually occurring was estimated, using heat-sensitive crayons, to vary between 600 and 800 F. Welding time per joint for a 16-in. width ran about three hours for the 1-3/4-in. plate and six to seven hours for the 3-in. plate, with one man performing the work. The welder was qualified by the Department for the type of welding done and the procedure followed was qualified on Michigan work and had been used in previous fabrication. For a listing of the welding wires and other variables used, see Table 1.

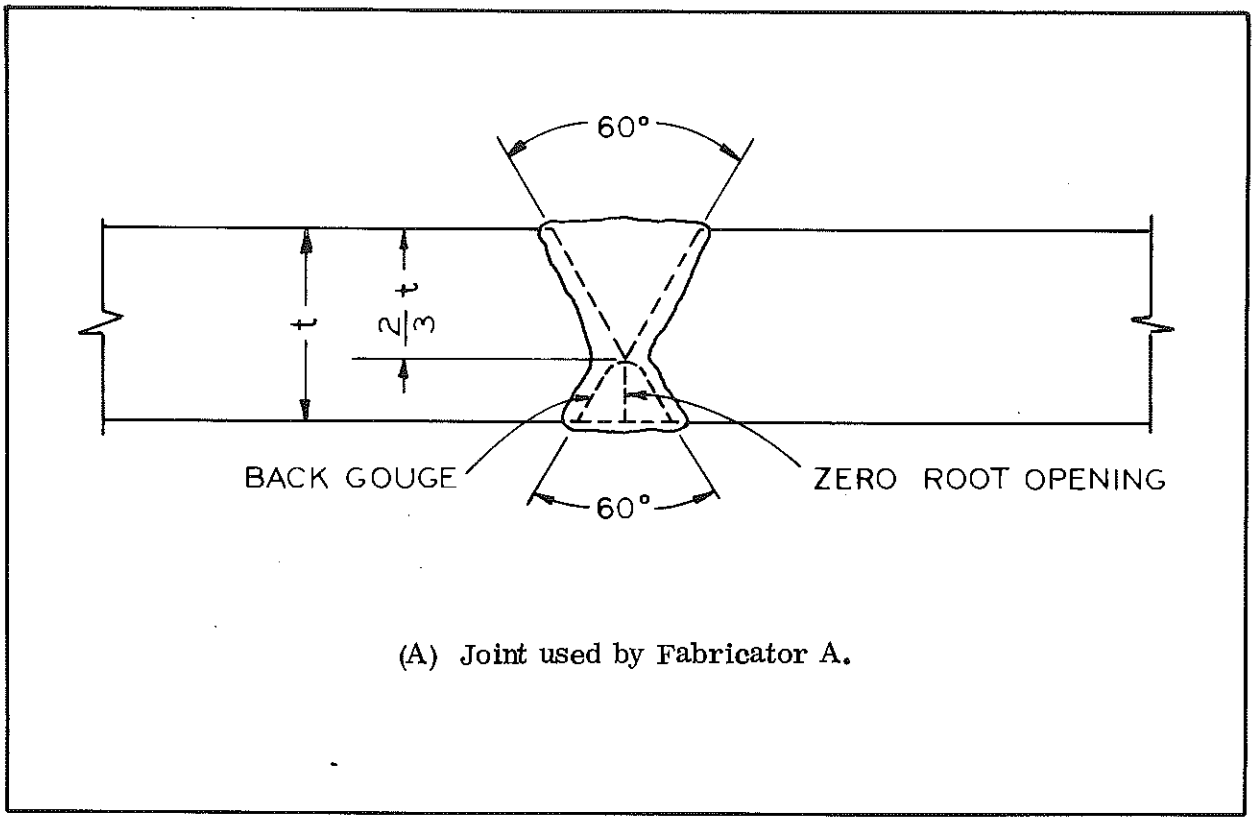

(A) Joint used by Fabricator A.

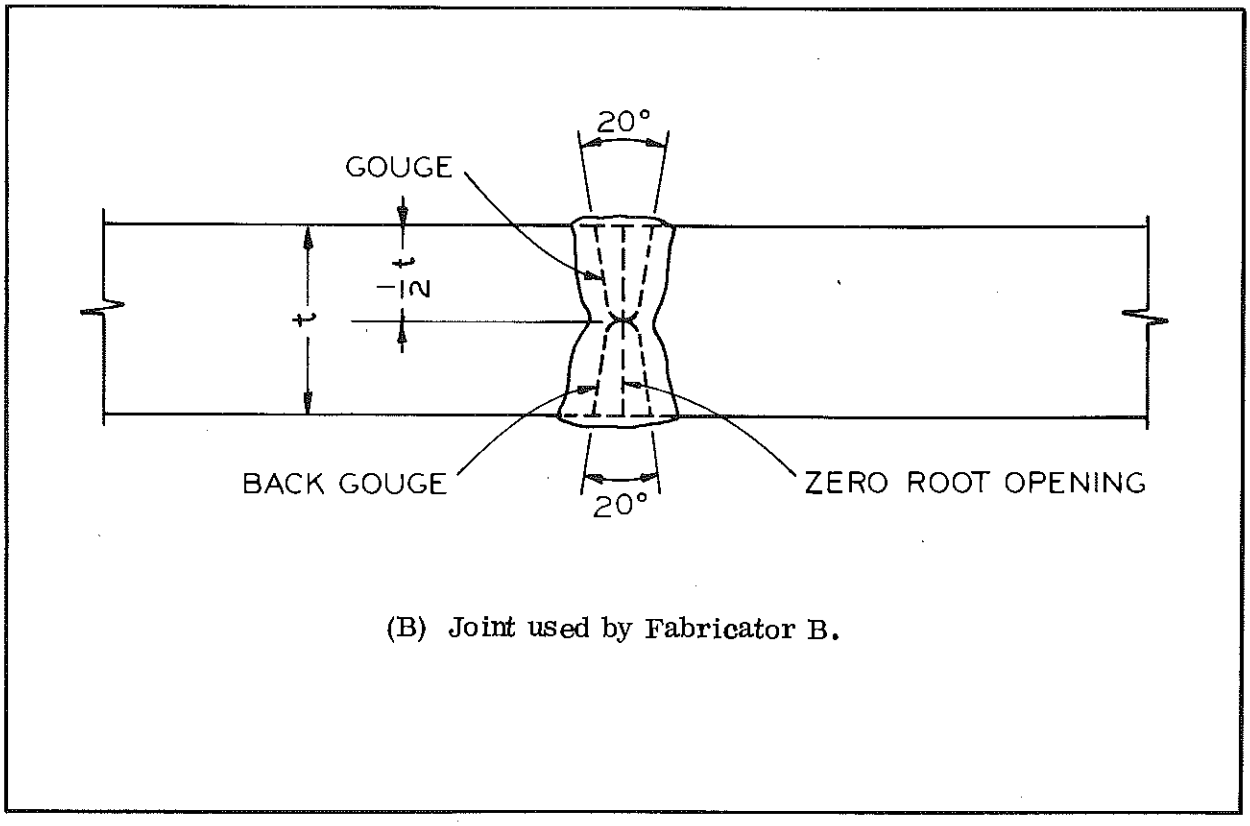

(B) Joint used by Fabricator B.

Figure 2. Submerged arc welded butt joint procedures.

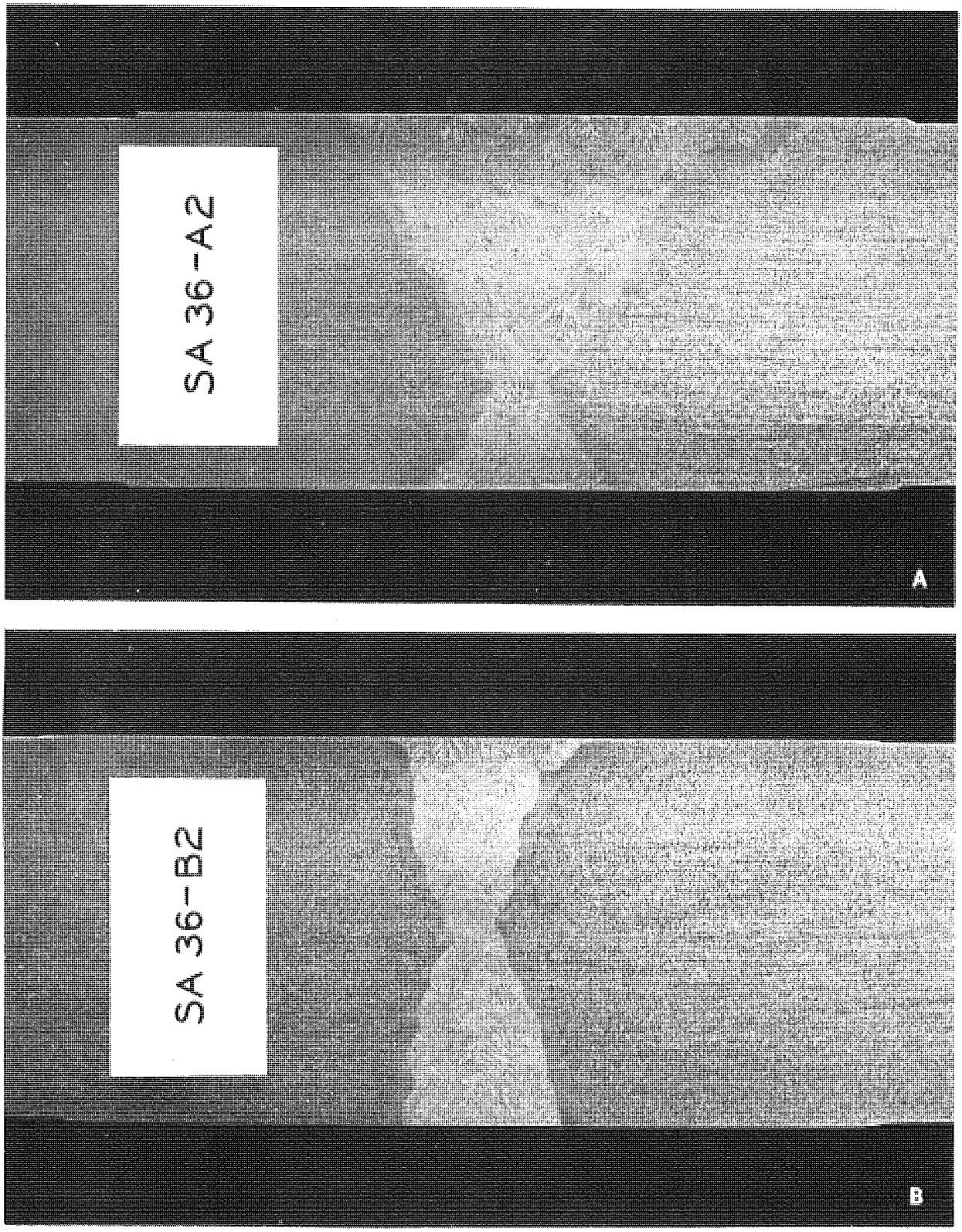

Figure 3. Typical macrostructures of submerged arc welded butt joints. (A) Joint made by Fabricator A, and (B) joint made by Fabricator B.

TABLE 1
WELDING VARIABLES - SUBMERGED ARC PROCESS

Weld Identification[1]	Base Metal ASTM Designation	Plate Thickness, in.	Electrode Type	Flux Type	Amps	Volts
SAW 588-A1	A 588	1-3/4	Raco 815	Lincoln 780	450	35
SAW 588-A2	A 588	3	Raco 815	Lincoln 780	450	35
SAW 36-A1	A 36	1-3/4	Lincoln L-60	Lincoln 780	450	35
SAW 36-A2	A 36	3	Lincoln L-60	Lincoln 780	450	35
SAW 588-B1	A 588	1-3/4	Linde 81	Linde 124	450	35
SAW 588-B2	A 588	3	Linde 81	Linde 124	450	35
SAW 36-B1	A 36	1-3/4	Linde 81	Linde 124	450	35
SAW 36-B2	A 36	3	Linde 81	Linde 124	450	35

[1]Identification Symbolism:
SAW - submerged arc weld
588 or 36 - ASTM A 588 or A 36 Base Metal
A or B - Fabricator A or B
1 or 2 - 1-3/4 or 3-in. plate thickness, respectively

Fabricator B selected a different procedure for making the submerged arc butt joints (Fig. 2). The plates to be welded were cut square on the ends, butted together and secured by welding a runoff block on each end of the joint. A groove was then air carbon-arc gouged in one side to the mid-thickness of the plate. After grinding smooth and cleaning, the groove was filled by depositing a sequence of weld beads. As before, some reinforcement was deposited when the plate surface was reached and later ground off smooth with the plate surface. The plates were then turned over and the same procedure was followed after back gouging until sound weld metal was reached. Total number of weld passes ran about 20 to 25 on the 1-3/4-in. plates and 35 on the 3-in. plates. A typical macrostructure of the resulting weldments is shown in Figure 3. As before, the welders paid no particular attention to interpass temperature since they were not accustomed to doing so in production welding. The maximum interpass temperature was estimated to run in excess of 600 F and at times a weld bead would be deposited in less than one minute after depositing the preceding bead. With the procedure used by Fabricator B, the volume of deposited weld metal was significantly less than that deposited by Fabricator A. The total welding time for a 16-in. width ran about two to three hours on the 1-3/4-in. plates and four to five hours on the 3-in. plates, including preparation time. Two qualified welders independently performed the work. The procedure used was qualified on Michigan work and had been used in previous fabrication. For a listing of the welding wires and other variables used, see Table 1.

Electroslag Welding Process

Electroslag welding is defined as ". . . a welding process wherein coalescence is produced by molten slag which melts the filler metal and the surfaces of the work to be welded. The weld pool is shielded by this slag which moves along the full cross-section of the joint as welding progresses. The conductive slag is maintained molten by its resistance to electric current passing between the electrode and the work. Consumable guide electroslag welding is a method of electroslag welding wherein filler metal is supplied by an electrode and its guiding member" (5). Welding by this process is done in the vertical position and joints are usually completed in a single pass for any plate thickness.

The physical setup used in consumable guide electroslag butt welding is shown in Figure 4. This is the method that was used in the fabrication of Michigan bridge beams and the method that was studied in this project. As the molten slag pool and weld pool move up the joint, they are contained by two copper molds or shoes that are clamped on the plate surfaces. These shoes are slightly recessed in the middle to allow weld reinforcement to be built up on the surface. The reinforcement is later ground off flush with the plates. The shoes may be solid copper or hollow for circulating cooling water, called, respectively, the "dry shoe" and the "cooled shoe" methods. Both methods have been used on Michigan work and are included in this study. A sump or starting tab is required at the bottom of the joint to assure that slag depth and fusion are adequate by the time the plates to be joined are reached. Likewise, runoff tabs are provided at the top edge of the plates to avoid lack of fusion and other flaws that occur at the stopping point of the weld. These starting and runoff tabs are later removed flush with the plate edges by flame cutting and grinding.

The main advantages and disadvantages of the electroslag welding process as applied to bridge beam fabrication are as follows:

Advantages:

1) Since electroslag welding is a single pass procedure with a minimum of joint preparation required, it offers a significant time savings in butt joint welding of plates from 1 to 8 in. The welding observed in this project showed about a 50 percent savings in welding time as compared to the submerged arc process.

2) Filler metal deposition rates are extremely high in electroslag welding, running from 25 to 45 lb per hr per electrode (6).

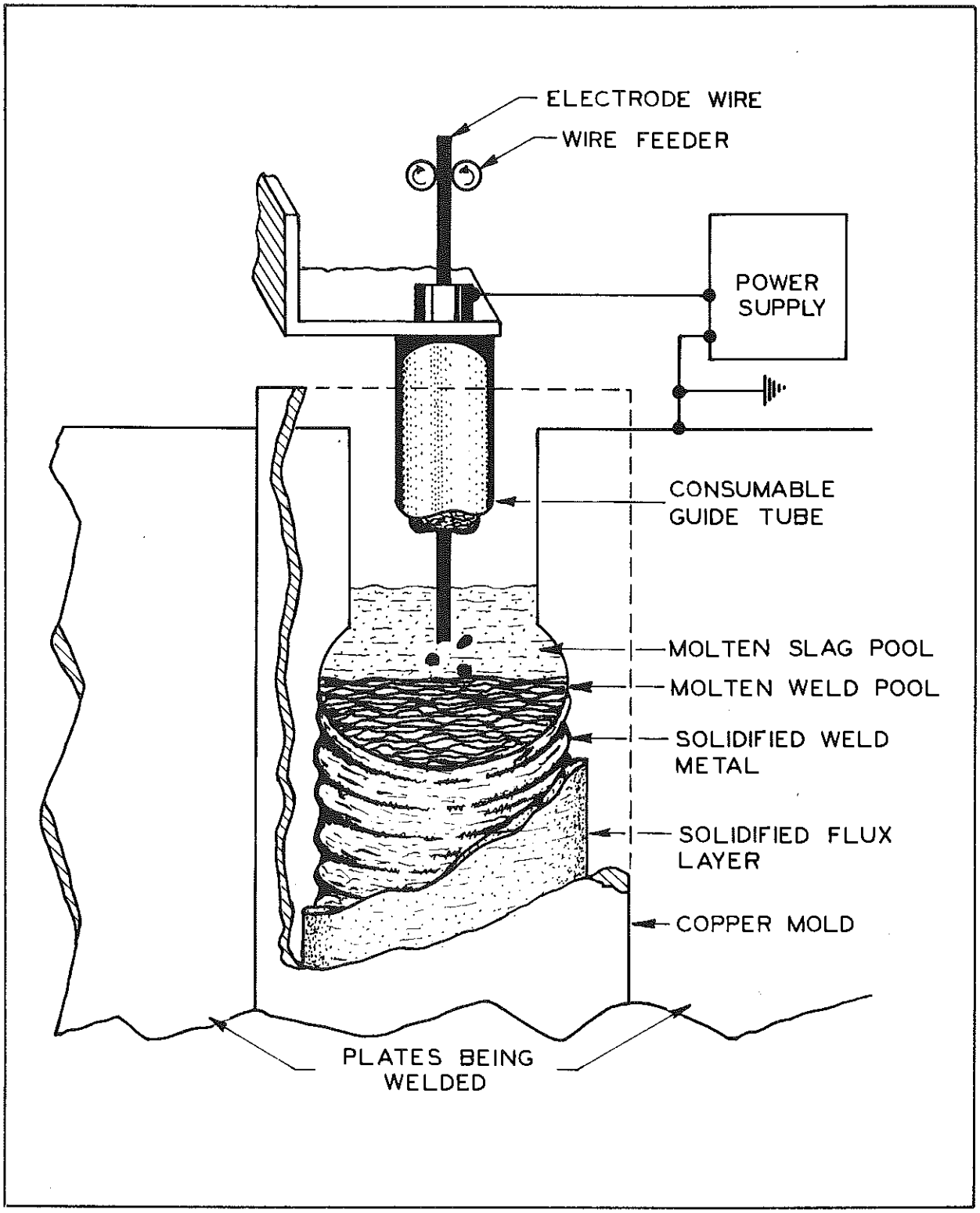

Figure 4. Schematic of consumable guide electroslag welding (after Ref. 6).

3) Since the weld metal pool stays molten for a long period of time and is completely covered with the molten slag pool, the deposited weld metal is generally free of inclusions and porosity.

4) The distortion occurring in an electroslag welded joint upon cooling is minimal and can be easily compensated for in the joint setup.

5) The residual stress pattern in an electroslag weldment is favorable since compressive stresses occur on the surface of the weld and the tensile stresses are confined to the inner core (9).

Disadvantages:

1) The primary disadvantages of the electroslag process is that its very high heat input results in a prolonged thermal cycle with very slow solidification and cooling rates. This thermal cycle results in an anisotropic, nonhomogeneous, large grained weld nugget and extremely large heat-affected zone (Fig. 5). This type of weld metal structure has many physical and metallurgical problems and is normally not acceptable for use in the "as welded" condition when Charpy V-notch impact requirements are specified (9).

2) If the welding parameters (amperage and voltage) are not carefully controlled the dendritic orientation will shift in the weld metal and a high incidence of centerline cracking can occur (6).

3) Once stopped, an electroslag weld cannot be restarted because of the discontinuities produced at the start-up point. An interrupted weld must be cut out and restarted in a sump.

4) Removal of the weld fixturing, such as the starting sump and run-off tabs, can introduce serious edge defects in actual production work. These defects require meticulous repair and are easily overlooked in inspection.

5) The metallurgical structure present in an electroslag weldment in the "as welded" condition has not been shown to be reliable for use in fatigue loading applications or in use with bare, unpainted exposures of steel beams with enhanced corrosion resistance, such as ASTM A 588 steel.

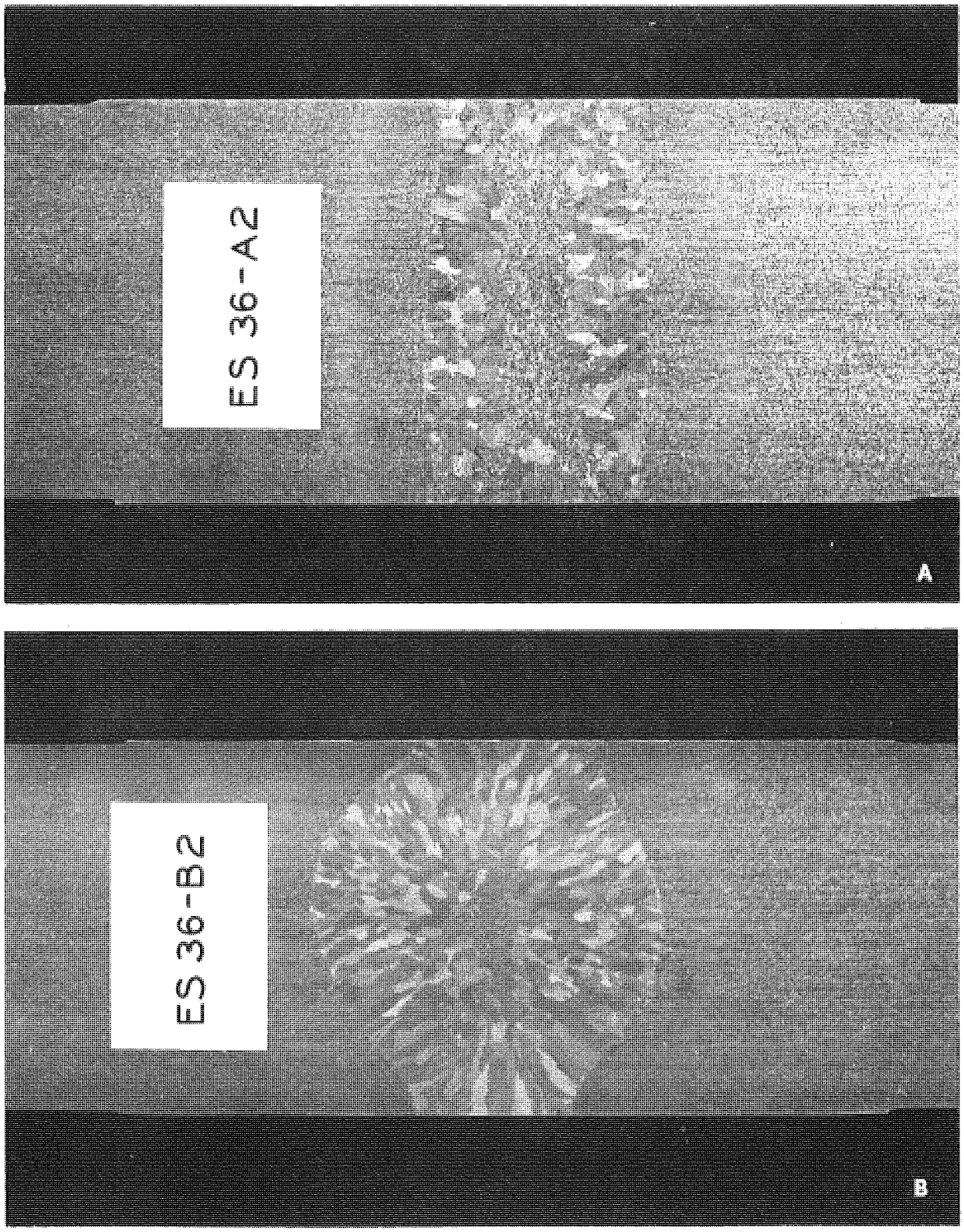

Figure 5. Typical macrostructures of electroslag welded butt joints. (A) Welded by Fabricator A with "cooled shoe" procedure, and (B) welded by Fabricator B with "dry shoe" procedure.

Test Weldments - Consumable Guide Electroslag Process

Test weldments for this project were produced by the two structural steel fabricators who were the prime users of the electroslag process, and during the period between early 1970 and July 1974 did the majority of Michigan's plate girder work. Butt joints were electroslag welded in 1-3/4 and in 3-in. thick plates, 16 in. wide, of both ASTM A 36 and A 588 steels. Plate length on either side of the joint varied between 3 and 4 ft. It was assumed that this length would provide an adequate heat sink for the weld joint. This was verified by monitoring the temperature change into the plate adjacent to the weld which revealed a negligible change in temperature beyond 12 in. from the edge of the retaining shoes. As in the submerged arc welding process, the philosophy applied to the fabrication was to produce welds exactly as would be done in production work and to observe no precautions that would not normally be considered.

Fabricator A, as previously described, used the cooled shoe method of consumable guide electroslag welding (Fig. 6). Joint preparation simply involved the grinding smooth of flame cut square ends. The plates were then aligned in a flat position with an initial gap width of 1 in. and tack welded together by the use of C plates or strong-backs. The 1-in. gap between the two work pieces was increased by 1/8 in. towards the joint top for every 12 in. of weld length, to compensate for the distortion that occurs upon cooling. The plates were then placed on edge in the vertical position and the starting sump and runoff tabs were tack welded in place (Fig. 7). Fabricator A used an oscillating guide tube technique in welding the 3-in. thick plates. The guide tube was aligned in the joint and the timing mechanism set so that the tube would dwell on one side for two seconds, then take two seconds to move across the joint where it would again dwell for two seconds, then back again. This technique provides for a uniform distribution of heat throughout the joint. Without oscillation, a single electrode is limited to less than 2-in. thick plates for a single pass procedure. The guide tubes used were bare metal of the same composition as the filler metal. Spacer rings made of flux were placed on the tube to prevent possible short circuiting with the edges of the work pieces. The electrode wire was then fed through the guide tube, the water-cooled shoes installed, and the setup was complete. A dry asbestos-foil tape was fitted between the edges of the retaining shoes and the plates to prevent any molten flux leakage where a loose fitup might occur. A ball of steel wool is placed in the bottom of the starting sump to produce a quick flash of high heat which aids in the starting of the electroslag process. A special starting flux is dumped in from the top of the joint and with the power on, the wire feed is started. After a few seconds of arcing in the bottom of the sump, a molten slag pool

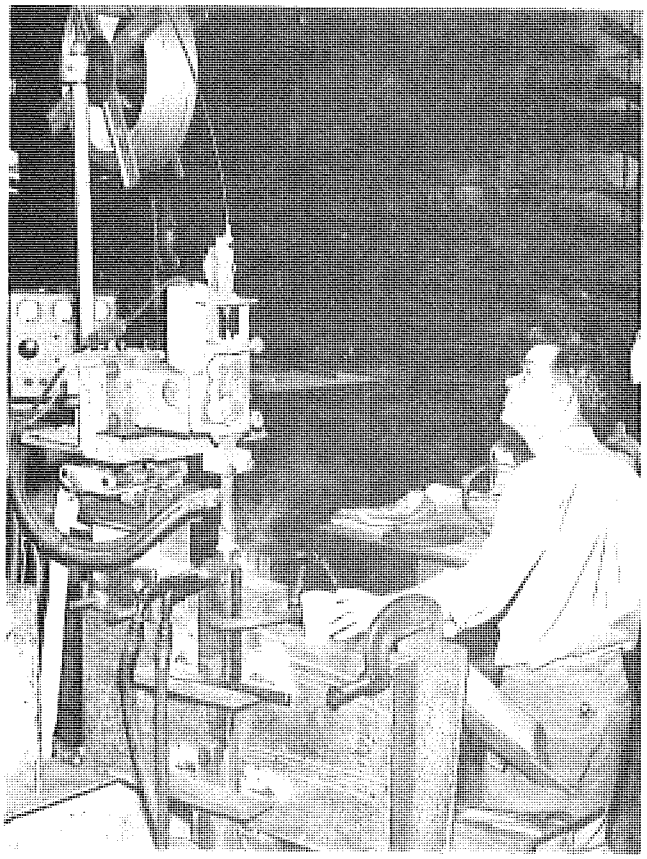

Figure 6. Electroslag welding procedure used by Fabricator A with water cooled retaining shoes.

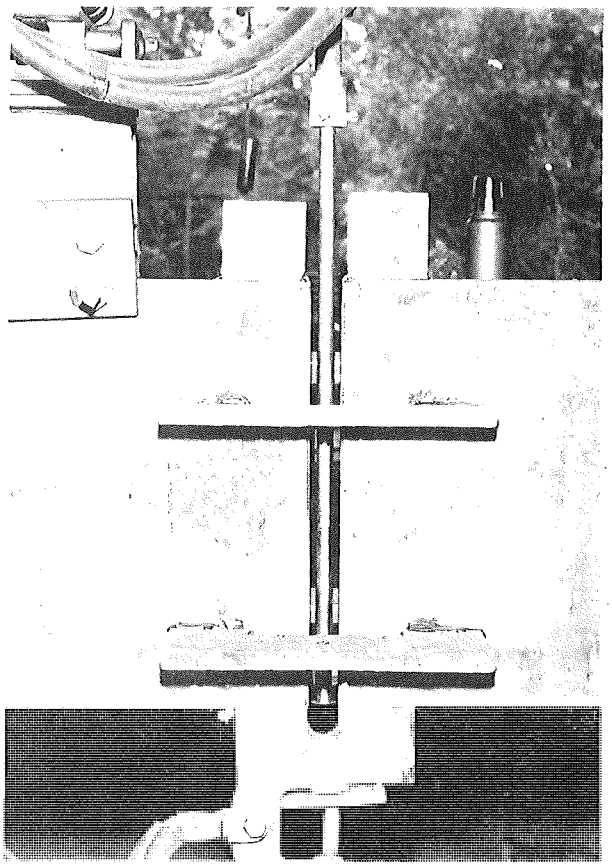

Figure 7. Fabricator A electroslag joint preparation showing strong-backs, starting sump, run-off tabs, consumable guide tube, and spacer ring.

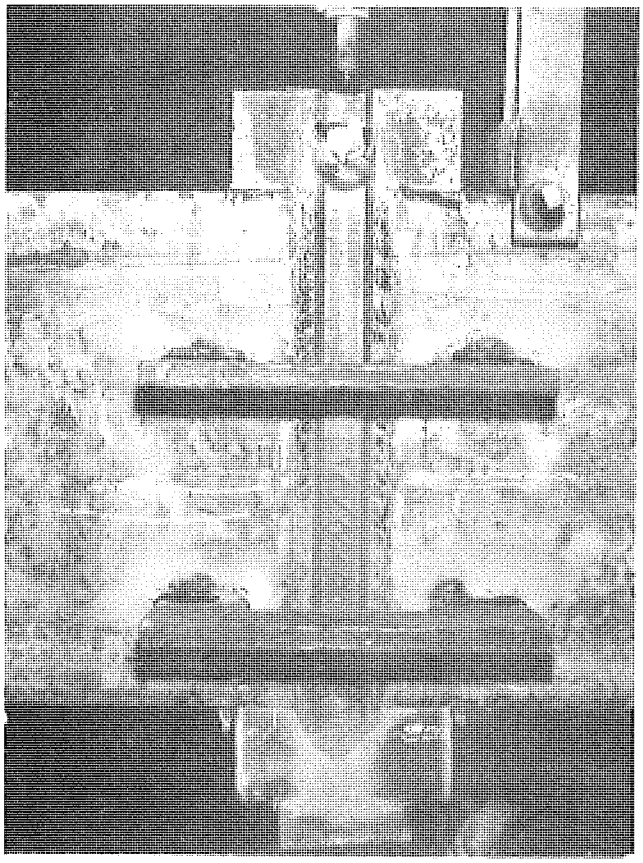

Figure 8. Completed electroslag weld with retaining shoes removed, strong-backs, sump and tabs still in place (Fabricator A).

forms over the arc and the process is started. A different running flux was used once the welding was started and this was added periodically by the operator from the top of the joint. Tap water was continuously circulated through the cooling shoes during the welding. Immediately upon completion of the weld, the water cooled shoes were removed and the joint was allowed to air cool (Fig. 8). The maximum temperature on the surface of the weld upon removal of the shoes was in excess of 1500 F. A typical macrostructure of the resulting weld is shown in Figure 5. Actual welding time per joint ran about 45 minutes for the 1-3/4-in. plates and one and one-half hours for the 3-in. plates, for a 16-in. wide plate splice. Including plate preparation and setup time, about one and one-half hours and two to three hours were required per joint in the 1-3/4 and 3-in. thick plates, respectively. The electroslag welding process required two men for operation of the equipment. For a listing of the weldments made and the welding variables, see Table 2.

TABLE 2
WELDING VARIABLES - ELECTROSLAG PROCESS

Weld Identification[1]	Base Metal ASTM Designation	Plate Thickness, in.	Electrode Type	Flux Type	Amps	Volts
ES 588-A1	A 588	1-3/4	Hobart 25P	(2)	600-650	36-38
ES 588-A2	A 588	3	Hobart 25P	(2)	750-800	42-44
ES 36-A1	A 36	1-3/4	Hobart 25P	(2)	600-650	36-38
ES 36-A2	A 36	3	Hobart 25P	(2)	750-800	42-44
ES 588-B1	A 588	1-3/4	Linde 36	Linde 124	525-550	36
ES 588-B2	A 588	3	Linde MC-70	Linde 124	1100	36
ES 588-B2a	A 588	3	Linde WS	Linde 124	1100	36-38
ES 36-B1	A 36	1-3/4	Linde 36	Linde 124	525-550	36
ES 36-B2	A 36	3	Linde MC-70	Linde 124	1100	36

[1] Identification Symbolism:
ES - electroslag weldment
588 or 36 - ASTM A 588 or A 36 steel
A or B - Fabricator A or B
1 or 2 - 1-3/4 or 3-in. plate thickness, respectively.
[2] Hobart - PF 203 - starting, PF 201 - running

Fabricator B used the dry shoe method of consumable guide electroslag welding (Fig. 9). In this method the only cooling supplied to the shoes is the heat loss to the surrounding air. Considerably more heat is built up and retained in the joint with this technique and the corresponding metallurgical structures reflect this. The welding preparation and procedure

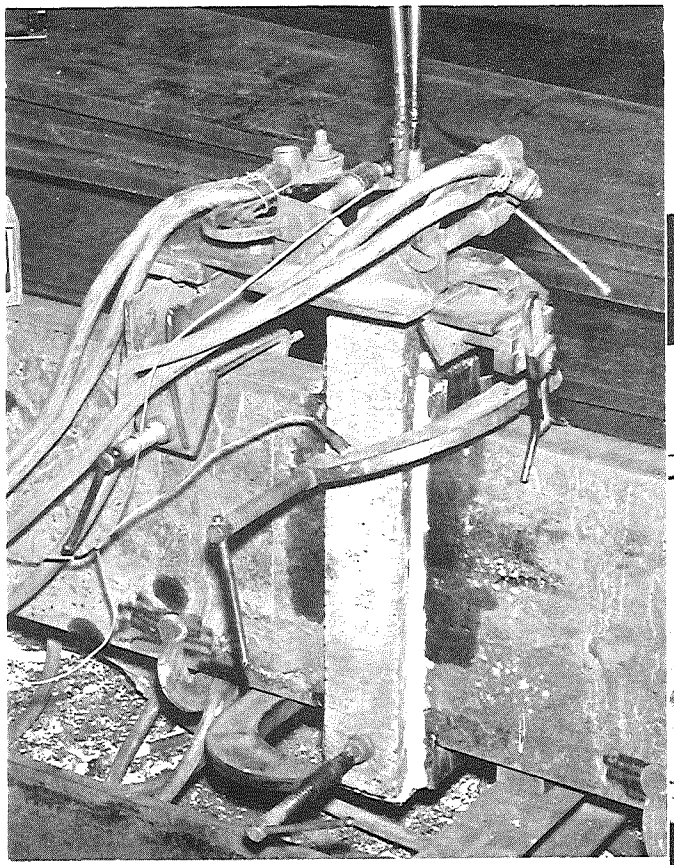

Figure 9. Electroslag welding procedure used by Fabricator B with dry retaining shoes.

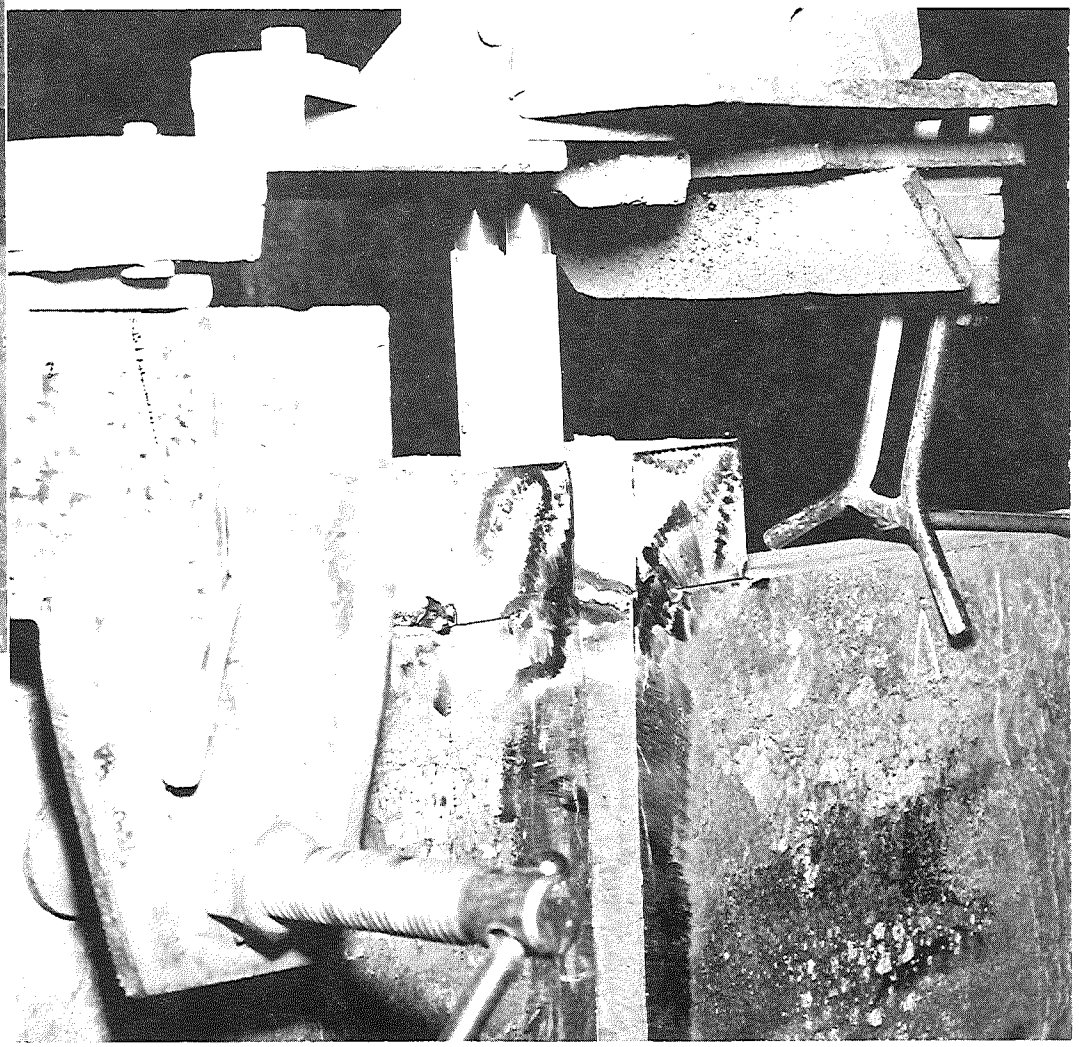

Figure 10. Double guide tube used in 3-in. thick joint by Fabricator B (note flux coating on guide tubes).

followed by Fabricator B were the same as those used by Fabricator A with the following exceptions. The plates to be welded were fixtured into alignment while standing in the vertical position, restraint being provided by support posts and the tack welded sump block. No strong-backs were attached across the joint and the weld retaining shoes were secured in place by large C-clamps. This technique eliminated tack welding in eight locations on the plate surfaces. An asbestos-water putty was used along the edge of the retaining shoe to keep the molten flux from escaping since a loose fitup with the plate occurred. A stationary guide tube was used by Fabricator B, and when the plate thickness exceeded 2 in. a double tube arrangement was used (Fig. 10). The guide tubes used were flux coated, supplying both the flux required to keep the weld running and the insulation needed to prevent short circuiting with the work piece. Each guide tube carried its own electrode and power supply. No special starting flux was used at the start up of a weld as was done by Fabricator A. When a weld was completed, the retaining shoes were left in place for about 30 minutes instead of being removed immediately as done by Fabricator A. The maximum temperature on the weld surface was about 700 F when the shoes were removed. External appearance of a joint welded by this dry shoe method was the same as that welded by the cooled shoe method. A typical macrostructure of the resulting weld is shown in Figure 5. The actual welding time to complete a 16-in. wide plate splice was about 25 minutes for the 3-in. thick plate using the double tube setup and about 40 minutes for the 1-3/4-in. thick plates using a single tube. Counting plate preparation, the time per joint was about two hours in each case, including the time lapse before the retaining shoes were removed. As before, this electroslag welding was a two man operation. For a listing of the weldments made and the welding variables, see Table 2.

General Weld Quality - Nondestructive Testing

With respect to internal flaws and inclusions electroslag deposited weld metal is of good quality. Since the molten weld pool remains in the liquid state for a relatively long time, and is always shielded by the molten flux pool, gases which can cause porosity, and other nonmetallic substances are expelled. With the submerged arc process the weld metal is in the molten state for a short period of time and thus is more susceptible to trapping gas or inclusions in the weld. However, a proper welding procedure and good quality control can practically eliminate the problem.

All test weldments used in this project were subjected to nondestructive testing by X-ray examination. Both the electroslag and the submerged

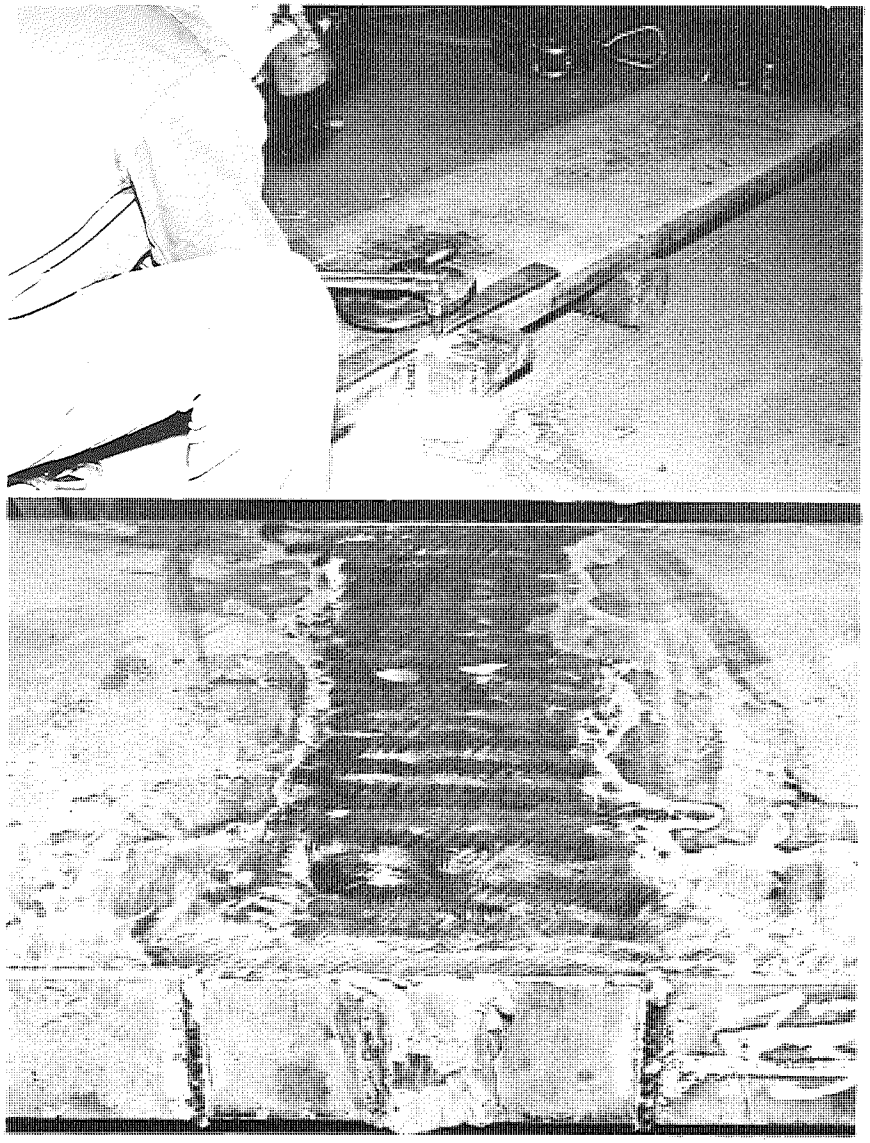

Figure 11. Method used for removing starting sump and run-off tabs in electroslag welding (above). Resulting edge condition before grinding (below).

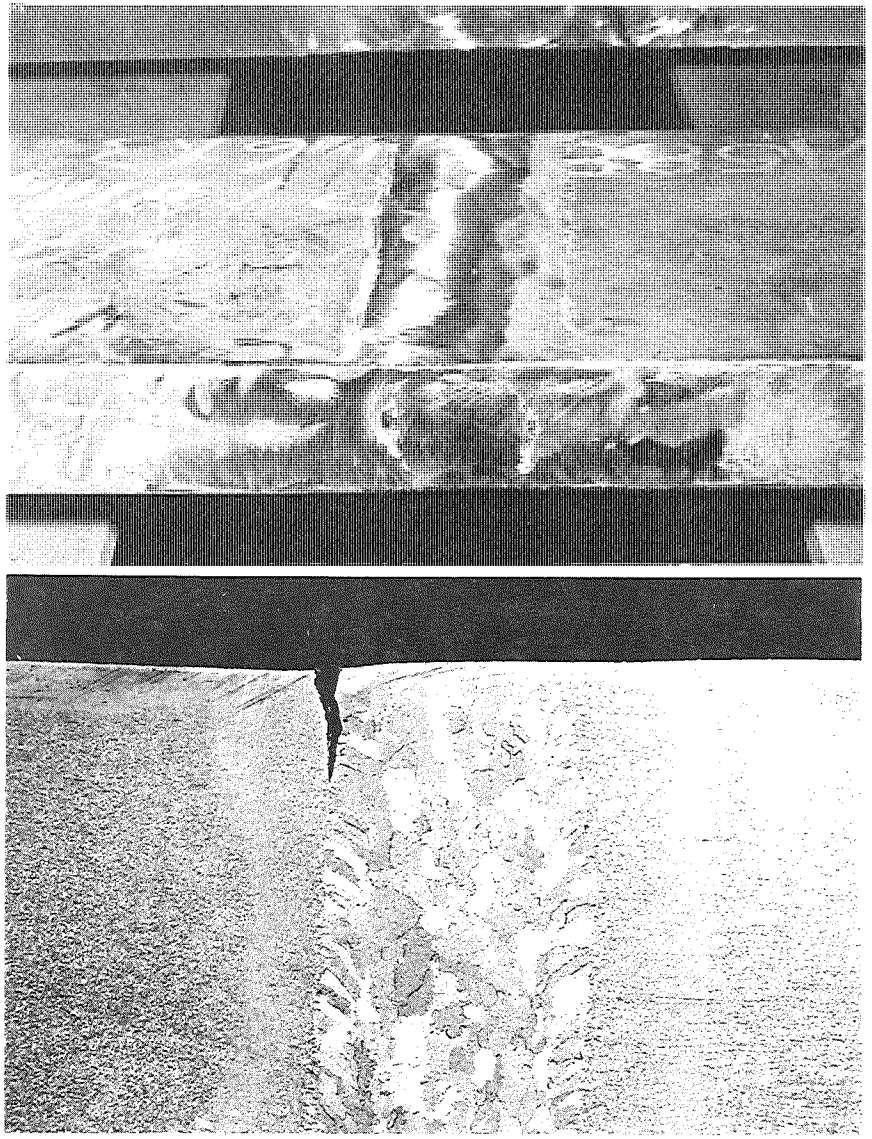

Figure 12. Lack-of-fusion edge defect that occurred in a dry shoe electroslag weld (above). Macrograph, below, shows the extent that such fusion defects may extend into the plate (about 1-in. in this case).

arc weldments were shown to be free of rejectable defects by this method. The only exception was that the electroslag weldments had a high incidence of edge defects, especially in the welds made by Fabricator B using the dry shoe method. In the 16 electroslag weldments produced by Fabricator B, 13 edge defects occurred that required either grinding or a manual weld repair. These edge defects were caused by the interaction of the starting sump or the runoff tabs with the molten weld pool as it passed the edge of the plate. Sometimes the edge tabs were undercut by the weld pool and sometimes lack of fusion would occur at the plate edge. The starting sump and runoff tabs were removed by flame cutting which left additional defects at the points where they were tack welded to the plates and also added a heat-affected zone on the edge. This heat-affected zone contains regions of untempered martensite, a very hard grain structure. Figures 11 and 12 show some of these defects. Fabricator A had similar problems with the edge defects caused by the attachment and removal of the starting sump and runoff tabs, but the cooled shoe process didn't seem to produce the lack-of-fusion problem at the plate edge. An additional type of surface defect was produced by Fabricator A because of the strong-backs used for fixturing the water cooled shoes in place. These strong-backs were tack welded to the plate surfaces in eight different locations. They were later removed by breaking them off with a sledge hammer. This procedure resulted in a metallurgical discontinuity at the tack welds with high residual stresses and usually a physical discontinuity where they were broken off (Fig. 13). The use of strong-back fixturing was prohibited shortly after these observations were made. Alternate fixturing techniques using C-clamps are easier to use and eliminate these surface defects.

Additional nondestructive testing was done on the test weldments produced by Fabricator A using ultrasonic gear. There has been some speculative concern about applying ultrasonic testing to electroslag weldments because of the potential for excessive back reflection and attenuation by the large grain boundaries. Some back reflection does occur due to the grain structure but it did not seem to lower the sensitivity threshold needed in this application. The results of the ultrasonics agreed with those of the X-ray, but several small, nonrejectable defects were located that did not show up on the X-ray films. Hence, ultrasonic testing may show greater resolution of defects than X-ray, especially in thick plates. The main disadvantages of using the ultrasonic inspection are the need for a highly skilled operator and the lack of a permanent record of the weld such as that given by the X-ray film.

Contrasting the quality of electroslag and submerged arc butt welds as evaluated by nondestructive testing makes them about equal. The multi-

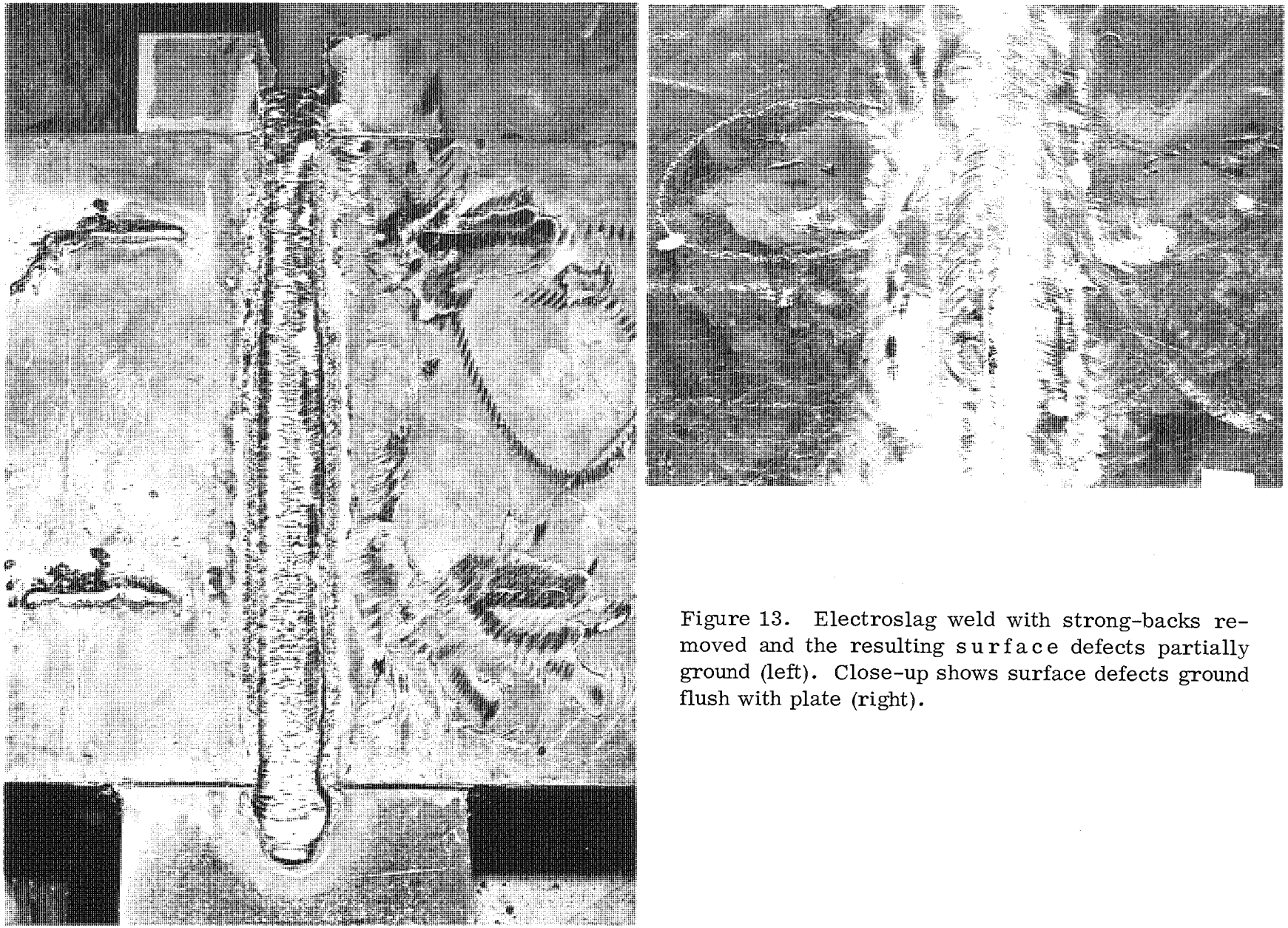

Figure 13. Electroslag weld with strong-backs removed and the resulting surface defects partially ground (left). Close-up shows surface defects ground flush with plate (right).

pass technique used in submerged arc welding gives a higher probability of an inclusion occurring in the weld which would require repair. This is offset in electroslag welding by the high incidence of edge defects, even though the deposited weld metal is usually defect free. Distortion due to shrinkage of the weld is easier to control in an electroslag weldment, but proper technique in submerged arc welding will yield the same result. The residual stress patterns present in an electroslag weldment are reported to have a favorable configuration since the weld surface is in compression and the central core is in tension (9). The residual stresses on the surface of a submerged arc weld are known to be tensile and of approximately yield point magnitude (4). This advantage in electroslag weldments is again offset by the repairs necessitated at the edge defects. The repair weld beads will produce residual tension stress approximately equal to the yield point of the weld metal.

Although not encountered in the fabrication of these test weldments, another flaw that can occur in electroslag welding is intergranular or hot cracks in the central portion of the weld metal. Weld metal chemistry and weld grain orientation, which is controlled by the shape of the molten weld pool, are the primary factors determining the resistance to hot cracking (10). If hot cracking were to occur, it should be found by either X-ray or ultrasonic testing. Repair of a joint with hot cracking would require removal of the entire joint and rewelding.

Metallurgical Structure and Alloy Composition of Weldments

The mechanical and corrosion properties of a weld metal are determined by its chemistry and grain structure. Once the chemistry of the weld has been established, the structure is a function of the heating and cooling cycle experienced by the weld and its adjacent heat-affected zones. In a submerged arc weld, the temperature of the weld puddle goes above the melting point very rapidly; however, the amount of weld metal at this temperature is very small relative to the surrounding weld and base metal. The amount of heat put into the joint in depositing a bead is just sufficient to provide fusion with the adjacent metal and to keep the weld molten long enough to expel any entrapped gas or inclusions. Hence the weld metal and adjacent heat-affected zone cool rapidly. If proper interpass temperature is maintained between passes, the time that the heat-affected zone adjacent to the fusion line is above the temperature where metallurgical changes can occur (approximately 1000 F) is only two minutes or less (10). This thermal cycle produces a weld metal that is fine grained relative to the base metal with one small heat-affected zone. In contrast, the electroslag welding process has a very high heat input that results in a prolonged thermal cycle with very slow solidification and cooling rates. The mass of molten slag

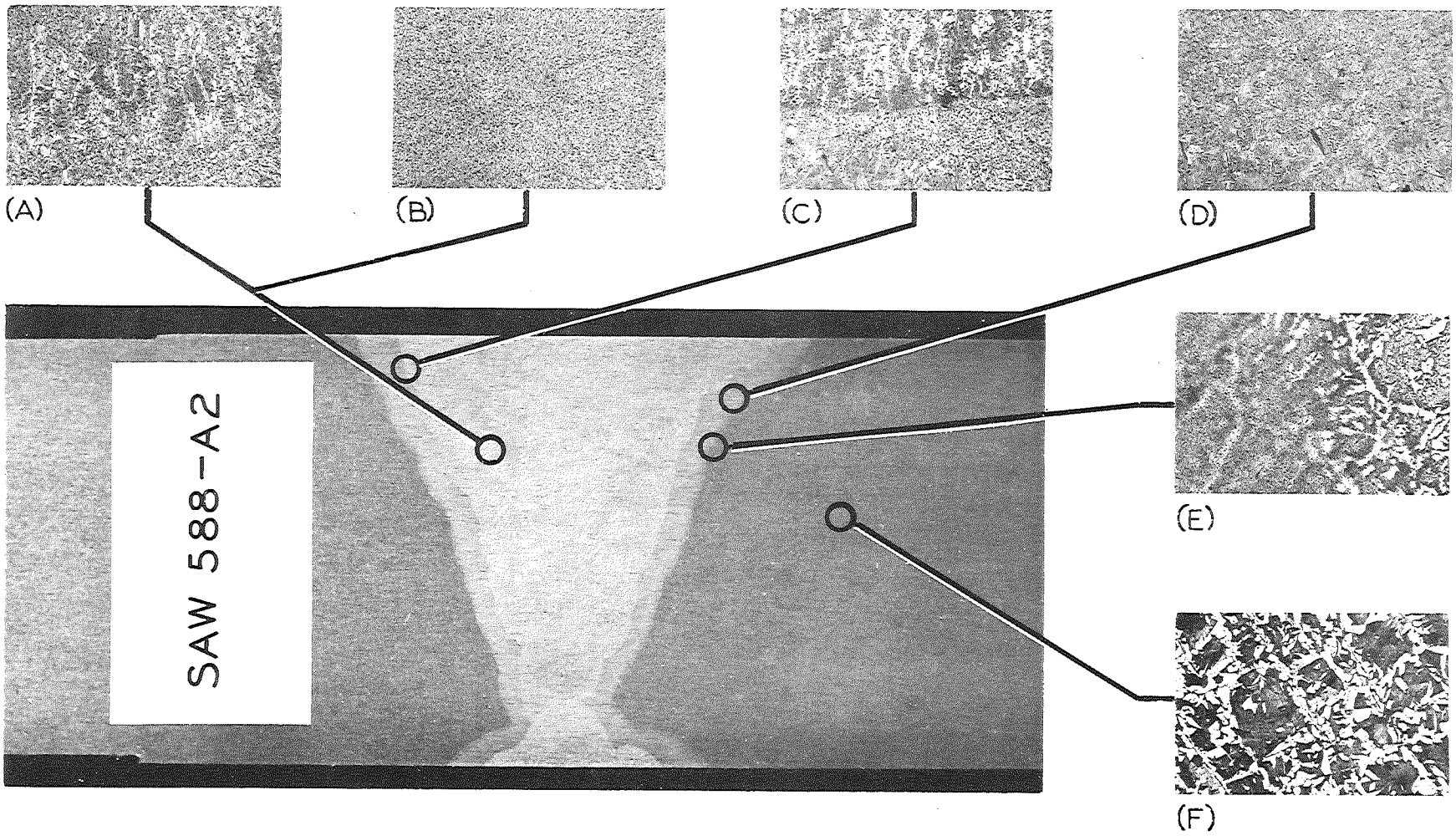

Figure 14. Submerged arc weld by Fabricator A on 3-in. A 588 steel. Microstructures shown are: A) as deposited weld metal, B) weld metal refined by a subsequent pass, C) fusion line (HAZ on bottom), D) HAZ beyond fusion line, E) interface between HAZ and base metal, F) unaffected base metal. (Microstructures at 100x, etchant 3 percent nital.)

and weld metal is relatively large and the surrounding metal and retaining shoes extract heat very slowly. On a thick plate (3 in.) the weld metal will be red in color (above 1200 F) for up to 15 minutes after the weld is completed. The time above 1000 F in the heat-affected zone adjacent to the weld has been measured as exceeding 20 minutes in a 4-in. thick electroslag weld (10). This thermal cycle results in a coarse grained weld metal with a structure resembling that of cast steel. The weld metal can contain as many as three metallurgically distinct zones with non-homogeneous and anisotropic grain structures, and at least two large heat-affected zones are produced.

The following section will attempt to document the grain structures produced by the submerged arc and electroslag welding processes as used in butt welding ASTM A 36 and A 588 steel plates. An introduction into these structures is essential to the understanding of the physical and metallurgical properties present in the weldments.

Submerged Arc Weld Metal Structure

In the construction grades of steel being studied in this project, weld metal deposited by the submerged arc welding (SAW) process has a very fine microstructure in comparison to the base metal. Figures 14 through 17 illustrate this for submerged arc weldments made by Fabricators A and B in 3-in. plates of A 588 and A 36 steel. The cross-sections of the weldments reveal that in the macrostructure of a SAW only one "macroscopic" weld zone and one heat-affected zone (HAZ) occur. The weld zone is composed of a mixture of "as deposited" and partially refined structure since the heat expended in depositing a weld bead will partially refine the weld bead underneath it. The weld metal does, however, behave homogeneously in mechanical testing and has no serious anisotropic (or directional) variations with respect to mechanical properties.

The primary structure of a steel refers to the configuration of the austenite grains present in the metal when the temperature was above the lower transformation temperature (around 1300 to 1400 F). When a low-carbon steel cools below this temperature the austenite phase transforms to pearlite and free ferrite, the relative amount of each depending mainly on the carbon content of the steel. These transformation products are referred to as the secondary structure and their size and distribution depends on the rate of cooling. High rates of cooling will yield fine grained secondary structures and slow rates yield large grained secondary structures. When the cooling rate is right, the primary structure in the steel will be revealed by ferrite bands which are formed by the deposition of free ferrite along the prior austenite grain boundaries just as transformation begins.

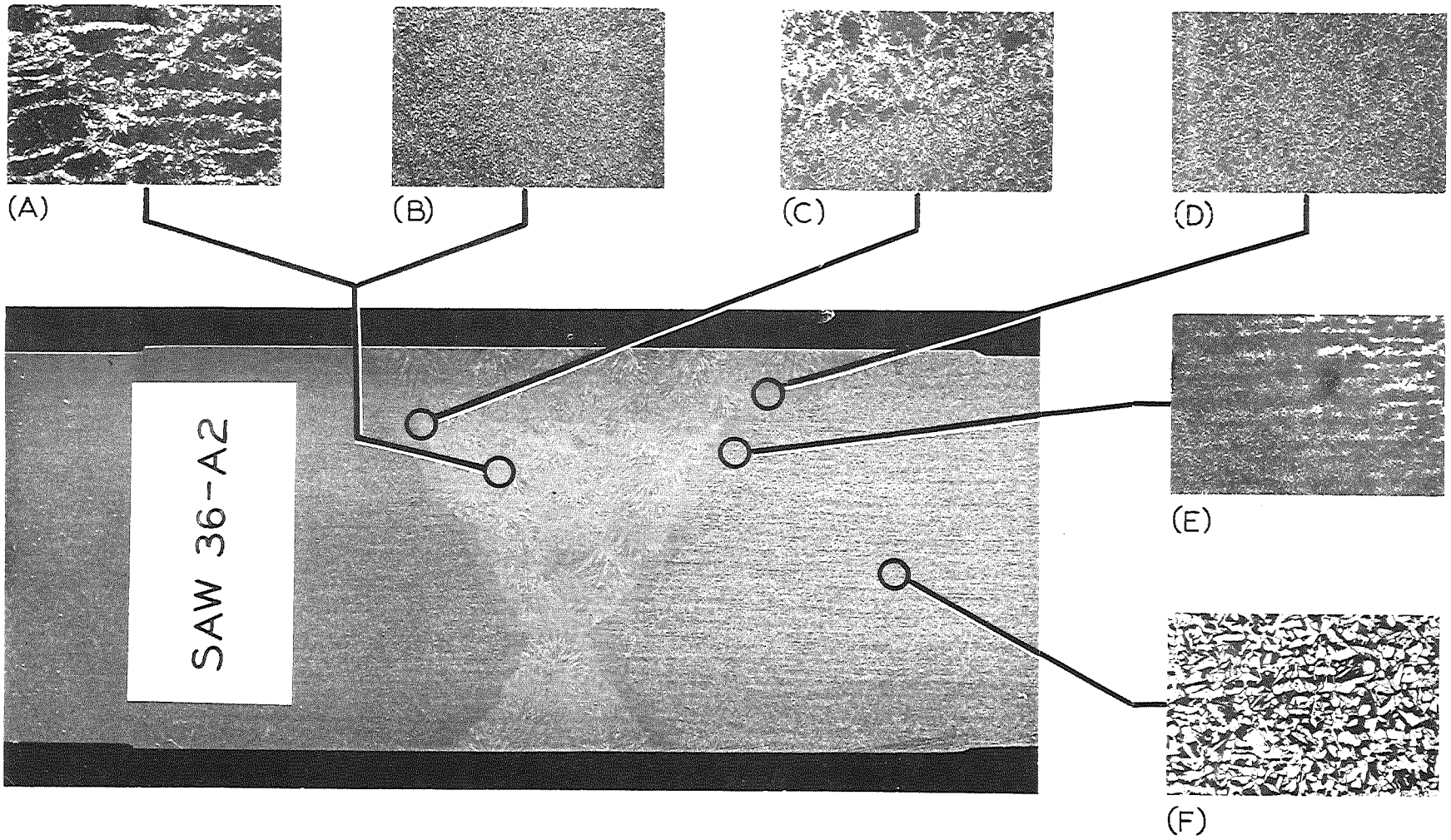

Figure 15. Submerged arc weld by Fabricator A on 3-in. A 36 steel. Microstructures shown are: A) as deposited weld metal, B) weld metal refined by a subsequent pass, C) fusion line (HAZ on bottom), D) HAZ beyond fusion line, E) interface between HAZ and base metal, F) unaffected base metal. (Microstructures at 100x, etchant 3 percent nital.)

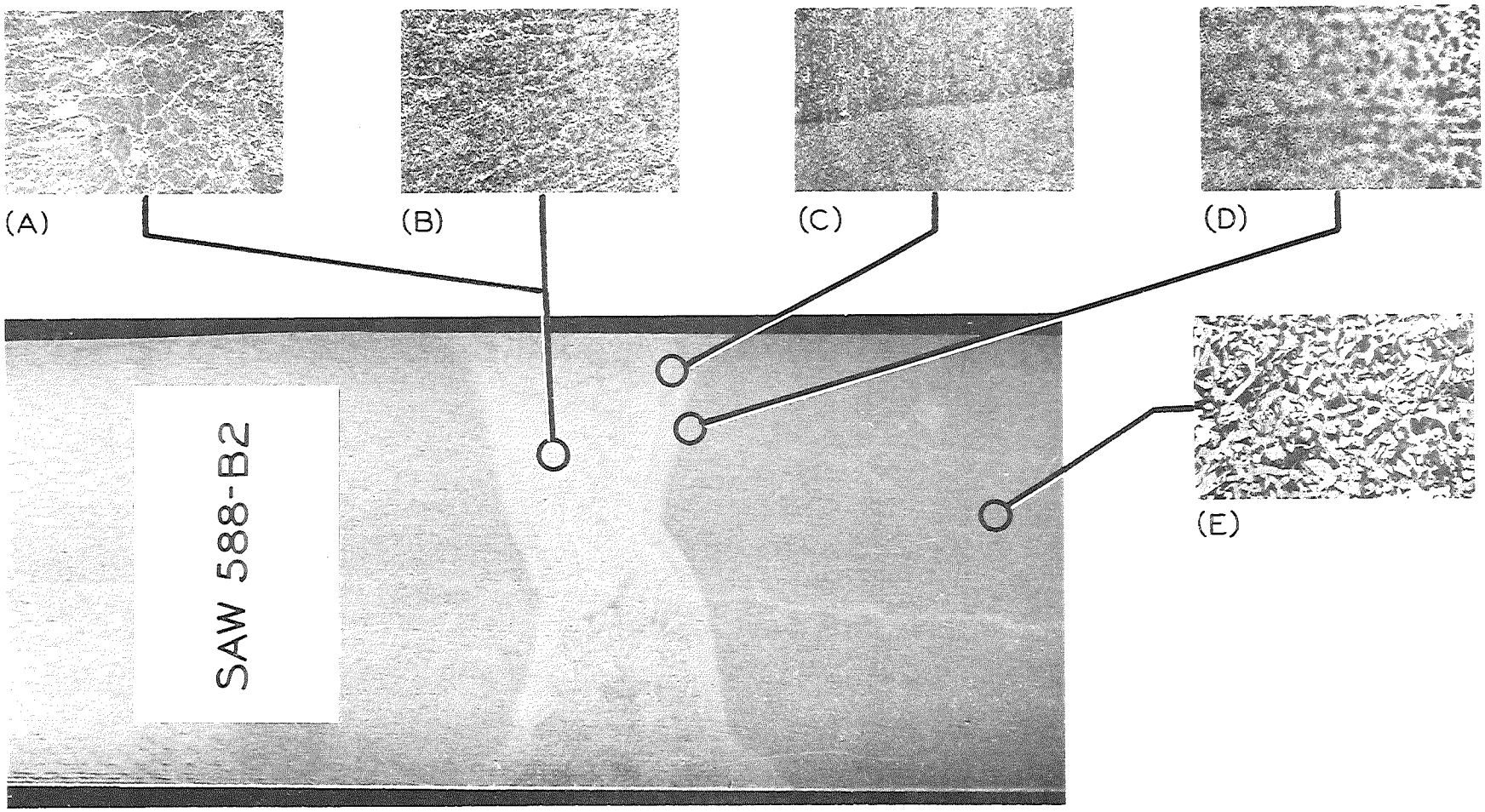

Figure 16. Submerged arc weld by Fabricator B on 3-in. A 588 steel. Microstructures shown are: A) as deposited weld metal with some refinement, B) weld metal refined by a subsequent pass, C) fusion line (HAZ on bottom), D) interface between HAZ and base metal, E) unaffected base metal. (Microstructures at 100x, etchant 3 percent nital.)

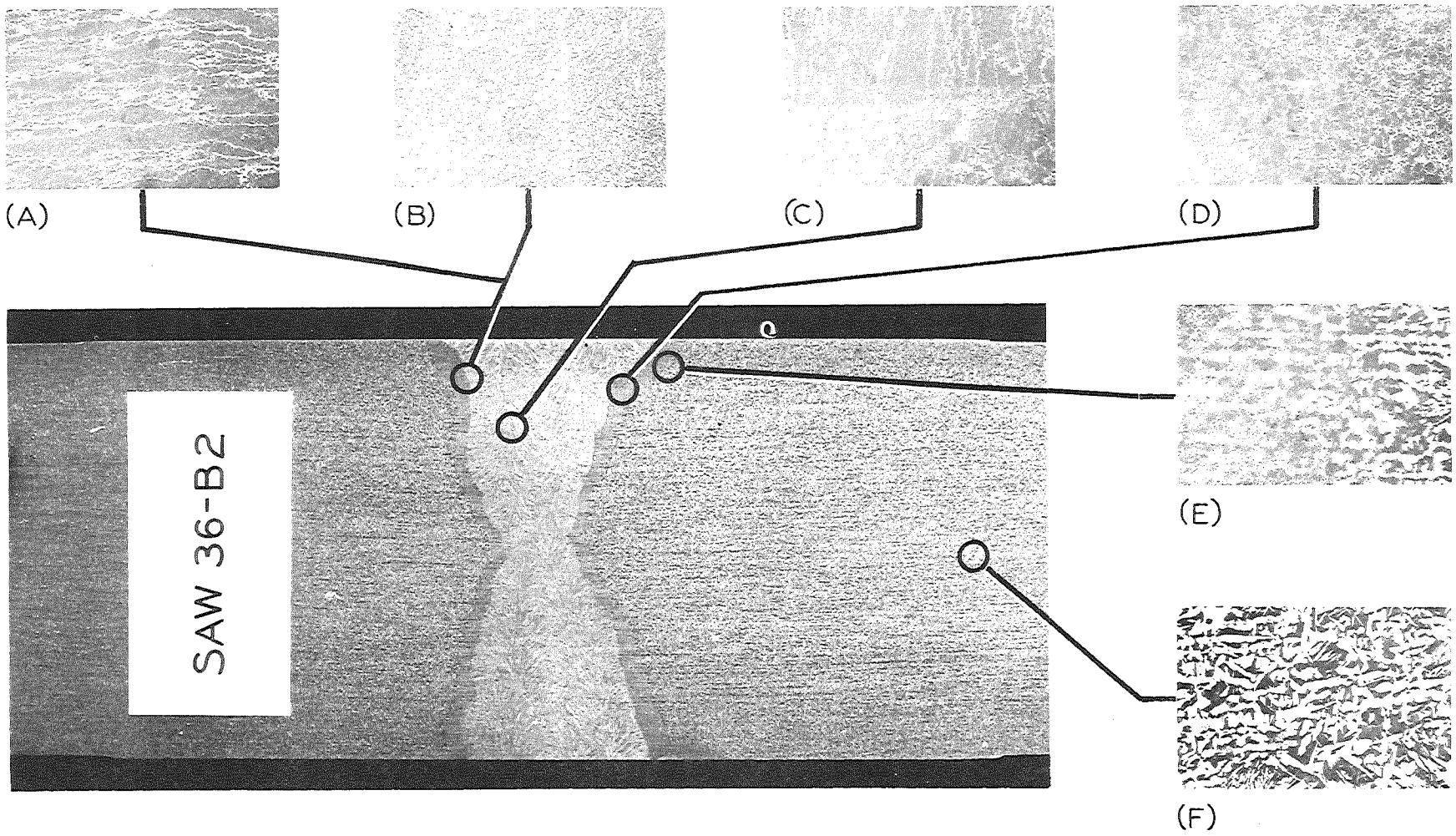

Figure 17. Submerged arc weld by Fabricator B on 3-in. A 36 steel. Microstructures shown are: A) as deposited weld metal, B) weld metal refined by a subsequent pass, C) fusion line (HAZ on bottom), D) HAZ beyond fusion line, E) interface between HAZ and base metal, F) unaffected base metal. (Microstructures at 100x, etchant 3 percent nital.)

The structure of submerged arc weld metal can be described as a dispersed system of pearlite and ferrite (secondary structure) with some ferrite banding along the prior austenite grain boundaries (primary structure) in the unrefined regions. These ferrite bands are destroyed in the regions where the heat from a subsequent weld pass elevated the metal above the lower transformation temperature, thus refining the structure. The primary and secondary structures of the weld metal are fine grained in comparison to base metal. The fusion line in a submerged arc weld is sharply defined and the base metal adjacent to it developes only one heat-affected zone. As long as the welding interpass temperature doesn't get too high, this HAZ is quite narrow (approximately 1/8 to 1/4 in.) and the effect is a refinement on the structure of the base metal. This is shown to elevate the hardness and impact properties of the HAZ above those of the base metal in the steel types being studied here. In quenched and tempered, high carbon, or high alloy steels, adverse effects can develop in this HAZ. As shown in the photomicrographs in Figures 14 through 17 the HAZ has a gradual transition into the unaffected base metal.

As illustrated by the macrostructures shown in Figures 14 through 17, the weld profile produced by the submerged arc process is governed by the initial shape of the plate edges being welded. Thus, a good weld profile is easily produced. Dilution of weld metal with base metal is kept to a minimum and occurs mainly along the fusion line. Thus, weld metal quality is not strongly dependent on base metal quality, since the alloy composition is controlled by the composition of the welding wire.

Electroslag Weld Metal Structure

According to Patton (10) over half of the heat extracted from an electroslag joint goes into the work pieces being welded. This can vary considerably as is seen in the use of dry or water cooled shoes. The method by which heat is extracted to a large extent determines the structure of the resulting weldment. In all electroslag welding techniques, heat is extracted very slowly as compared to the submerged arc process and large crystalline structures result. Crystallization or solidification of the weld pool proceeds from the partially fused grains of the base metal and the weld metal lying below the pool. Since the crystals grow in the directions of heat flow, the shape of the weld pool determines the orientation of the crystal growth (Fig. 18). Crystals grow in from the outer periphery of the weld with an upward deflection towards the weld pool, the dendrites pointing in the direction of welding. A deep weld pool produces crystals which meet at an obtuse angle in the center of the weld and a shallow pool produces crystals meeting

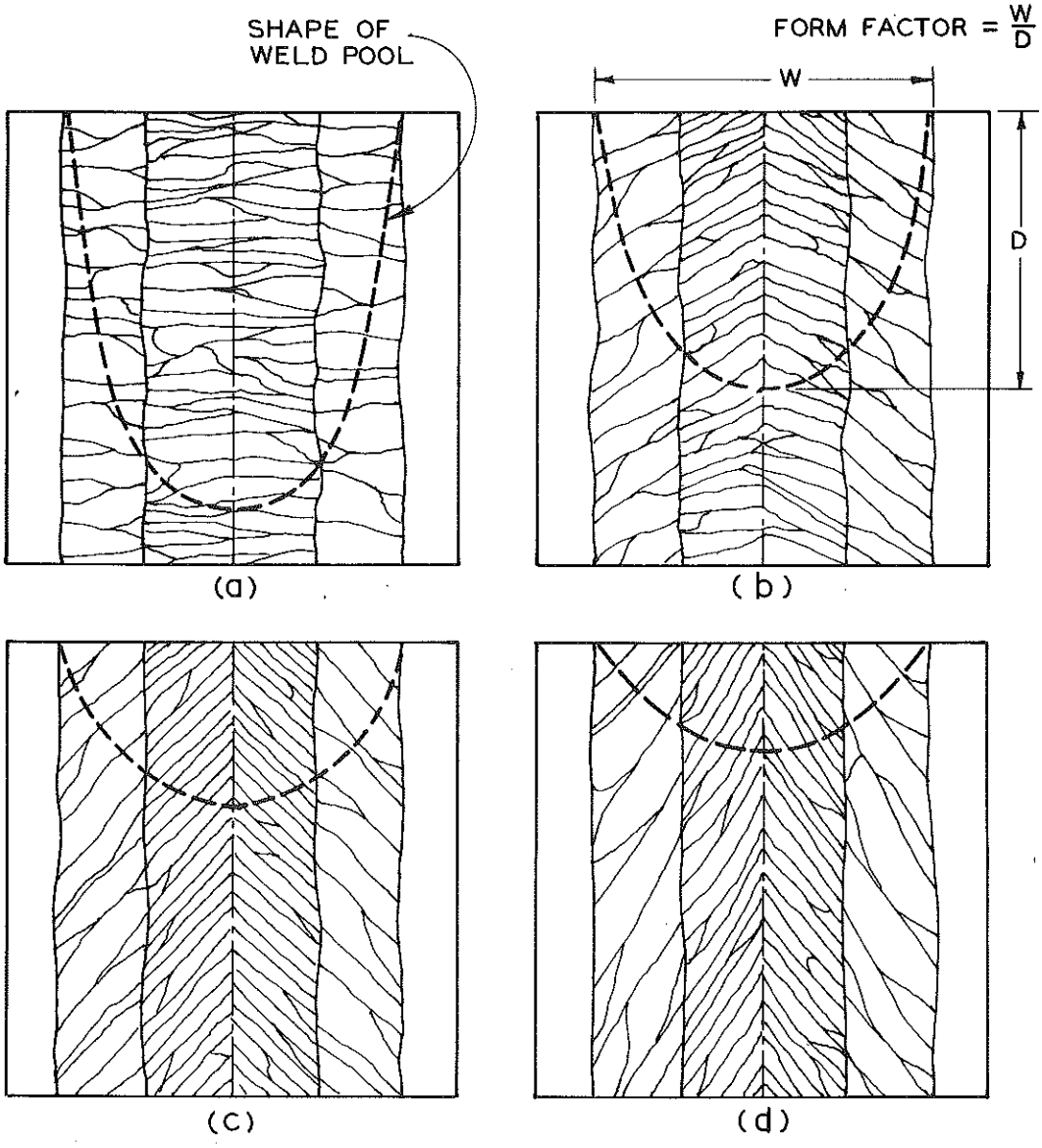

Figure 18. Sketch of longitudinal sections through electroslag weldments showing the variations in the orientation of the columnar crystals as a result of the weld pool shape:

(A) junction at butt ends of crystals (form factor 0.8),
(B) crystals meet at obtuse angle (form factor 1.2),
(C) crystals meet at acute angle (form factor 2.0),
(D) crystals meet at lateral faces (form factor 3.0).
Direction of welding is up (after Ref. 10).

at an acute angle. The form factor of an electroslag weld is defined as the width of the weld pool divided by its depth. Deep weld pools have low form factors and are very susceptible to intergranular cracking. Shallow weld pools with a high form factor (two or greater) are very resistant to such cracking (10). Electroslag welding is thus run with as shallow a pool as possible which results in crystallites that meet at an acute angle in the center. The depth of the slag pool above the weld pool must likewise be carefully controlled. It has been shown that microcracking can occur along the ferrite rich prior austenite grain boundaries when the slag pool is too shallow (11). This microcracking has been attributed to the penetration of diffusible hydrogen into the weld metal and to the increased entrapment of nonmetallic inclusions, both conditions resulting from a shallow slag pool. Solidification of the weld pool is a noncontinuous process and the longitudinal surface of the weld shows a slightly laminar structure because of this (10). In Ref. (10) Patton describes four different types of grain structure arrangements that can be produced in electroslag weldments (Fig. 19). Type I weld structure consists of an outer zone of coarse columnar crystals and an interior zone of thin, elongated columnar crystals. For purposes of discussion we will define the fine columnar crystals occurring in the center of the weld as Zone 1 weld metal and the coarse columnar crystals as Zone 2 weld metal. Type II welds have in addition to the coarse and fine columnar crystals of Type I, a zone of coarse, equiaxed crystals in the very center of the weld. Type III welds consist of only coarse columnar crystals throughout the cross-section and Type IV consists of only fine columnar crystals. All weldments studied in this project were either of Type I with coarse and fine columnar crystals zones or Type III with only a coarse columnar zone. Welds of Type IV with only a fine columnar zone have been encountered in some of Michigan's fabrication work with the cooled shoe electroslag welding, but these joints were not included in this study.

Figures 20 through 23 illustrate the various electroslag weldment structures produced by Fabricator A using the cooled shoe technique. The figures show transverse cross-sections taken normal to the longitudinal axis of the weld. The macrosections shown reveal the primary structure of the welds as belonging to Type I defined above. In the center of the weld, the Zone 1 type of thin columnar crystals appear and at the periphery of the weld the coarse columnar Zone 2 crystals appear. This structure is viewed on another plane in Figures 24 and 25 which are longitudinal sections taken at the mid-thickness of the plate. These sections show the columnar nature of the crystals with the Zone 1 crystals being nearly aligned with the weld axis and the Zone 2 crystals growing inward and upward, pointing in the direction of welding. Microstructures on the transverse plane are repeated in Figures 24 and 25 for comparison with the microstructures on

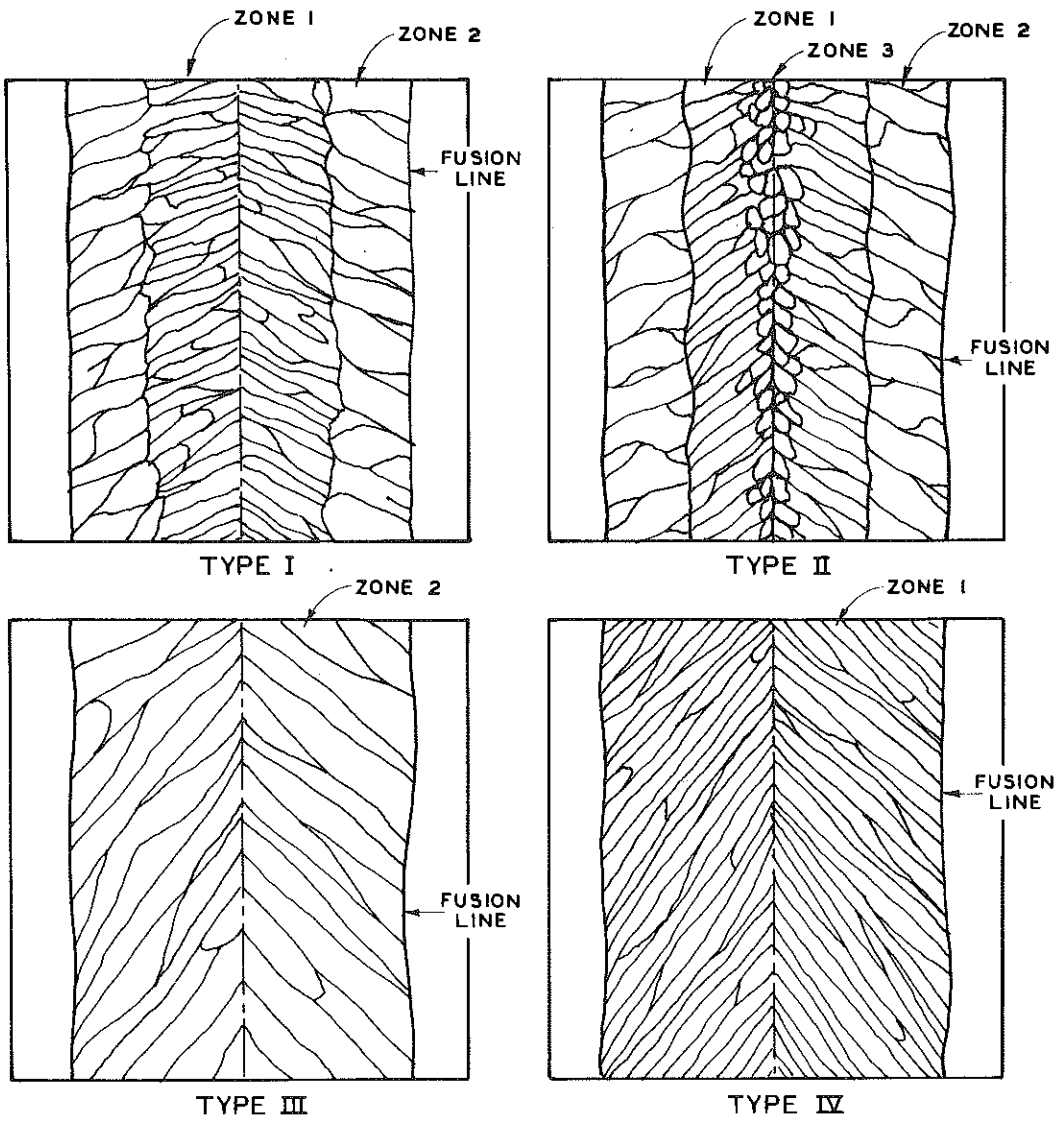

Figure 19. Sketch of electroslag joint types, longitudinal section through the weld. Type I - coarse (Zone 2) and fine (Zone 1) columnar crystals. Type II - Zones 1 and 2 plus coarse, equiaxed crystals (Zone 3). Type III - all Zone 2 crystals. Type IV - all Zone 1 crystals (after Ref. 10).

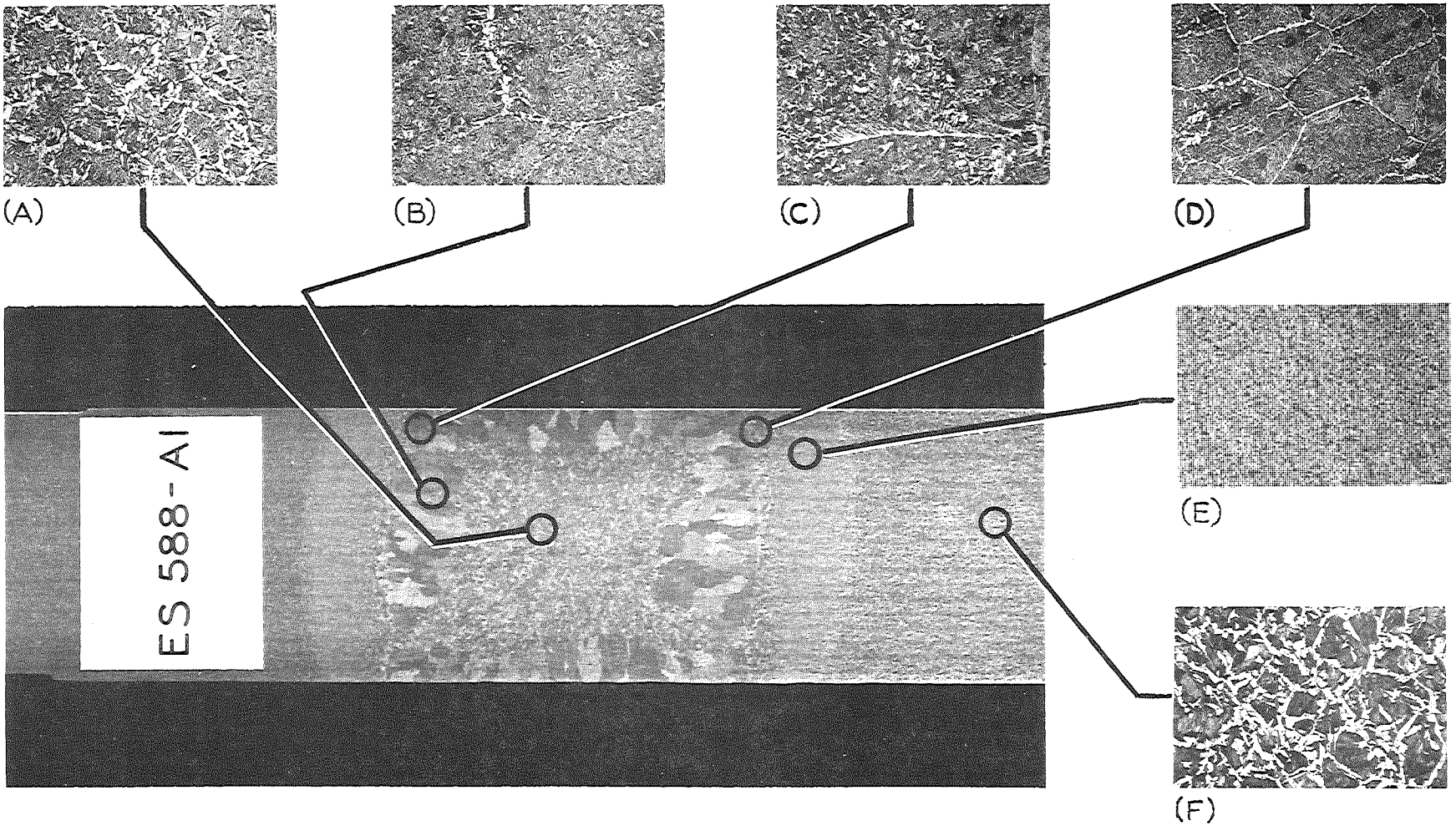

Figure 20. Cooled shoe electroslag weld by Fabricator A on 1-3/4-in. A 588 steel. Microstructures shown are: A) Zone 1 weld metal, B) Zone 2 weld metal, C) fusion line (HAZ 1 on right), D) HAZ 1 beyond the fusion line, E) HAZ 2, F) unaffected base metal. (Microstructures at 100x, etchant 3 percent nital.)

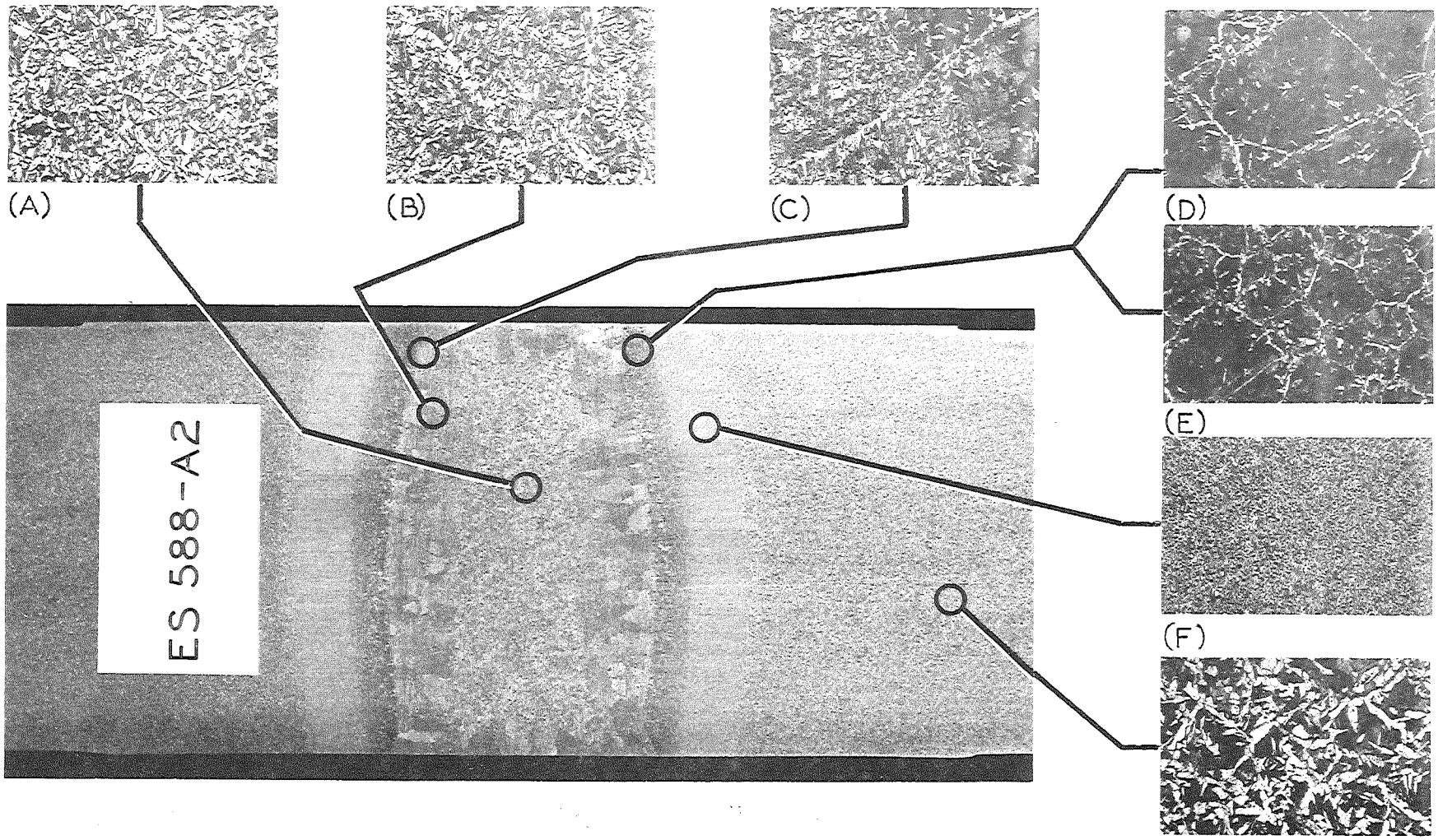

Figure 21. Cooled shoe electroslag weld by Fabricator A on 3-in. A 588 steel. Microstructures shown are: A) Zone 1 weld metal, B) Zone 2 weld metal, C) fusion line (HAZ 1 on right), D) HAZ 1 just beyond fusion line, E) HAZ 1 further out, F) HAZ 2, G) unaffected base metal. (Microstructures at 100x, etchant 3 percent nital.)

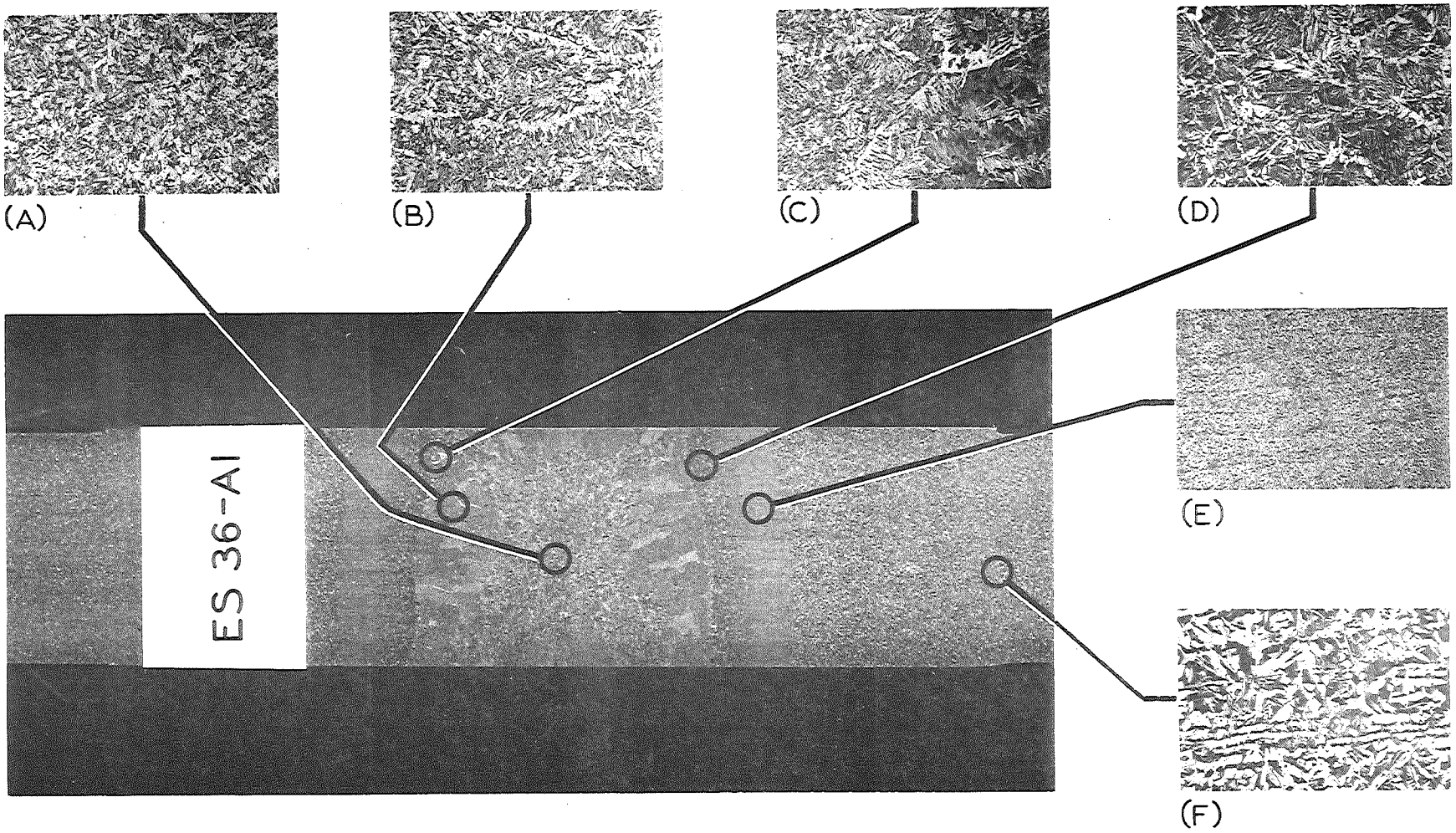

Figure 22. Cooled shoe electroslag weld made by Fabricator A on 1-3/4-in. A 36 steel. Microstructures shown are: A) Zone 1 weld metal, B) Zone 2 weld metal, C) fusion line (HAZ 1 on right), D) HAZ 1 beyond fusion line, E) HAZ 2, F) unaffected base metal. (Microstructures at 100x, etchant 3 percent nital.)

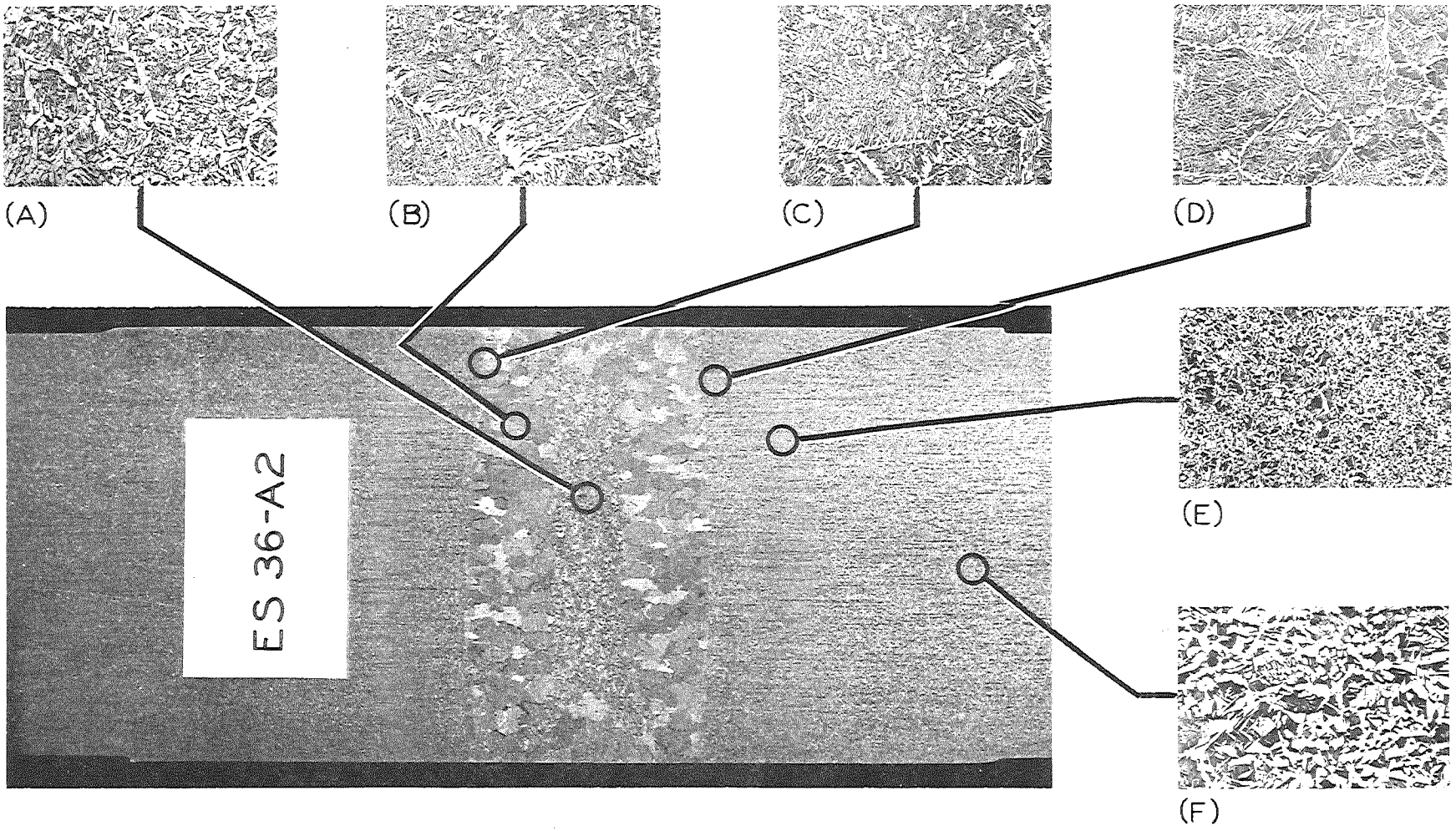

Figure 23. Cooled shoe electroslag weld by Fabricator A on 3-in. A 36 steel. Microstructures shown are: A) Zone 1 weld metal, B) Zone 2 weld metal, C) fusion line (HAZ 1 on bottom), D) HAZ 1 beyond fusion line, E) HAZ 2, F) unaffected base metal. (Microstructures at 100x, etchant 3 percent nital.)

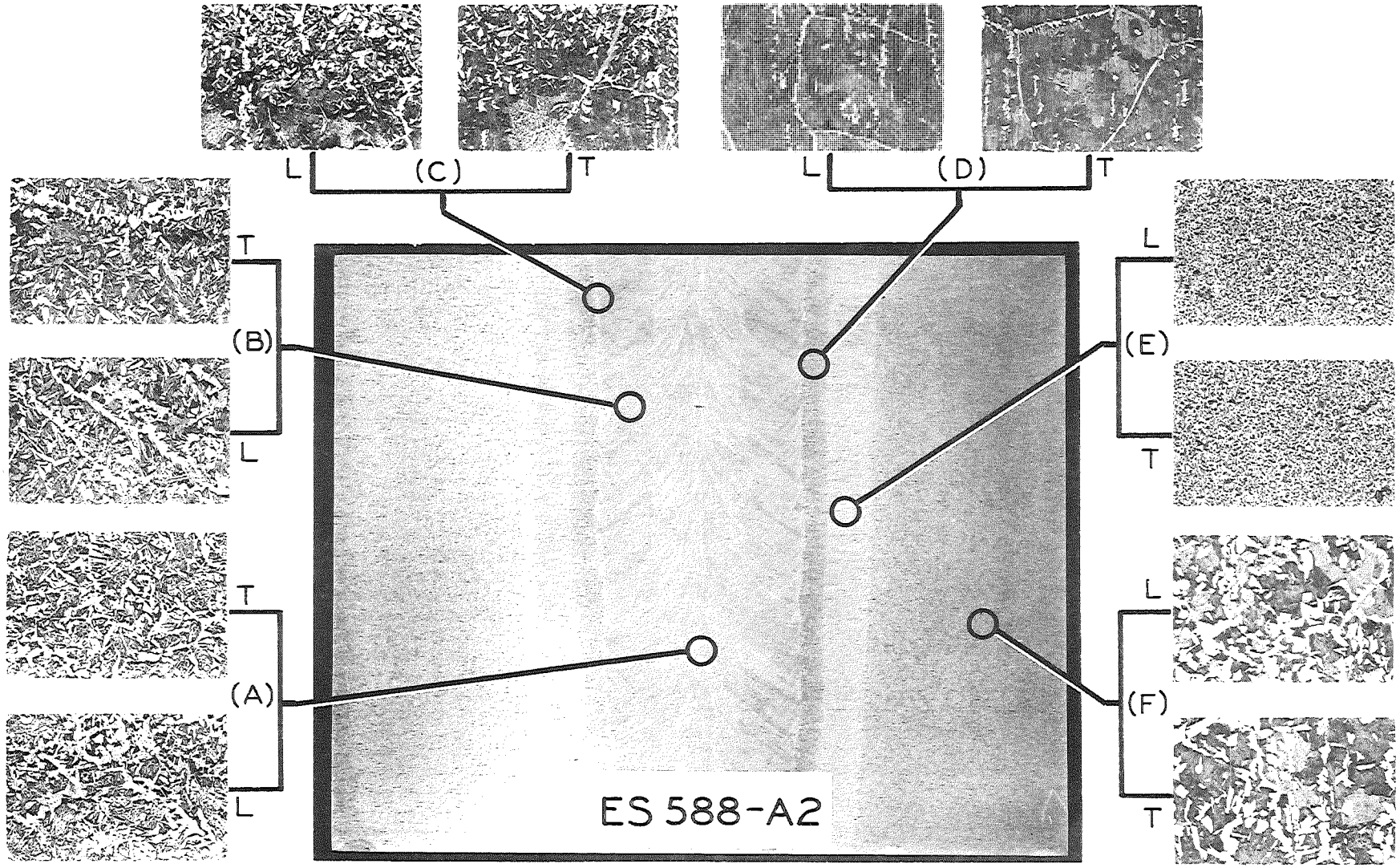

Figure 24. Typical mid-thickness longitudinal section through a cooled shoe electroslag weld by Fabricator A on 3-in. A 588 steel. (Microstructures marked "L" are taken in the longitudinal plane shown and "T" are in the transverse direction, i.e., normal to the plane of the page.) A) Zone 1 weld metal, B) Zone 2 weld metal, C) fusion line (HAZ 1 on bottom), D) HAZ 1, E) HAZ 2, F) unaffected base metal. (Microstructures at 100x, etchant 3 percent nital.)

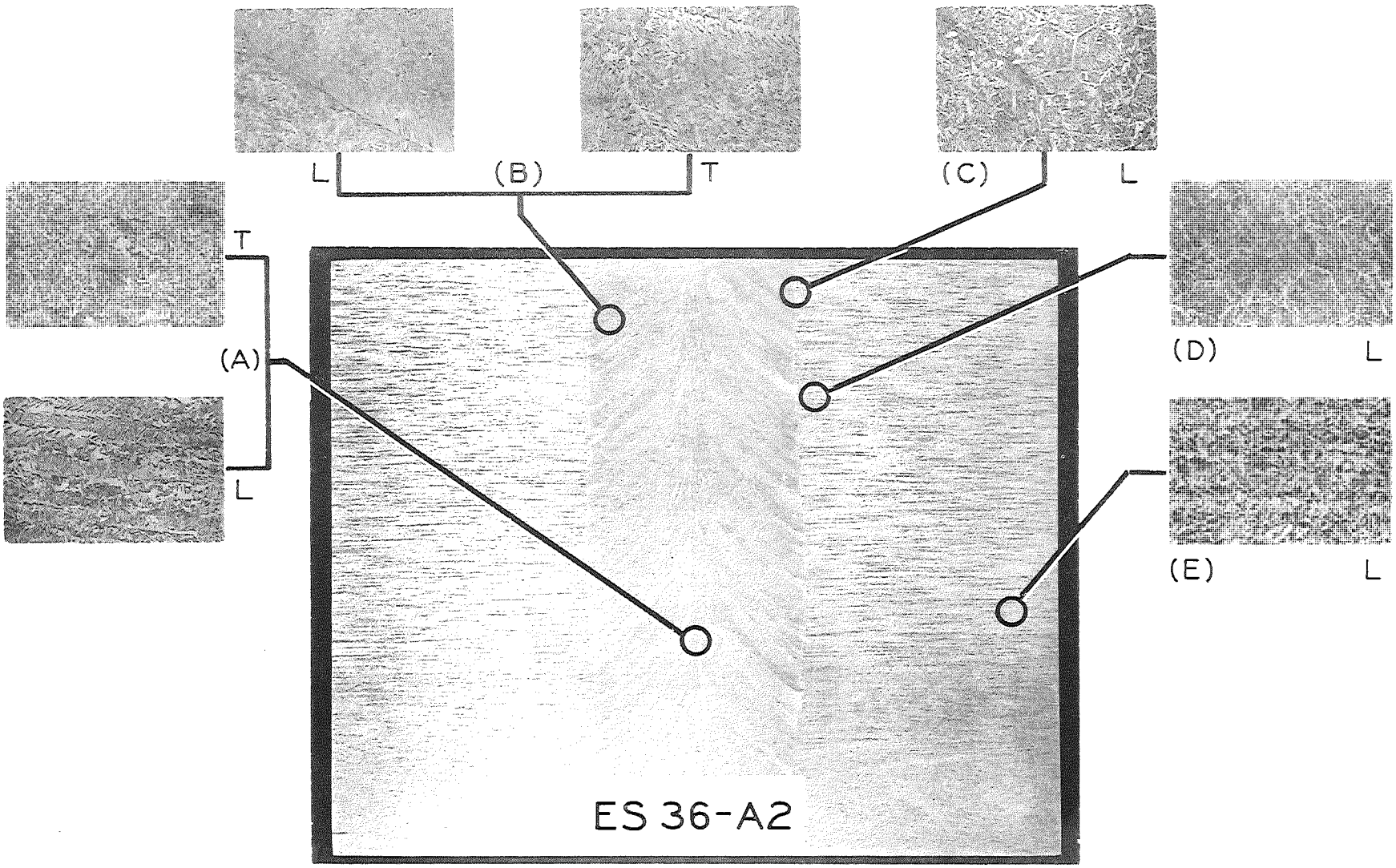

Figure 25. Typical mid-thickness longitudinal section through a cooled shoe electroslag weld by Fabricator A on 3-in. A 36 steel. (Microstructures marked "L" are taken in the longitudinal plane shown and "T" are in the transverse direction, i.e., normal to the plane of the page.) A) Zone 1 weld metal, B) Zone 2 weld metal, C) fusion line (HAZ 1 on right), D) HAZ 1 beyond fusion line, E) unaffected base metal. (Microstructures at 50x, etchant 3 percent nital.)

the longitudinal plane. Between the fusion line and the outlying base metal, two heat-affected zones appear. The first one, denoted as HAZ 1, appears dark in the macrosection and is a zone of grain coarsening as is shown in the accompanying microstructures. The grains in HAZ 1 decrease in size as the second heat-affected zone (denoted as HAZ 2) is approached. HAZ 2 appears light in the macrosection and is a zone of grain refinement. An etched section along a longitudinal plane at the surface of the weld, as seen in Figure 26, shows the Zone 2 weld metal as it occurs on the exposed surfaces of the welded plate after removal of the weld reinforcement. As in the midplane section, the coarse columnar grains along the fusion line are seen to point in the direction of welding. The coarse grains in the center region appear to be aligned almost parallel with the weld axis, but this occurs because 1/4 in. or more of the weld reinforcement deposited on the surface has been removed. Thus the figures are showing sectioned columnar grains of the same type seen angling up from the fusion line in the direction of welding.

Figures 27 through 30 are transverse sections illustrating the various electroslag weldments produced by Fabricator B using the dry shoe method. A much wider weld profile is seen in these cross-sections than in the cooled shoe weldments, as a result of the higher heat accumulation occurring in the dry shoe method. Additional widening of the weld contour occurs in the 3-in. thick weldments since they were made with the double stationary tube setup, which further increases the heat input over the single oscillating tube procedure. The dry shoe method is seen to produce Type I weldments containing fine and coarse columnar crystal zones and also Type III weldments in plates less than 2 in. thick, which contain only the coarse columnar Zone 2 (Figs. 27 and 29). The production of the Type III weldment is evidently due to the longer heat retention time occurring in a dry shoe electroslag weld. This long dwell time at temperatures above 1300 to 1400 F allow the coarse columnar grain zone to extend to the center of the weld. In the cooled shoe process, after the coarse grains have grown towards the center for some distance, the cooling rate accelerates and the remainder of the weld metal in the center solidifies in the fine columnar structure. This fine columnar structure is likewise produced in the central region of the 3-in. thick dry shoe weldments, but covers a much smaller area. In some instances, as shown in Figure 30 on weldment ES 36-B2, the Zone 1 weld metal region occurs over a very small region in the center of the weld and may appear and disappear intermittently along the length of the weld. Figures 31 and 32 show longitudinal sections taken at the mid-thickness of the plate (no such section was available for the Type III weldments). As before, the coarse columnar crystals are seen to deflect upwards from the fusion line in the direction of welding. Note that in both the cooled shoe

Figure 26. Typical longitudinal surface of the weld in cooled shoe electroslag weldments made by Fabricator A in 3-in., (A) A 588 steel and (B) A 36 steel.

Note: Vertical markings on the plate in the regions outside of the etched area are heat-affected zones resulting from the attachment of the strong-back plates. The zones are still present with nearly 1/4 in. of plate removed.

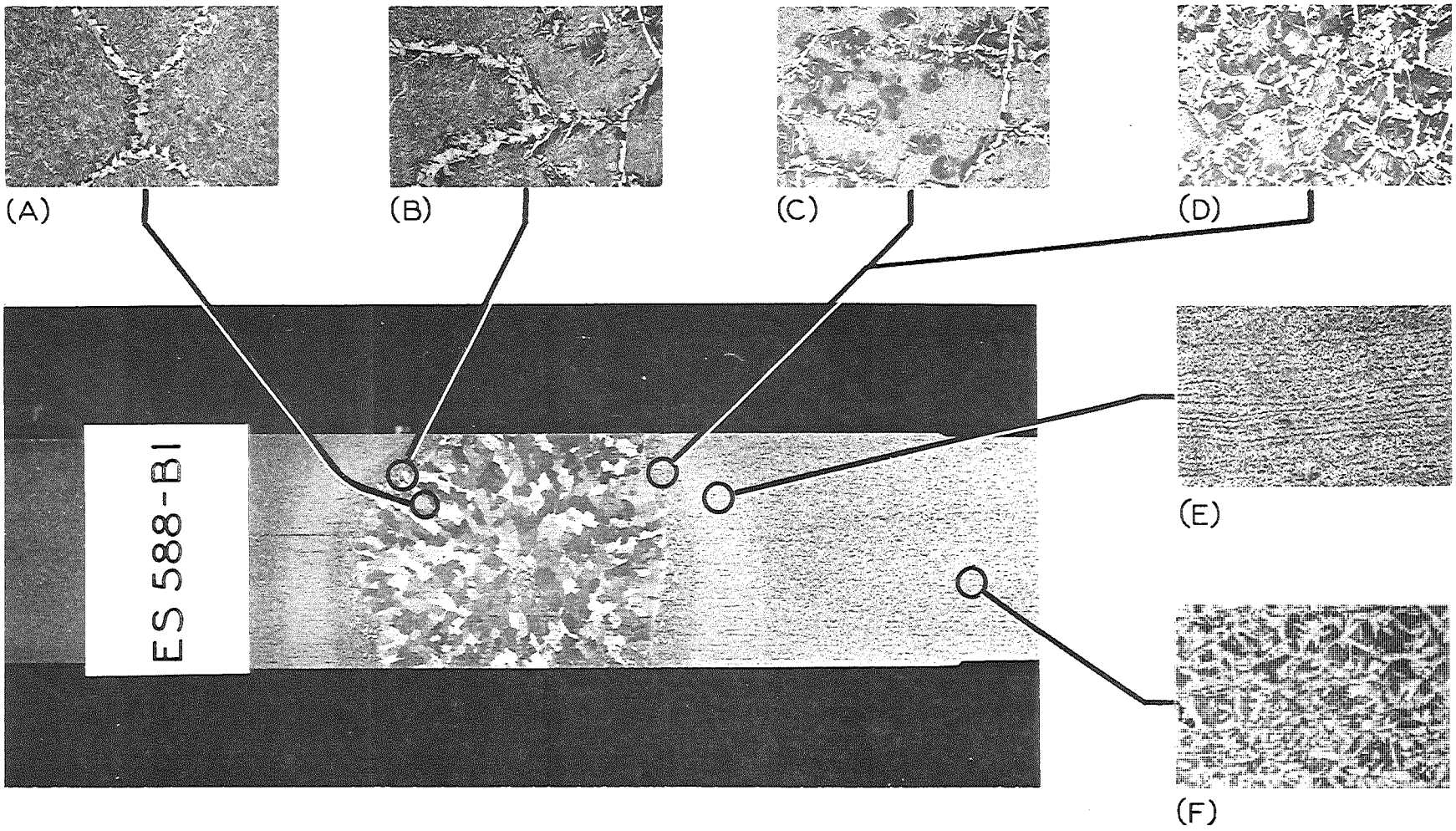

Figure 27. Dry shoe weld made by Fabricator B on 1-3/4-in. A 588 steel. Microstructures shown are: A) Zone 2 weld metal, B) fusion line (HAZ 1 on right), C) HAZ 1 next to fusion line, D) HAZ 1 further out, E) HAZ 2, F) unaffected base metal. (Microstructures at 100x, etchant 3 percent nital.)

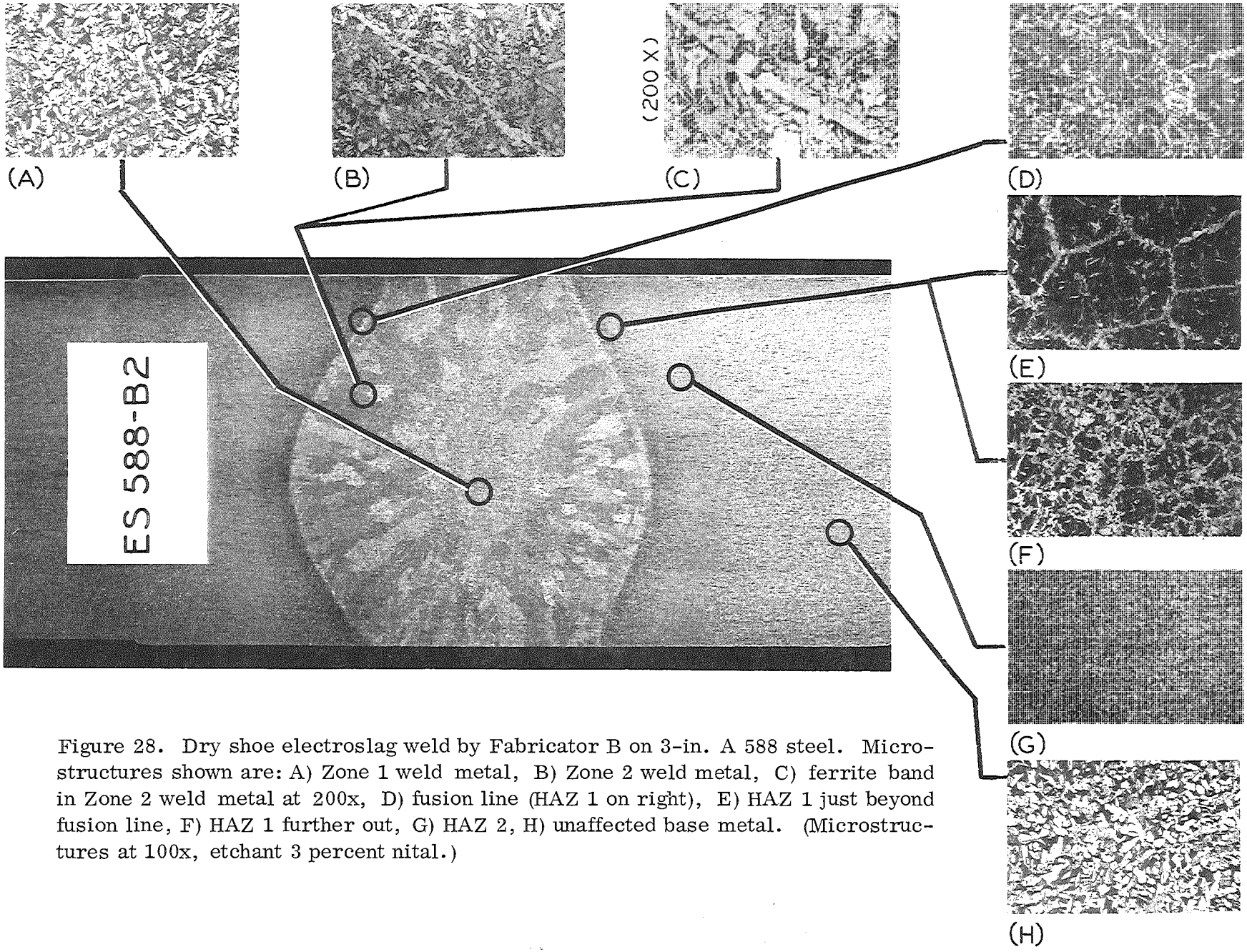

Figure 28. Dry shoe electroslag weld by Fabricator B on 3-in. A 588 steel. Microstructures shown are: A) Zone 1 weld metal, B) Zone 2 weld metal, C) ferrite band in Zone 2 weld metal at 200x, D) fusion line (HAZ 1 on right), E) HAZ 1 just beyond fusion line, F) HAZ 1 further out, G) HAZ 2, H) unaffected base metal. (Microstructures at 100x, etchant 3 percent nital.)

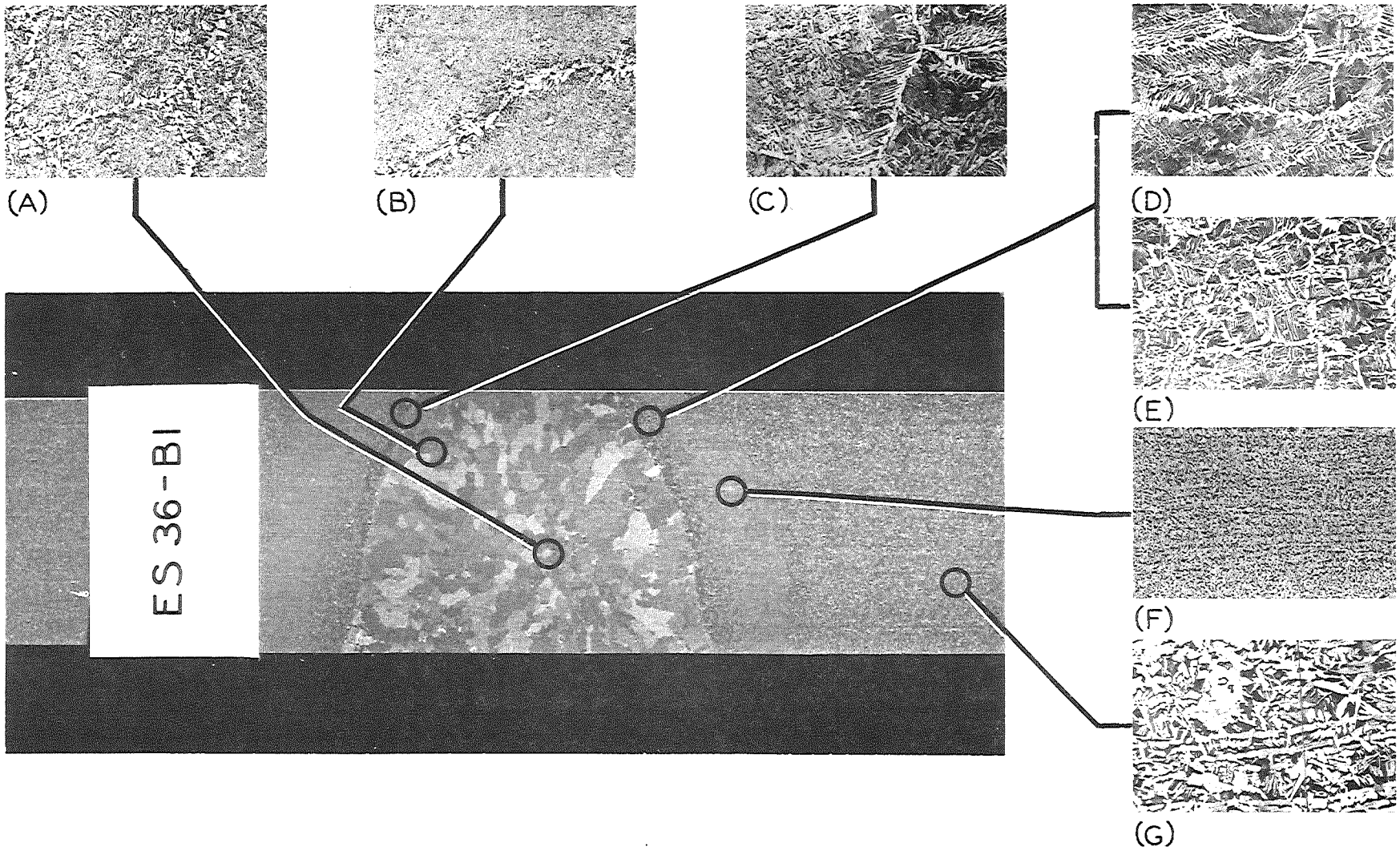

Figure 29. Dry shoe electroslag weld made by Fabricator B on 1-3/4-in. A 36 steel. Microstructures shown are: A) Zone 2 weld metal in center, B) Zone 2 weld metal near edge, C) fusion line (HAZ 1 on the right), D) HAZ 1 beyond fusion line, E) HAZ 1 further out, F) HAZ 2, G) unaffected base metal. (Microstructures at 100x, etchant 3 percent nital.)

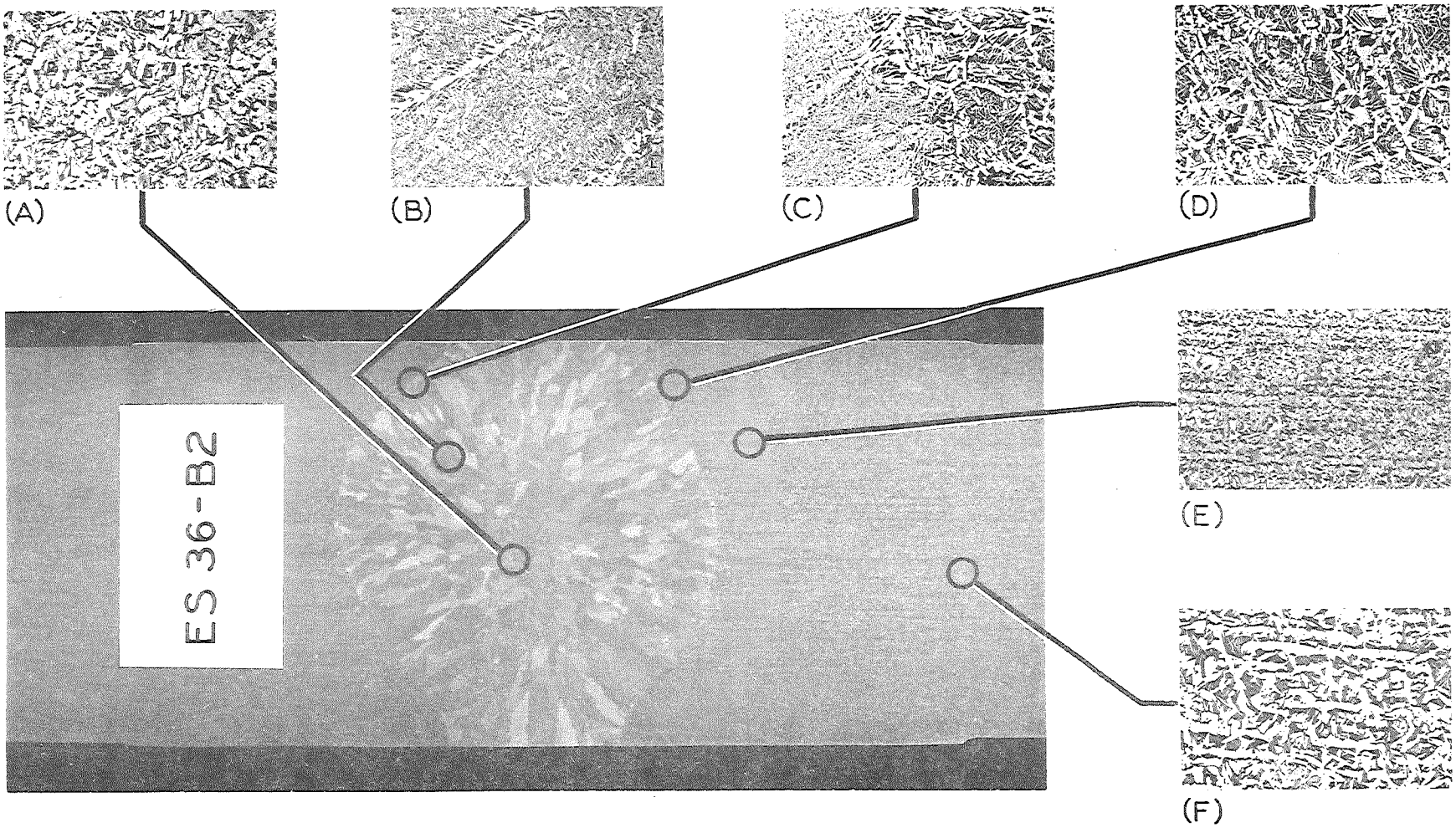

Figure 30. Dry shoe electroslag weld made by Fabricator B on 3-in. A 36 steel. Microstructures shown are: A) Zone 1 weld metal, B) Zone 2 weld metal, C) fusion line (HAZ 1 on right), D) HAZ 1 beyond fusion line, E) HAZ 2, F) unaffected base metal. (Microstructures at 100x, etchant 3 percent nital.)

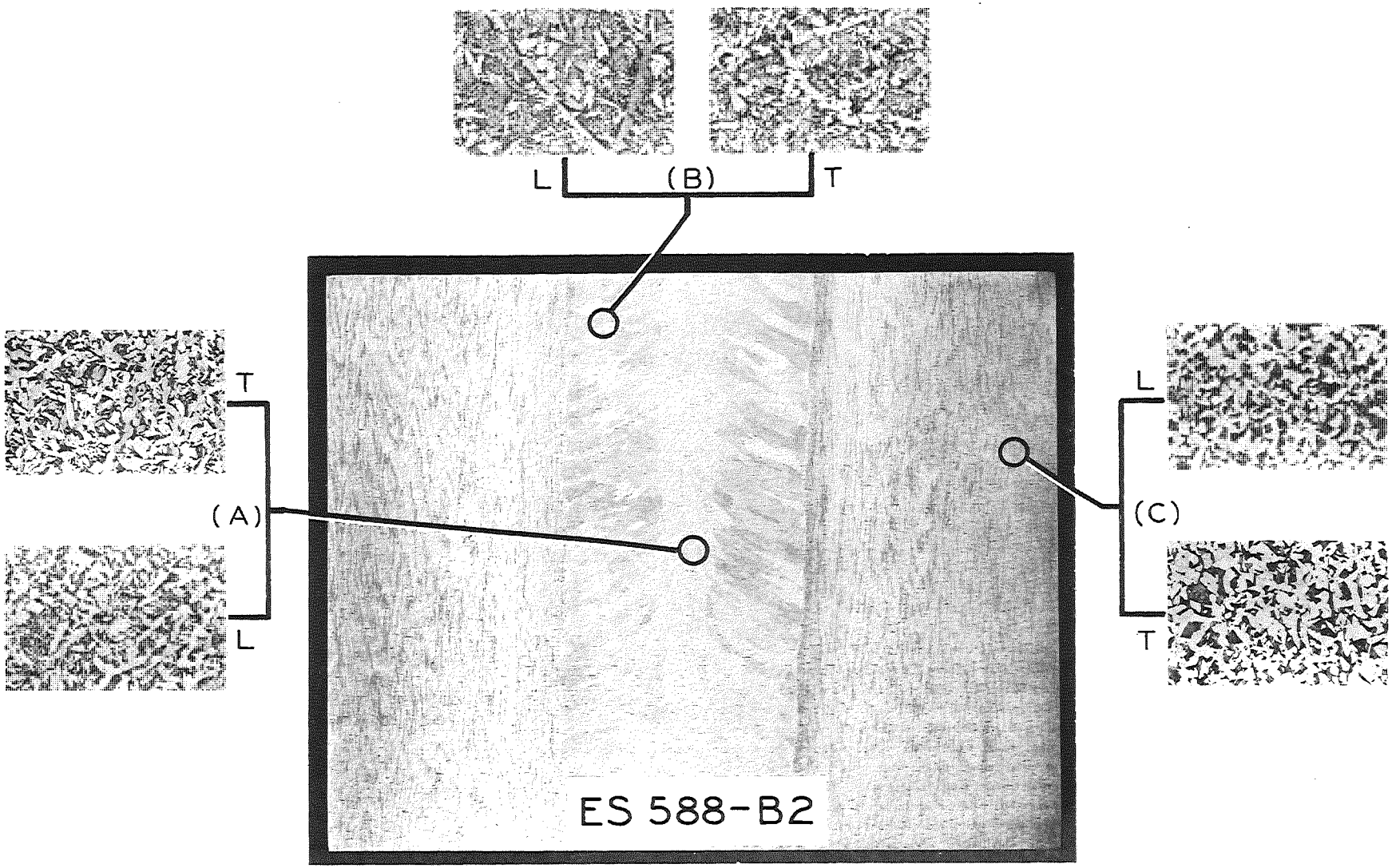

Figure 31. Typical mid-thickness longitudinal section through a dry shoe electroslag weld by Fabricator B on 3-in. A 588 steel. (Microstructures marked "L" are taken in the longitudinal plane shown and "T" are in the transverse direction, i.e., normal to the plane of the page.) A) Zone 1 weld metal, B) Zone 2 weld metal, C) unaffected base metal. (Microstructures at 100x, etchant 3 percent nital.)

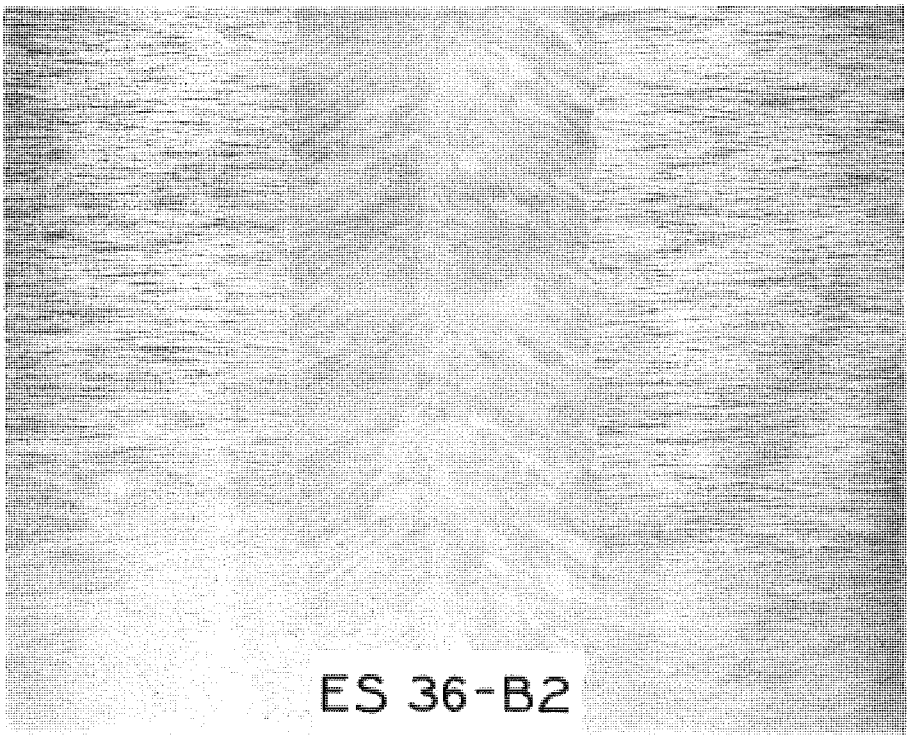

Figure 32. Typical mid-thickness longitudinal section through a dry shoe electroslag weldment by Fabricator B on 3-in. A 36 steel.

and the dry shoe welds produced for this project, the angle at which the Zone 1 (and Zone 2) crystals meet at the center is acute, thus indicating a relatively shallow weld pool (high form factor) and a resulting high resistance to intergranular cracking. Because of the favorable form factor achieved, no such cracking was encountered in the weldments produced. The heat-affected zones produced in the dry shoe weldments are seen to be the same HAZ 1 with grain coarsening and HAZ 2 with grain refinement that occur in the cooled shoe weldments. The main discernable differences between the dry and cooled shoe weldments appears to be the enlargement of the weld profile and the occurrence of a Type III weldment in the thinner sections with the dry shoe method or a Type IV weldment in thin sections with the cooled shoe method. Figure 33 shows two etched sections along the longitudinal surface of the dry shoe weldments. Note how the weld profile will meander along the plate as the heat accumulation fluctuates. Without the continual extraction of heat provided by the water cooled shoes, the weld profile is hard to control.

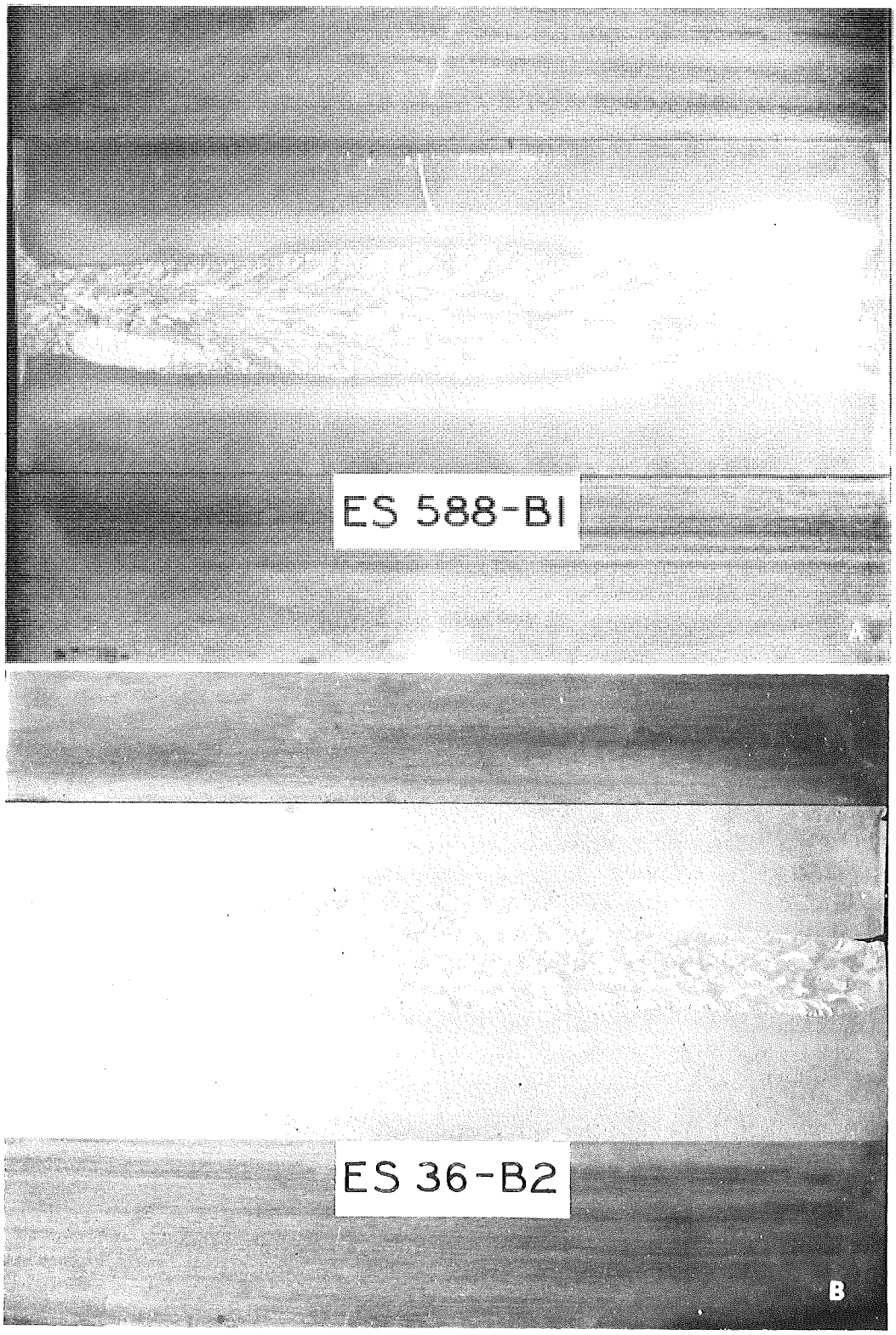

Figure 33. Typical longitudinal surface of the weld in dry shoe electroslag weldments made by Fabricator B in: A) 1-3/4-in. A 588 steel, B) 3-in. A 36 steel (see Fig. 12 on lack-of-fusion defect).

The primary structures of the electroslag weldments are typical of structures formed in the casting of low alloy steels. Due to the slower cooling experienced in the dry shoe method, the coarse columnar crystal region becomes larger than the cooled shoe method, covering the entire joint in plates under 2 in. thick. The growth of these large crystals progresses as long as the weld metal is kept above the lower transformation temperature (around 1350 to 1400 F), i.e., in the recrystallization region. As noted before, the crystal growth proceeds in line with the direction of heat flow from the weld pool, which is normal to the solid-liquid interface. This is why the weld pool shape is so important in getting proper crystal orientation. The Zone 1, fine columnar crystals that appear in the center of Type I weldments are oriented nearly aligned with the weld axis in the weldments produced for this study. Figure 25(a) illustrates the needlelike nature of the fine columnar crystals found in Zone 1 weld metal. The microstructure in the longitudinal plane reveals the length of the crystal, and that in the transverse plane reveals their cross-sectional shape. (It will be shown that this crystal orientation explains why Zone 1 weld metal has lower Charpy impact strength than the Zone 2 weld metal when tested in the standard direction, across the plate.) The orientation of the Zone 1 crystals coincides with the direction of heat flow, down from the bottom of a shallow weld pool. Zone 1 weld metal has a much shorter dwell time at temperatures in the recrystallization region than Zone 2 weld metal. Thus, the columnar crystals produced are quite fine in cross-section as compared to those found in Zone 2. In the microstructures shown, the prior austenite grain boundaries (i.e., primary structures) are seen as a network of ferrite bands. This occurs because ferrite is deposited on the austenite grain boundaries just as the transformation at the lower transformation temperature (1350 to 1400 F) begins. On a longitudinal plane (Figs. 24 and 25) ferrite is seen to grow at an angle to the prior austenite boundary in long, acicular strands. These strands also appear on the transverse sections but are not as massive and are oriented at nearly right angles to the ferrite bands. These strands are more pronounced in the A 36 steel than in the A 588, which is probably due to the A 588 being closer to the eutectoid composition with all the additional alloying elements it contains. The role of the ferrite strands in crack propagation and the mechanism of their formation is not clear. However, the ferrite bands that outline the prior austenite grain boundaries do offer a path of least resistance for a propagating crack, which leads to an intergranular type of failure through these zones. A continuous fracture path is provided for long distances throughout the zones with these ferrite bands. Crack propagation along this ferrite network requires far less energy than that required for a transgranular failure. As will be seen later, the orientation of the bands (or primary crystal boundaries) greatly influences the impact strength of the weld metal.

The secondary structure (i.e., the size and distribution of the ferrite and pearlite within the primary crystal boundaries) of the electroslag weld metal zones is seen in the microstructures as consisting of pearlite (dark areas) surrounded by ferrite (light) distributed in a Widmanstatten pattern, and grain boundary ferrite. This Widmanstatten ferrite is characterized by its acicular or needlelike, spiny appearance and is a nonequilibrium phase that is characteristic of a cast metal. The secondary structure appearing in Zone 1 weld metal is usually considerably coarser than that occurring in Zone 2 weld metal as is illustrated in Figures 23, 28, and 30. This is due to the formation of larger deposits of ferrite in Zone 1 as a result of the slower cooling rate that it experiences below the austenite transformation temperature. Note in Figure 29, a dry shoe electroslag weldment in 1-3/4 in. A 36 steel, that a well defined Zone 1 does not appear in the macrostructure. However, the secondary transformation products seen in the Zone 2 weld metal from the center of the weld are coarser than those seen in Zone 2 near the edge. This type of weld structure is commonly produced by the dry shoe method on plates less than 2 in. thick and Zone 1 weld metal can appear and disappear intermittently along the length of the weld.

The heat-affected zones that are produced in the base metal beyond the fusion line are similar for both the dry shoe and cooled shoe electroslag weldments. The first zone, denoted as HAZ 1, is seen to be a region of grain coarsening as illustrated in the macro and microstructures of Figures 20 through 25, and 27 through 32. As in the weld metal, grain boundary ferrite displays the large prior austenite grain size produced in HAZ 1 by the overheating experienced during welding. This grain size decreases steadily as you move away from the fusion line. Note in Figures 24 and 25 that the longitudinal sections of the heat-affected zones show that they are equiaxed. The secondary structure of the HAZ 1 is pearlite (dark areas) with an acicular ferrite distribution. Comparing the structure of HAZ 1 with the heat-affected zone produced by the submerged arc process (Figs. 14 through 17) we see that this grain coarsening is one of the major metallurgical problems encountered in electroslag welding. Even if modifying agents are used in the weld metal to refine its structure, the grain coarsening of HAZ 1 can only be eliminated through postweld heat treatment. The second heat-affected zone, denoted as HAZ 2, is seen in Figures 20 through 25, and 27 through 32 to be a zone of grain refinement as compared to the base metal. This structure appears to be a normalized base metal with a fine dispersion of pearlite and ferrite. HAZ 2 presents no problems, at least in the low alloy steels tested, and in most cases shows a marked improvement over base metal in impact strength. The hardness in HAZ 2 is slightly lower than that of base metal indicating a possible small reduc-

tion in the yield strength. The grain structures produced in HAZ 1 and HAZ 2 had no deleterious effect on the static or impact properties of the two base metals evaluated in this study. They could, however, have a profound effect on the properties of higher strength, high alloy, or quenched and tempered steels. Some effect is seen in the HAZs on the fatigue properties of the steel and these will be discussed later.

The metallurgical structures shown for the various electroslag weldments give rise to many problems in electroslag weld metal. The distribution and orientation of the fine and coarse columnar crystals produce significant nonhomogeneities and anisotropies in the mechanical properties of the weld. Chemical segregation in these structures is also a potential threat. During solidification, solute elements are rejected by the solidifying iron-rich phase into the surrounding liquid. This leads to high alloy impurities, or carbon concentrations in the interdendritic regions of the solidified mass. If these segregated elements are not completely diffused during the remainder of the cooling cycle, dendritic segregation will be present in the final structure. No investigation of microsegregation of alloying elements was undertaken by this project, but such work needs to be done. Dendritic segregation, which is a common occurrence in steel castings, could be present in electroslag weld metal and would exert an influence on its mechanical and corrosion properties. Another place for alloy segregation to occur is at the ferrite network that outlines the prior austenite grain boundaries. The manner in which this ferrite is deposited does give rise to microsegregation which should be quantitatively assessed. The ferrite bands are preferentially followed by a propagating crack, as will be seen in the impact and fatigue testing, and uncontrolled segregation along the bands could further influence their role in failure.

Chemistry of Weld Metal

In a submerged arc weldment produced by a multipass technique, the dilution of the weld metal by the base metal is low and occurs mainly along the edge of the fusion line. Thus, weld metal chemical composition is controlled mainly by the filler metal used. In the electroslag welding process, the high heat input spreads the fusion area to the extent that the weld metal is diluted by 40 to 60 percent with base metal throughout the entire cross-section of the weld. Even in the thinner plates produced for this project, dilution rates ran about 50 percent. Due to this high dilution, the resulting weld metal chemistry in electroslag weldments is highly dependent on the base metal chemistry. Hence, in electroslag welding, the weld metal chemistry cannot be controlled without carefully controlling the base metal chemistry.

The alloy chemistry of the various submerged arc weldments, electroslag weldments, and welding electrodes are listed in Tables 3 through 6. The percent compositions listed for the submerged arc weldments in Tables 3 and 4 represent values determined from samples of weld metal, and values reported for base metal in the mill analyses, which were verified by check analyses on the base plates. In Tables 5 and 6 for electroslag weldments, values are listed for both Zone 1 and Zone 2 weld metal when both zones occurred in the weld, and for base metal from the mill analyses, which were verified by check analyses. Table 7 lists the typical analyses of the various welding electrodes as published by the manufacturers. Check analyses were not run on the electrode wires. Compositions of the various fluxes were not available since they are proprietary mixtures. In general, fluxes will usually add manganese and silicon and sometimes copper, chromium, and vanadium to the deposited weld metal.

The chemical compositions that are reported here are average alloy concentrations as determined by macroscopic quantitative analysis. They do not give any indication of the manner in which the various elements are dispersed throughout the microstructure. Note that on this macroscopic scale, Zone 1 and Zone 2 weld metal in the electroslag weldments have virtually identical alloy compositions. This is a significant fact because it implies that the different grain structures produced in the two weld metal zones must be primarily a function of the different cooling cycles experienced and not due to a difference in alloy composition. Analyses were also run on HAZ 1 and HAZ 2 found in electroslag weldments and their compositions are identical to base metal. Thus, even though a significant amount of grain coarsening occurs in HAZ 1 due to overheating, no measurable diffusion of alloy elements takes place (on the macroscopic scale).

The type of cast structures present in electroslag weld metal do lead to alloy segregation on the microscopic level. No equipment was available in the laboratory for exploration of such segregation, but previous investigation (12) has shown that at the ferrite bands in Zone 2 weld metal, low carbon and high manganese and sulfur concentrations can occur. Microhardness measurements conducted in this project reveal that the softest ferrite is found in the prior austenite grain boundaries, indicating a chemical variation there. This type of chemical segregation within the microstructure can have a deleterious effect on the mechanical and corrosion properties of the electroslag weld metal. The occurrence and effects of alloy microsegregation in electroslag weldments needs to be carefully investigated, especially when the deposited weld metal is placed in an unpainted exposure of ASTM A 588 steel.

TABLE 3
CHEMICAL COMPOSITIONS OF SUBMERGED ARC WELDMENTS IN A 588 STEEL

Weldment Type (See Table 1)	Typical Analysis (weight, percent)										Electrode/Flux Type
	C	Mn	P	S	Si	Ni	Cr	Cu	V	Al	
SA 588-A1											
Weld Metal	0.07	1.70	0.025	0.019	0.76	0.66	0.49	0.42	0.02	0.03	Raco 815/
Base Metal	0.17	1.17	0.006	0.026	0.24	0.18	0.56	0.30	0.05	0.04	Lincoln 780
SA 588-A2											
Weld Metal	0.07	1.54	0.026	0.019	0.74	0.72	0.47	0.48	0.02	0.03	Raco 815/
Base Metal	0.19	1.14	0.015	0.022	0.22	0.15	0.54	0.32	0.05	0.04	Lincoln 780
SA 588-B1											
Weld Metal	0.08	1.48	0.030	0.02	0.56	0.10	0.18	0.20	0.02	0.02	Linde 81/
Base Metal	0.13	1.00	0.012	0.02	0.25	0.39	0.61	0.32	0.04	0.01	Linde 124
SA 588-B2											
Weld Metal	0.05	2.06	0.030	0.023	1.20	0.01	0.07	0.18	0.02	0.03	Linde 81/
Base Metal	0.18	1.15	0.014	0.022	0.23	0.13	0.53	0.31	0.05	0.03	Linde 124
Specified Weld Metal Composition Range [1]	0.12 max.	0.50/ 1.10 [2]	0.03 max.	0.04 max.	0.35/ 0.80	0.40/ 0.80	0.45/ 0.70	0.30/ 0.75	0.05 max. [3]		

[1] MDSHT Supplemental Specifications for Welding Structural Steel (13), for unpainted exposures.
[2] AWS D1.1-72 requires 0.50/1.30 Mn.
[3] Applies only when postweld heat-treated is required.

TABLE 4
CHEMICAL COMPOSITIONS OF SUBMERGED
ARC WELDMENTS IN A 36 STEEL

Weldment Type (See Table 1)	Typical Analysis (weight, percent)[1]							Electrode/Flux Type
	C	Mn	P	S	Si	Cu	V	
SA 36-A1								
Weld Metal	0.08	1.76	0.032	0.014	0.84	0.38	0.02	Lincoln L-60/
Base Metal	0.21	1.00	0.012	0.020	0.22	0.05	0.01	Lincoln 780
SA 36-A2								
Weld Metal	0.06	1.39	0.031	0.013	0.63	0.08	0.02	Lincoln L-60/
Base Metal	0.23	1.07	0.012	0.018	0.23	0.05	0.01	Lincoln 780
SA 36-B1								
Weld Metal	0.10	1.61	0.023	0.019	0.70	0.11	0.01	Linde 81/
Base Metal	0.21	1.00	0.012	0.020	0.22	0.05	0.01	Linde 124
SA 36-B2								
Weld Metal	0.08	1.54	0.021	0.018	0.65	0.13	0.01	Linde 81/
Base Metal	0.23	1.07	0.012	0.018	0.23	0.05	0.01	Linde 124

[1] No specification on weld metal composition, except 0.05 max. V when post weld heat-treatment is required.

The Michigan Specification (13) for welding on A 588 steel to be used in an unpainted exposure requires the weld metal to possess the following chemical composition: 0.12 max carbon, 0.50 - 1.10 manganese, 0.03 max phosphorus, 0.04 max sulfur, 0.35 - 0.80 silicon, 0.40 - 0.80 nickel, 0.45 - 0.70 chromium, 0.30 - 0.75 copper. The specification found in AWS D2.0-69 (1) requires only that the "deposited weld metal" possess corrosion resistance and coloring characteristics similar to those of the base metal and that the manufacturer's recommendations be followed. The AWS Structural Welding Code D1.1-Rev. 74 requires a "filler material" chemical composition identical to the Michigan specification on weld metal with the exception of a manganese range of 0.50 - 1.30. The AWS Code has no requirement on the resulting weld metal that appears in the finished weldment.

Analysis of the compositions listed for submerged arc welding in Table 3 reveals that all the welds placed in A 588 steel have an excessive amount of manganese. A manganese content in excess of 1.6 percent is considered to have a detrimental effect on the notch toughness of submerged arc weld metal (14). Thus, even though all the weld metals exceed the specification of 1.10 maximum manganese, welds SA 588-A1 and SA 588-B2 are the most likely to suffer low notch toughness, since they exceed 1.60 manganese.

TABLE 5
CHEMICAL COMPOSITION OF ELECTROSLAG WELDMENTS IN A 588 STEEL

Weldment Type (See Table 2)	Typical Analysis (weight, percent)										Electrode/Flux Type
	C	Mn	P	S	Si	Ni	Cr	Cu	V	Al	
ES 588-A1											
Zone 1 Weld Metal	0.15	1.20	0.018	0.021	0.39	0.06	0.26	0.15	0.02	0.01	Hobart 25P/ Hobart PF 201
Zone 2 Weld Metal	0.16	1.19	0.017	0.021	0.41	0.07	0.25	0.15	0.03	0.01	
Base Metal	0.17	1.17	0.006	0.026	0.24	0.18	0.56	0.30	0.05	0.04	
ES 588-A2											
Zone 1 Weld Metal	0.15	1.18	0.019	0.018	0.42	0.05	0.18	0.12	0.02	0.01	Hobart 25P/ Hobart PF 201
Zone 2 Weld Metal	0.15	1.20	0.019	0.017	0.45	0.06	0.20	0.13	0.02	0.01	
Base Metal	0.19	1.14	0.015	0.022	0.22	0.15	0.54	0.32	0.05	0.04	
ES 588-B1											
Zone 2 Weld Metal	0.14	1.29	0.012	0.020	0.22	0.20	0.35	0.20	0.03	0.01	Linde 36/ Linde 124
Base Metal	0.13	1.00	0.012	0.020	0.25	0.39	0.61	0.32	0.04	0.01	
ES 588-B2											
Zone 1 Weld Metal	0.12	1.28	0.015	0.020	0.30	0.09	0.28	0.19	0.03	0.01	Linde MC-70/ Linde 124
Zone 2 Weld Metal	0.13	1.30	0.013	0.021	0.31	0.09	0.32	0.20	0.03	0.01	
Base Metal	0.18	1.15	0.014	0.022	0.23	0.13	0.53	0.31	0.05	0.03	
ES 588-B2a											
Zone 2 Weld Metal	0.16	0.92	0.006	0.026	0.25	0.30	0.52	0.37	0.04	0.01	Linde WS/ Linde 124
Base Metal	0.16	1.23	0.011	0.016	0.28	----	0.56	0.32	0.06	----	
Specified Weld Metal Composition Range [1]	0.12 max.	0.50/ 1.10 [2]	0.03 max.	0.04 max.	0.35/ 0.80	0.40/ 0.80	0.45/ 0.70	0.30/ 0.75	0.05 max. [3]		

[1] MDSHT Supplemental Specifications for Welding Structural Steel (13), for unpainted exposures.
[2] AWS D1.1-72 requires 0.50/1.30 Mn.
[3] Applies only when post weld heat-treatment is required.

In addition, weld SA 588-B2 exceeds the silicon limitation by a considerable amount. It has been established that silicon in amounts greater than 0.60 percent is usually detrimental to the notch toughness. Weldments SA 588-B1 and SA 588-B2 are seen to be deficient in nickel, chromium, and copper which are some of the main elements required to give the weld metal the enhanced corrosion resistance required of A 588 steel. These deficiencies can produce a lighter colored rusting of the weld metal in an unpainted exposure and create a potential for accelerated corrosion of the weld (15). Also, nickel improves weld metal notch toughness, so these deficiencies may lower the toughness of the weld (14).

TABLE 6
CHEMICAL COMPOSITIONS OF ELECTROSLAG WELDMENTS IN A 36 STEEL

Weldment Type (See Table 2)	Typical Analysis (weight, percent) [f]							Electrode/Flux Type
	C	Mn	P	S	Si	Cu	V	
ES 36-A1								
Zone 1 Weld Metal	0.14	1.10	0.019	0.021	0.41	0.05	0.01	Hobart 25P/ Hobart PF 201
Zone 2 Weld Metal	0.15	1.11	0.017	0.020	0.38	0.05	0.01	
Base Metal	0.21	1.00	0.012	0.020	0.22	0.05	0.01	
ES 36-A2								
Zone 1 Weld Metal	0.14	1.10	0.018	0.022	0.40	0.05	0.01	Hobart 25P/ Hobart PF 201
Zone 2 Weld Metal	0.14	1.12	0.017	0.020	0.40	0.05	0.01	
Base Metal	0.23	1.07	0.012	0.018	0.23	0.05	0.01	
ES 36-B1								
Zone 2 Weld Metal	0.17	1.34	0.016	0.016	0.22	0.06	0.01	Linde 36/ Linde 124
Base Metal	0.21	1.00	0.012	0.020	0.22	0.05	0.01	
ES 36-B2								
Zone 2 Weld Metal	0.16	1.28	0.016	0.016	0.28	0.01	0.01	Linde MC-70/ Linde 124
Base Metal	0.23	1.07	0.012	0.018	0.23	0.05	0.01	

[f] No specification on weld metal composition, except 0.05 max. V when post weld heat-treatment is required.

There is no specified composition range on weld metal in ASTM A 36 steel. High manganese and silicon levels as seen in Table 4 for weld SA 36-A1 can have the same effect of lowering the notch toughness of the weld metal. Since A 36 steel is never used in the unpainted condition, nickel and chromium are not normally added to the composition and copper up to about 0.50 percent will exert little influence on strength or toughness (14).

Table 5 gives a listing of the compositions found in all the various A 588 steel electroslag weldments tested. Note that in all but one case, the

carbon content of the weld metal exceeds the maximum limitation. This is undoubtedly due to the very high dilution of the weld metal with base metal. With increasing carbon content, carbides begin to form in the weld structure and this leads to a decrease in ductility and notch toughness. Small increases in carbon content lead to a sharp rise of the notch toughness transition temperature (14). All the weldments, except one, slightly exceed the limitation for manganese but are below the 1.6 percent point considered to be the maximum before notch toughness is lowered. Note that the electroslag weldments made by the dry shoe method used by Fabricator B all show a deficiency in silicon, being below the 0.35 percent minimum. Silicon is important as a deoxidizer in the weld metal and deficiencies such as those experienced here can lead to problems with porosity (14). Silicon is also very important in developing weld metal corrosion resistance and these deficiencies will adversely affect the weatherability of unpainted weld metal (15). No explanation is offered for the low silicon content of electroslag weldments produced by the dry shoe method, which also occurs in the A 36 weldments as shown in Table 6. (The Hobart 25P wire used in the cooled shoe electroslag welding is seen in Table 7 to have a high silicon content which accounts for the higher silicon content of the weldments by Fabricator A.) Adequate silicon should be picked up by the weld metal from the flux, as apparently happens in submerged arc welding. The electroslag process doesn't appear to pick up silicon in the same manner. The high heat accumulation and prolonged cooling cycle must adversely affect the pickup of silicon in the weld metal assuming that it is available in the flux. We see that with the exception of weldment ES 588-B2a which was produced with a special "weathering steel" wire and was deficient only in nickel, gross deficiencies in nickel, chromium, and copper exist in the electroslag deposited weld metal. As with the carbon, this seems to be a problem introduced by the high dilution of weld metal with base metal as well as a deficiency of these elements in the welding wires used. These deficiencies will decrease the corrosion resistance of the weld metals and the low nickel will be degrading to the notch toughness. Additional unknown effects may arise due to microsegregation of the deficient elements within the electroslag weld structure and the electrochemical potentials that may exist between the weld metal and the base metal at the fusion line. These factors could further degrade the corrosion resistance of unpainted weld metal. It is interesting to note here that the weldment ES 588-B2a that was made with the special weathering steel wire and had a composition most nearly in conformance with the specification, had very poor notch toughness. This underscores the fact that macrochemistry alone does not lead to good weldments in the electroslag process. The percentage of vanadium is seen to be quite low in the electroslag deposited weld metal. Slight increases in this element could have the beneficial effect of decreasing the ferrite grain size in the microstructure and thereby increasing the notch toughness (14).

TABLE 7
CHEMICAL COMPOSITIONS OF WELDING ELECTRODES

Electrode Type	Typical Manufacturers Analysis (weight, percent)								
	C	Mn	P	S	Si	Ni	Cr	Cu	V
Raco 815 [1]	0.09	0.52	0.020	0.034	0.26	0.50	0.50	0.32	----[2]
Lincoln L-60	0.07-0.15	0.35-0.60	0.018	0.027	0.045 max.			0.01	----
Linde 81	0.15	1.10	0.017	0.024	0.25			----	----
Linde 36	0.14	2.00	0.017	0.024	0.03			----	----
Linde MC-70 [3]	0.10	1.25	-----	-----	0.35	----	----	----	----
Linde WS	0.09	0.75	0.020	0.025	0.30	0.50	0.50	0.45	----
Hobart 25P	0.11	1.20	0.020	0.019	0.50	----	----	0.20 [4]	0.03 [4]

[1] Actual wire analyses have been found to vary considerably from these typical values advertised by the manufacturers.
[2] Dashes indicate that amount of the element is not specified. Blank spaces indicate that element is not present.
[3] As deposited in A 441 steel using Linde 124 flux and the submerged arc process.
[4] Added to the weld metal by the Hobart PF 201 running flux.

Table 6 shows that the electroslag weldments produced in A 36 steel also have carbon content excessively high for weld metal in all cases as a result of high base metal dilution. Again, note the low silicon content present in the weldments produced by the dry shoe method in comparison to the cooled shoe welds. As in A 588 steel, increasing the vanadium content would probably be beneficial in refining the secondary structure of the weld metal.

Tensile Properties of Weldments

The tensile properties and side bend test results for electroslag weldments are shown in Table 8 for A 588 steel and Table 9 for A 36 steel. Also listed in the tables are the specified yield strength, tensile strength, and elongation requirements for electroslag weld metal. The specifications require the deposited electroslag weld metal to match those properties required in the base metal being welded.

The only type of weldment that did not meet the minimum requirement on yield strength was ES 538-A2, which was the cooled shoe electroslag weldments produced in 3-in. A 588 steel. In this case, both Zone 1 and Zone 2 weld metal had yield strengths less than the required minimum of 50,000 psi, Zone 1 being the lowest of the two. Note that the general trend in all of the electroslag weldments is for Zone 1 to have a lower yield point

TABLE 8
TENSILE PROPERTIES AND BEND TEST RESULTS FOR ELECTROSLAG WELDMENTS IN A 588 STEEL

Weldment Type (See Table 2)	Yield Strength,[1] psi	Tensile Strength, psi	Elongation, percent, (2 in. gage)	Reduction of Area, percent	Guided Side Bend Test
Values Required by Specification [2]	50,000	70,000	21	--	
ES 588-A1					
Zone 1 Weld Metal	53,100	80,900	27	65	Pass
Zone 2 Weld Metal	54,200(2)[3]	82,400	29	51	Pass
Base Metal	66,700	95,200	22	--	
ES 588-A2					
Zone 1 Weld Metal	47,400(2)	76,400	32	65	Pass
Zone 2 Weld Metal	49,400(2)	77,500	--	57	Pass
Base Metal	66,600	96,000	22	--	Pass
ES 588-B1					
Zone 2 Weld Metal	57,600(3)	82,500	26	51	Pass
Base Metal	67,500	97,000	25	--	Pass
ES 588-B2					
Zone 1 Weld Metal	52,000(2)	79,700	32	66	Pass
Zone 2 Weld Metal	56,200(2)	82,800	27	47	Pass
Base Metal	56,100	83,200	32	--	Pass
ES 588-B2a					
Zone 1 Weld Metal	54,000(1)	83,000	--	67	Fail
Zone 2 Weld Metal	57,500(2)	85,500	24	45	Fail
Base Metal	57,400	86,400	26	--	Pass

[1] 0.2 percent offset method used for weld metal, 0.5 percent extension under load method used for base metal.

[2] Require electroslag weld metal to match the properties of the base metal (13), single values shown are minimum requirements.

[3] Numbers in parenthesis are the number of specimens tested (when greater than one) to give the average values shown.

and tensile strength than the Zone 2 weld metal. This is in agreement with results previously reported (10) and is a result of the metallurgical structures present in the weld metal zones and their role in the yielding and failure of the tensile specimens. The Zone 1 weld metal is composed of the long, needlelike crystals which are oriented in the direction of applied stress in the tensile specimen. This structure exhibits a low yield point when tested in this direction but does show good ductility as measured by percent elongation and reduction of area. The Zone 2 weld metal is composed of the coarse columnar crystals which are oriented at various acute angles with the direction of stress applied in the tensile specimen. When tested at this orientation, Zone 2 grain structure exhibits a fairly high yield point and tensile strength but low ductility as measured by the reduction of area. This loss of ductility is a result of the failure occurring over an extended area by the slippage of the large columnar crystals along their boundaries, thus reducing the amount of necking that occurs at the break. The fractograph shown in Figure 34 displays the jagged appearance of a tensile failure in Zone 2 weld metal in contrast to the "cup and cone" type of fracture exhibited by the Zone 1 weld metal, which is the normal failure mode for mild structural steel and its weldments.

The extensive anisotropy present in the structures of Zone 1 and Zone 2 electroslag weld metal will undoubtedly have an effect on the tensile properties when the applied stress direction is varied from that tested. Under service loading conditions the applied stress on a welded joint is normal to the direction tested in the "all weld metal" tension test. In the service loading direction the large columnar structure of Zone 2 weld metal would have approximately the same orientation to the applied stress as in the test specimen. Hence no great difference would be anticipated. However, the thin columnar crystals of Zone 1 weld metal will be oriented normal to the applied stress instead of parallel to it, as they are in the tensile test. This could cause a drastic change in properties, especially in the reduction of the weld metal ductility. These zones are not large enough to test in the service loading direction with the standard tensile specimen. A specimen taken transverse to the weld with small gage lengths contained entirely within these zones of interest might produce valid measurements of the tensile properties in the service loading direction. This testing has not been done in this project but will be attempted in the near future.

Side bend test specimens taken from electroslag weldments show the effect of the large crystal structures by exhibiting a multitude of yield bands along the ferrite network tracing out the prior austenite grain boundaries. When such welds fail a bend test it is normally due to intergranular cracking along these bands such as is shown in Figure 35a for weldment ES 36-B1 in Table 9. Weldment ES 588-B2a (Table 8) had such poor ductility that the

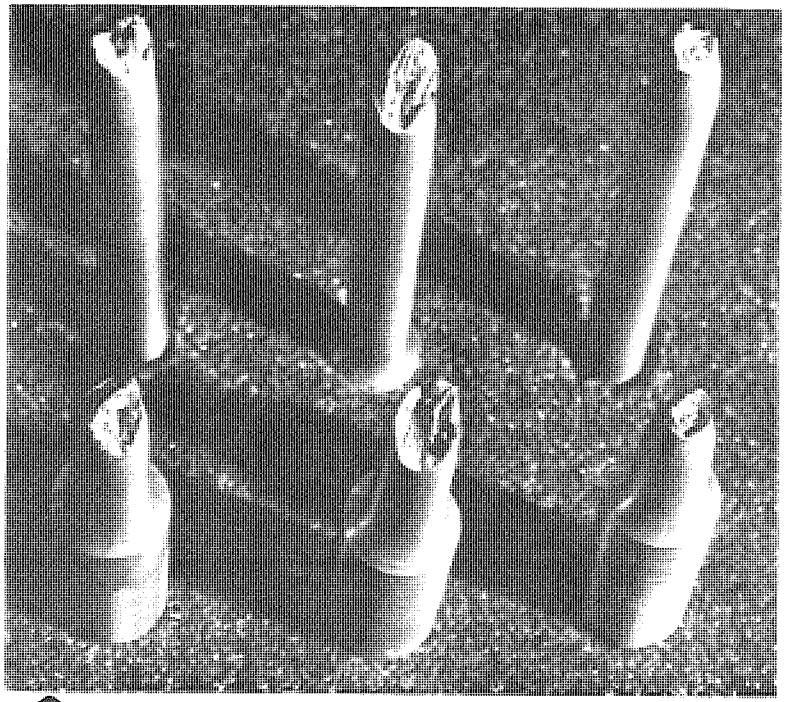

Figure 34. Fractured tensile specimens from an electroslag weld (ES 588-B2a) showing the effect of the weld metal structure on the mode of failure. The first two specimens on the left show the type of fracture occurring in Zone 2 weld metal, which fails along the prior austenite grain boundaries. The specimen on the right shows the common "cup and cone" failure mode exhibited by the Zone 1 weld metal.

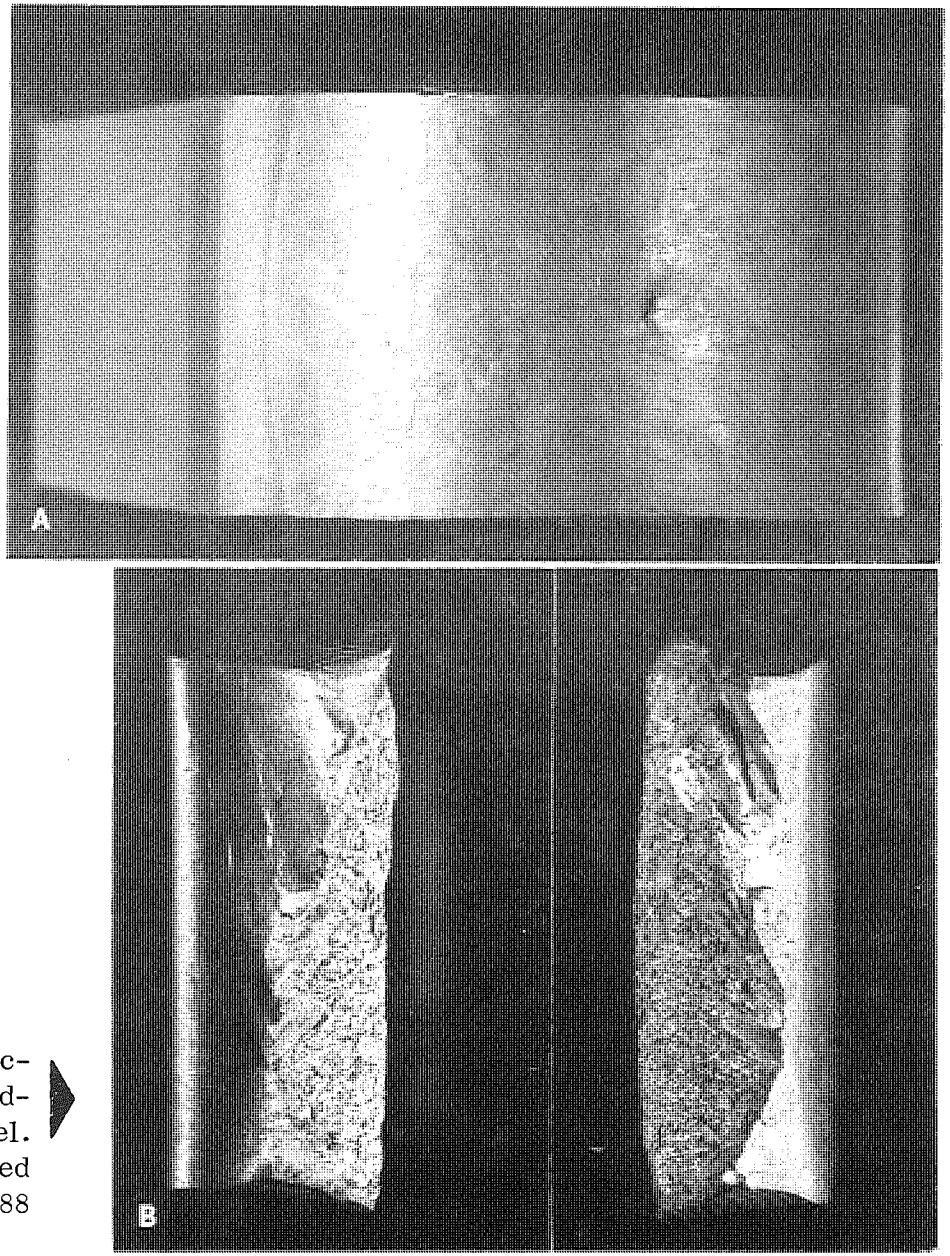

Figure 35. Side bend test specimen failures in electroslag weldments, (A) intergranular cracking in weldment ES 36-B1, a dry shoe weldment in A 36 steel. (B) Complete fracture due to poor ductility exhibited by weldment ES 588-B2a, a dry shoe weldment in A 588 steel that had an A 588 type of weld chemistry.

TABLE 9

TENSILE PROPERTIES AND BEND TEST RESULTS FOR ELECTROSLAG WELDMENTS IN A 36 STEEL

Weldment Type (See Table 2)	Yield Strength,[1] psi	Tensile Strength, psi	Elongation percent, (2 in. gage)	Reduction of Area, percent	Guided Side Bend Test
Values Required by Specification [2]	36,000	58,000-80,000	24	--	
ES 36-A1					
Zone 1 Weld Metal	43,000(2)[3]	74,100	33	64	Pass
Zone 2 Weld Metal	49,300	75,400	--	59	Pass
Base Metal	40,700	71,400	32	--	Pass
ES 36-A2					
Zone 1 Weld Metal	46,100(2)	73,800	--	69	Pass
Zone 2 Weld Metal	48,000(2)	75,500	28	64	Pass
Base Metal	39,000	64,400	33	--	Pass
ES 36-B1					
Zone 2 Weld Metal	48,100(3)	74,000	28	63	Fail
Base Metal	40,700	71,400	32	--	Pass
ES 36-B2					
Zone 2 Weld Metal	42,700(3)	70,700	34	65	Pass
Base Metal	39,000	64,400	33	--	Pass

[1] 0.2 percent offset method used for weld metal, 0.5 percent extension under load method used for base metal.

[2] Require electroslag weld metal to match the properties of the base metal (13), single values shown are minimum requirements.

[3] Numbers in parenthesis are number of specimens tested (when greater than one) to give the average values shown.

TABLE 10
TENSILE PROPERTIES AND BEND TEST RESULTS FOR SUBMERGED ARC WELDMENTS IN A 588 AND A 36 STEELS

Weldment Type (See Table 1)	Yield Strength,[1] psi	Tensile Strength, psi	Elongation percent, (2 in. gage)	Reduction of Area, percent	Guided Side Bend Test
A 588 Weldments					
Weld Metal Requirements [2]	60,000	72,000-95,000	22	--	
Base Metal Requirements	50,000	70,000	21	--	
SA 588-A1					
Weld Metal	83,750(2)[4]	118,750	19	34	Pass
Base Metal	66,700	95,200	22	--	Pass
SA 588-B1					
Weld Metal	72,250(2)	96,100	26	55	Pass
Base Metal	67,500	97,000	25	--	Pass
A 36 Weldments					
Weld Metal Requirements [3]	50,000	62,000-80,000	22	--	
Base Metal Requirements	36,000	58,000-80,000	24	--	
SA 36-A1					
Weld Metal	70,000(2)	84,750	31	63	Pass
Base Metal	40,700	71,400	32	--	Pass
SA 36-B1					
Weld Metal	68,900(2)	87,250	30	59	Pass
Base Metal	41,900	73,900	32	--	Pass

[1] 0.2 percent offset method used for weld metal, 0.5 percent extension under load method used for base metal.

[2] AWS-Flux Classification F71-EXXX, AWS Specification A5.17-69, (13), single values are a minimum.

[3] AWS-Flux Classification F61-EXXX, AWS Specification A5.17-69, (13), single values are a minimum.

[4] Numbers in parenthesis are the number of specimens tested to give the average values shown.

bend specimens actually fractured into two pieces as shown in Figure 35. As a rule, the ductility of the weldments as tested by the bend test does not indicate good or bad impact notch toughness. However, extreme loss of ductility as experienced by ES 588-B2a did coincide with a corresponding low notch toughness. It is interesting to note that weldment ES 588-B2a was the only A 588 weld deposit that closely matched the alloy chemistry requirement (Table 5). This chemistry, however, when present in the electroslag weld structure, exhibited both poor ductility and low notch toughness. This at least indicates that it is difficult to achieve the required ductility and toughness in an A 588 electroslag weldment when the chemistry range must be one that is suitable for use in an unpainted exposure. Post-welding heat treatment is possibly the only means of achieving this.

A point that should be noted is the need for offsetting a bend test specimen from the center of the weld and centering it on the fusion line in order to give a valid test of the fusion line and heat-affected zones. The normal electroslag weld nugget spreads from 2 to 3 in. in cross-section and a bend specimen that is centered on the weld puts very little bending into the fusion line area. No fusion line or heat-affected zone failures were encountered in the weldments tested in this manner. These zones, however, always require careful evaluation in electroslag welding since the grain coarsening that occurs is known to cause a decrease in both ductility and fracture toughness in steels of other alloy contents and higher yield strength.

The tensile properties and side bend test results for the submerged arc weldments are shown in Table 10. The "all weld metal" tension tests were performed only on the 1-3/4-in. submerged arc weldments. The tensile properties of weld metal from a multipass submerged arc weldment are not highly dependent on the joint thickness. As long as the thermal cycle of each pass is approximately the same the weld metal will be quite homogeneous in its tensile behavior. A constant weld bead size is normally used to build up a joint regardless of the total joint thickness.

This is recognized by the AWS Specifications (2) in requiring a procedure qualification test weld of only 1 in. in thickness for qualifying welding on unlimited thickness. (As will be shown in the Charpy impact evaluations, the toughness properties of the weld metal are quite sensitive to the grain coarsening that occurs in the thicker joints when interpass temperature is not strictly controlled.) The electrode-flux combinations used in the submerged arc weldments of this project were the same for the 1-3/4-in. and 3-in. plate thicknesses (Table 1). Since the other welding variables were held constant, the tensile properties of the 1-3/4-in. weldments should be representative of the 3-in. thickness as well.

The Michigan Specification (13) requires the use of welding wire and flux that will meet the AWS flux classifications F61-EXXX or F71-EXXX for submerged arc welding on A 36 or A 588 steel, respectively. Prior to December 1974 this specification was enforced only to the extent of requiring the electrode manufacturer to certify that the wire would meet the requirements of the flux classification when tested in accordance with AWS 5.17, Specification for Bare Mild Steel Electrodes and Fluxes for Submerged-Arc Welding. No additional testing was required to determine the tensile properties being produced by the welding procedure being used in fabrication. Thus, the weld metal tensile requirements listed in Table 10 cannot be strictly applied to the weld metal taken from the test weldments, since the specification did not require this at the time. In December 1974 the Michigan Supplemental Specification for Welding Structural Steel was modified to require that the procedure qualification test weld be capable of meeting the tensile requirements of the appropriate AWS flux classification. This action was taken to improve the quality control of weldments being used in bridge structures. The option of requiring the procedure qualification test weldment to produce all of the flux classification properties is given to the Welding Engineer in Section 4.12.1 of the AWS Structural Welding Code (2). It is interesting to note that the tensile requirements for submerged arc welding call for an "overmatching" of the base metal being welded. This is a traditional approach to welding which provides a factor of safety for the weld metal which must function in the presence of residual stresses and undetected fabrication flaws. The requirements listed for electroslag weld metal (Tables 8 and 9) do not require this overmatching of the base metal. The only justification for this is, apparently, the inability of the electroslag weld to consistently produce a weld metal that is stronger than the base metal being welded. Thus, an electroslag weld does not offer the same safety factor that a submerged arc weld does, even when both weldments meet specifications.

The first set of weldments listed in Table 10 are the submerged arc welds in A 588 steel. The weldment SA 588-A1 was produced by Fabricator A by a welding procedure that produced a poor microstructure in the weld. The yield strength and tensile strength of this weld metal are excessively high and the weld metal ductility is low. (This lack of ductility in the weld metal will also be seen in a low Charpy impact toughness of this weldment.) The weldment SA 588-B1 has properties that are nearly in conformance with those specified for the flux classification F71-EXXX. Both weldments passed the side bend test. The second set of weldments in Table 10 are the submerged arc welds in A 36 steel. The tensile strength of both SA 36-A1 and SA 36-B1 are seen to exceed the maximum requirement of the flux classification F61-EXXX. The ductility of both weldments, how-

ever, is very good as seen in the percent elongation and reduction of area measurements. Note the overmatch of the A 588 and A 36 weldments in comparison to the base metal. It's not uncommon for the yield point of the A 588 steel plate itself to greatly exceed the 50,000 psi minimum required, as seen in the weldments of Tables 8 and 10. When this occurs, electroslag weld metal can actually be undermatched in yield strength compared to the base metal being joined.

Typical hardness surveys across the weldments are shown in Figures 36 through 38. In the electroslag weldments made in A 588 steel, the HAZ 1, where grain coarsening occurs, is seen to have an increase in hardness and in HAZ 2, where the base metal grain structure has been refined, the hardness decreases. The maximum hardness usually occurs near the fusion line. The large columnar crystal Zone 2 weld metal shows a higher hardness than the fine columnar crystal Zone 1 weld metal. (This is also indicated by the Zone 1 yield strength being lower than the Zone 2 yield strength.) These trends are also present in the hardness surveys across A 36 electroslag weldments but the variations in magnitude are smaller. In the submerged arc weldments, the hardness of the base metal will increase as the fusion line is approached and hardness reaches a maximum at the fusion line. Hardness through the weld metal fluctuates slightly about some representative average value.

Microhardness testing using a Vickers indenter revealed nothing unusual except the fact that the ferrite present in the ferrite network tracing out the prior austenite grain structure in the electroslag weld metal is slightly softer than the free ferrite present inside of this network. This seems to be evidenced by the deformation that occurs along the ferrite bands in the failure of various tensile and side bend specimens. One notable exception to this was in the weldment ES 588-B2, which had grain boundary ferrite that was harder than the intergranular ferrite. This weldment also exhibited unusually low impact toughness in the Zone 2 weld metal which could be partially due to the increased hardness of the ferrite bands in this particular case. The ferrite bands in Zone 2 are usually included in the fracture path for an impact fracture and the increased hardness would increase the brittleness of the ferrite.

Charpy Impact Evaluation of Weldments

Three series of Charpy V-notch impact tests were performed on the butt welds. The first series involved the evaluation of both the electroslag and the submerged arc weldments at a temperature of 0 F to compare their impact properties with the existing acceptance criteria. Second, impact tests were conducted over the temperature range of -40 to +40 F on both

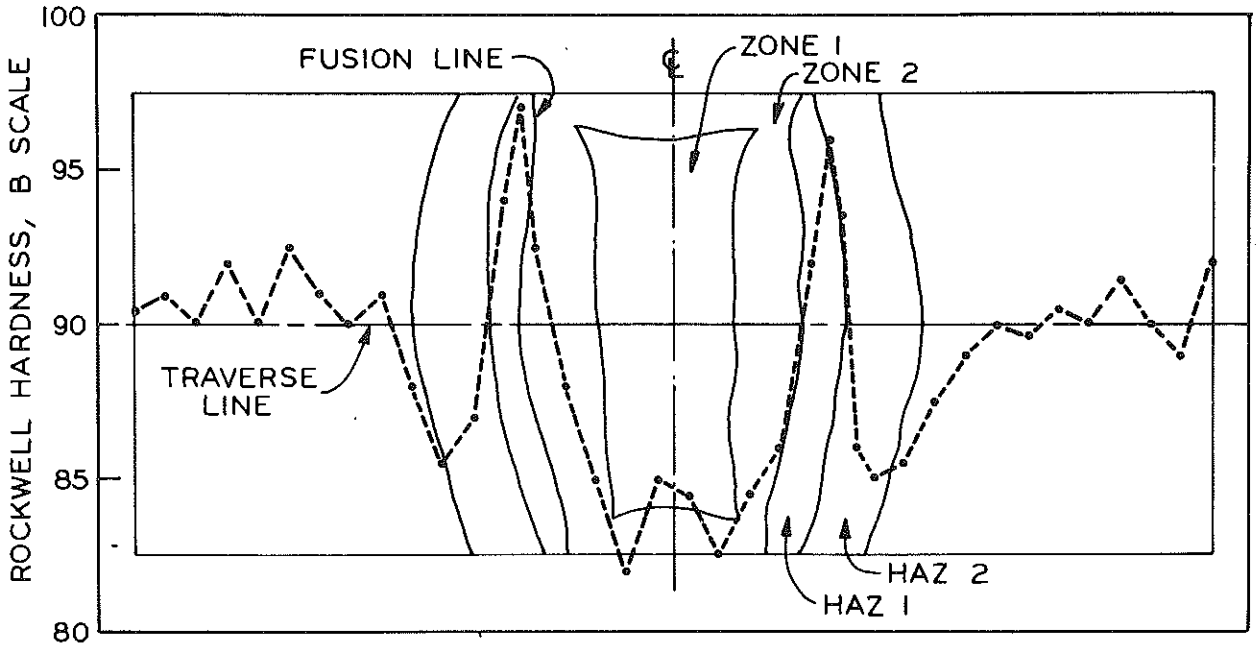

(A) Cooled shoe electroslag weldment in 3-in. thick A 588 steel (ES 588-A2).

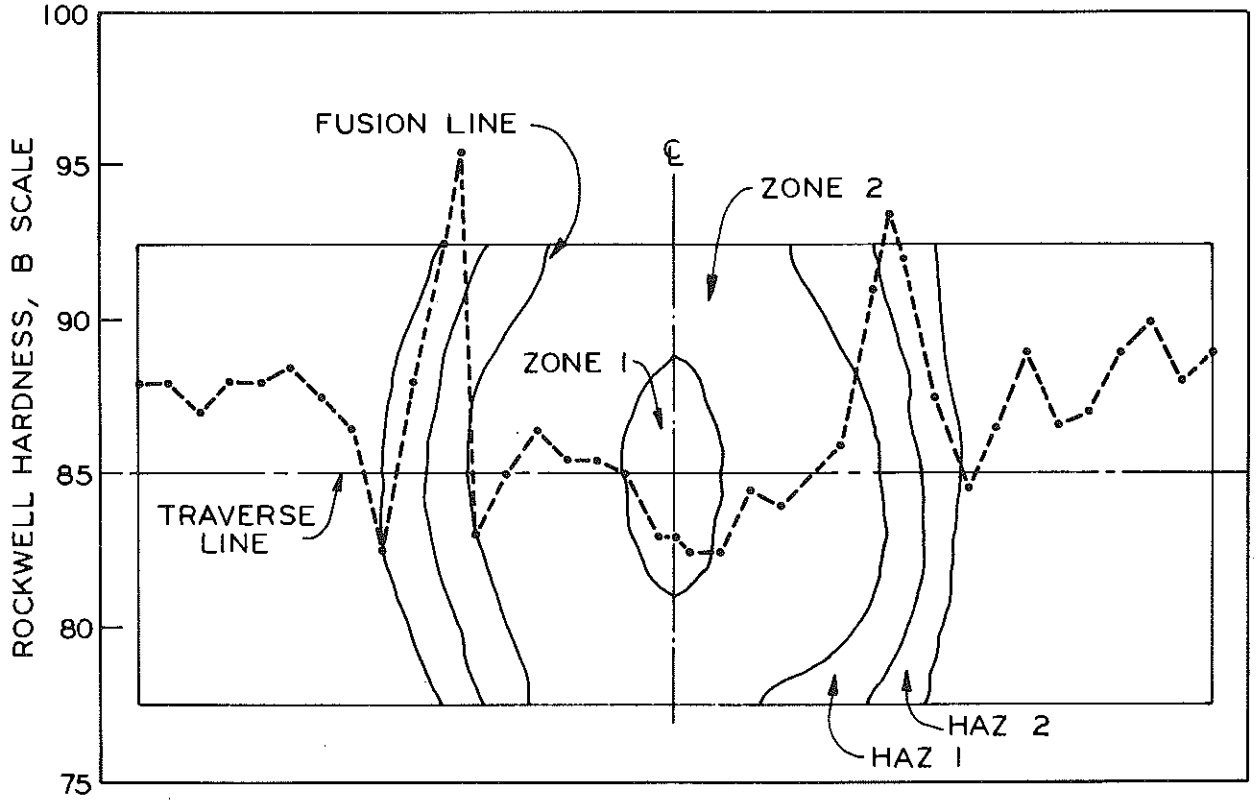

(B) Dry shoe electroslag weldment in 3-in. thick A 588 steel (ES 588-B2).

Figure 36. Hardness traverses across electroslag welds in A 588 steel.

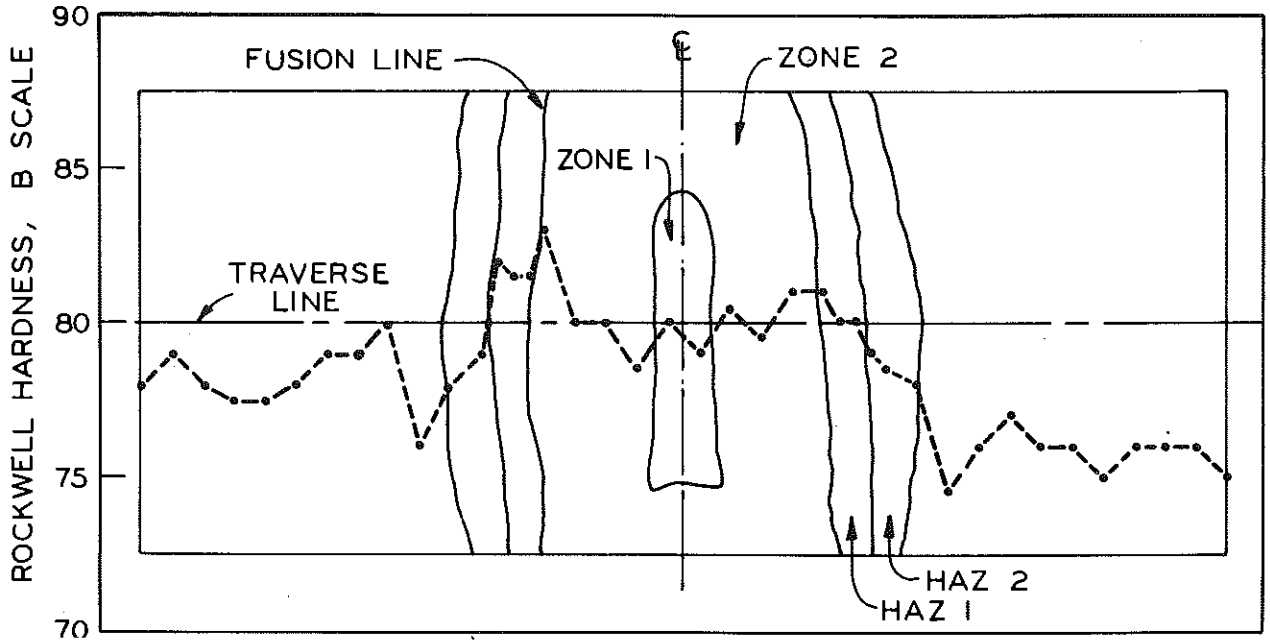

(A) Cooled shoe electroslag weldment in 3-in. thick A 36 steel (ES 36-A2).

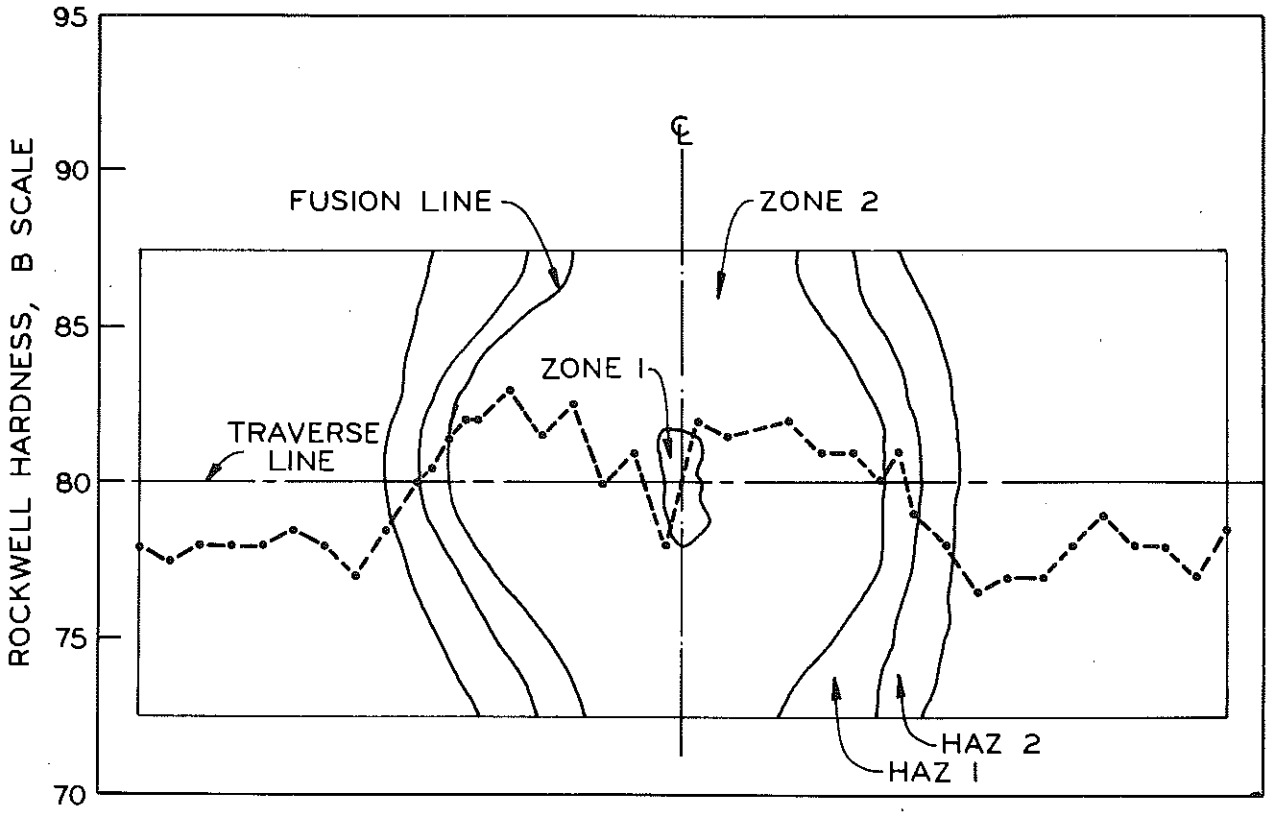

(B) Dry shoe electroslag weldment in 3-in. thick A 36 steel (ES 36-B2).

Figure 37. Hardness traverses across electroslag welds in A 36 steel.

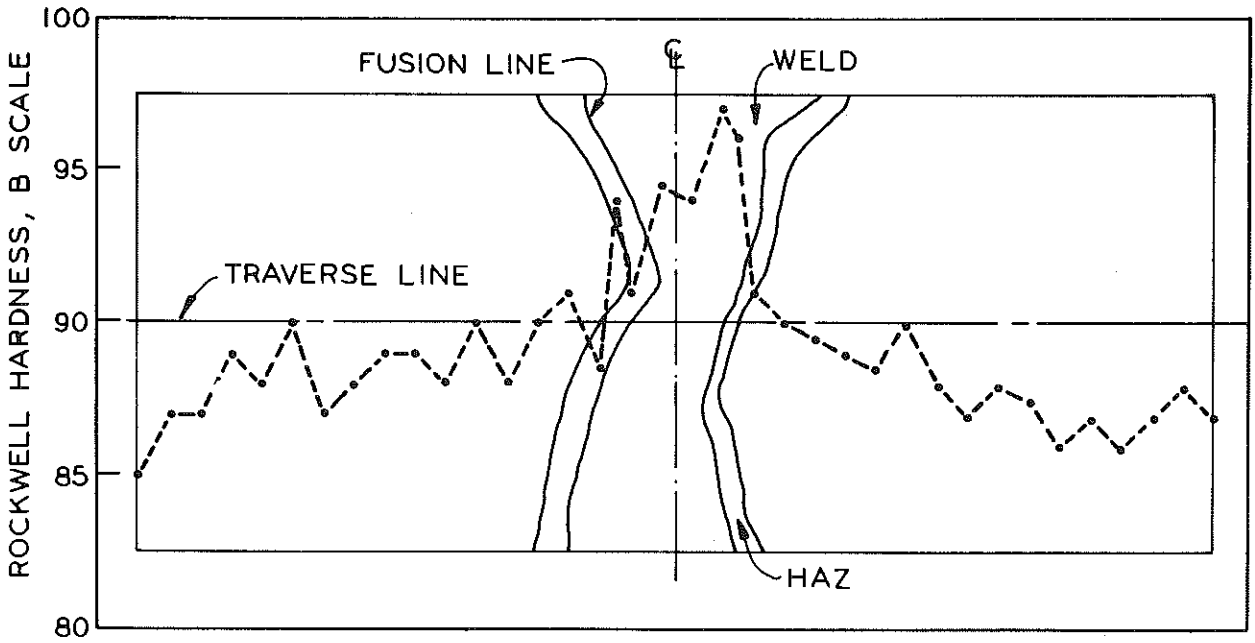

(A) Submerged arc weldment in 3-in. thick A 588 steel (SA 588-B2).

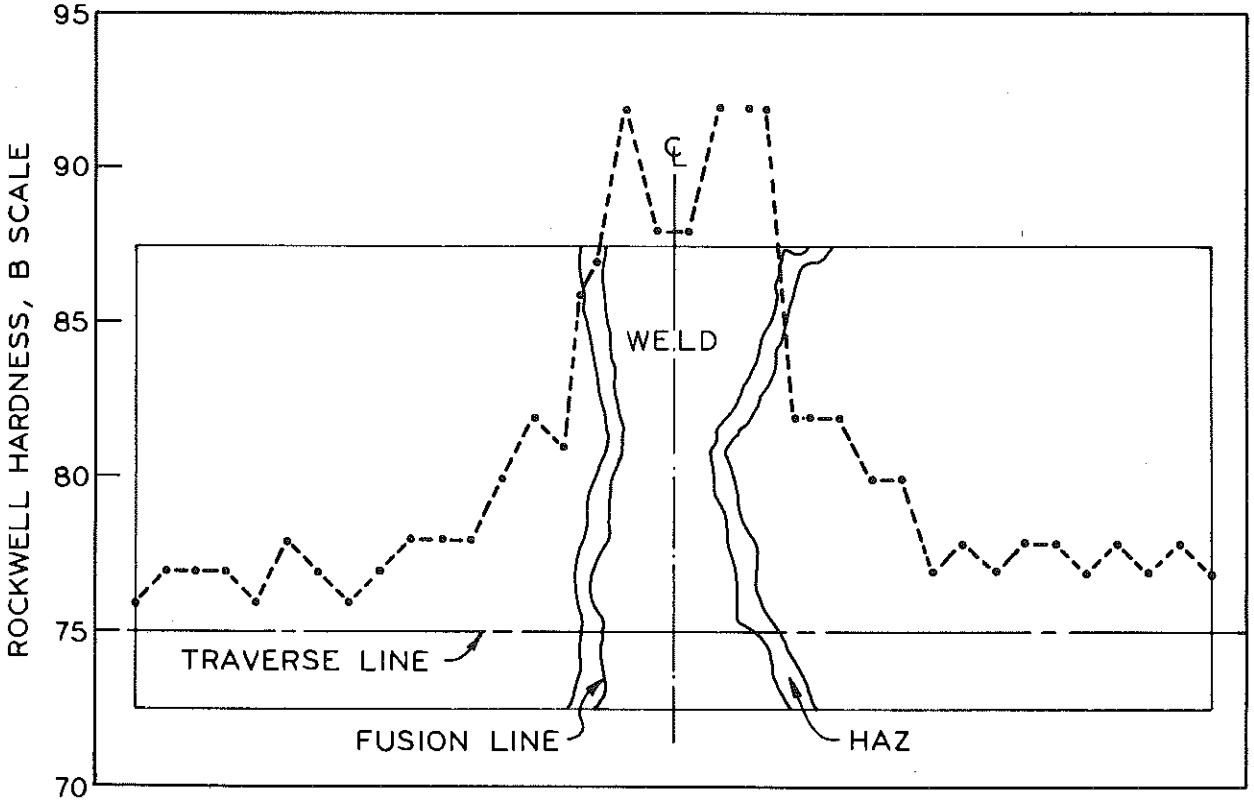

(B) Submerged arc weldment in 3-in. thick A 36 steel (SA 36-B2).

Figure 38. Hardness traverses across submerged arc welds.

the electroslag and the submerged arc weldments to determine their temperature transition characteristics. Third, the directional variation or anisotropic nature of the impact properties of the electroslag weld metal was determined by varying the orientation of the specimens with respect to the grain structures present in the two zones of the weld metal.

Series I - Acceptance Testing

The impact requirements for butt welds are found in the AWS specifications of Refs. (1) and (2). Five specimens are required from each weld assembly. These specimens are removed from the weld with their longitudinal centerline oriented transversely to the weld axis, and the base of the notch is machined perpendicular to the plate surface. For materials of thickness greater than 1/2 in. the longitudinal centerline of the specimen is located as near as practicable to a point midway between the surface and the center of thickness of the plate. These impact specimens are machined and tested in accordance with the "ASTM Specification for Notched Bar Impact Testing of Metallic Materials," E 23, for Type A (simple beam) impact specimens. These specimens are tested at 0 F, and then the average is computed by discarding the extreme high and low values of the set of five and averaging the remaining three. The minimum average impact values required are 15 ft-lb for an electroslag weldment and 20 ft-lb for a submerged arc weldment. In addition, the minimum impact value permitted on one specimen only in the set of three is 10 and 15 ft-lb for electroslag and submerged arc weldments, respectively. The Michigan Specification (13) calls for mandatory impact testing for procedure qualification of both submerged arc and electroslag butt weldments and since 1974 have imposed additional restrictions on the testing and use of electroslag weldments. These additional requirements were not in effect at the beginning of this project and will be listed in the concluding section of this report.

Approximately 3 in. of plate was saw cut from both the starting end and the top (finishing) end of the electroslag weldments. A cross-sectional surface of each weld block was then ground smooth and macro-etched to reveal the metallurgical structures present in the weld. In removing the Charpy specimens from the weld, all the specifications for impact testing were adhered to except for the positioning of the test specimens in the cross-section of the plate. Sets of five specimens were located at various positions throughout the weldments to test all the weld metal zones and heat-affected zones present. Several sets of impact specimens were also taken from the base plates surrounding the welds. Specimens were similarly located in pieces cut from each end of the submerged arc weldments.

TABLE 11
IMPACT TOUGHNESS (CVN) OF ELECTROSLAG WELDMENTS IN A 588 STEEL
(Test Temperature 0 F)

Weldment Type (See Table 2)	Impact Toughness, ft-lb				
	Zone 1 Weld Metal	Zone 2 Weld Metal	HAZ 1	HAZ 2	Base Metal
ES 588-A1					
Top end	18*	46	N. T.[1]	81	13
Starting end	13*	34	N. T.	69	13
ES 588-A2					
Top end	11*	35	18	77	12
Starting end	14*	29	18	123	14
ES 588-B1					
Top end	N. P.[2]	22	8	128	14
Starting end	20	34	N. T.	52	9
ES 588-B2					
Top end	6*	14*	18	30	16
Starting end	5*	7*	25	33	18
ES 588-B2a					
Mid-section[3]	5*	6*	N. T.	N. T.	51

* An asterisk denotes that the set of specimens failed to meet the specified impact requirements.
[1] N. T. denotes that the zone was present but was not tested.
[2] N. P. denotes that the zone was not present in the weldment.
[3] Specimens were located in accordance with AWS D2. 0-69, Fig. A-10.

TABLE 12
IMPACT TOUGHNESS (CVN) OF ELECTROSLAG WELDMENTS IN A 36 STEEL
(Test Temperature 0 F)

Weldment Type (See Table 2)	Impact Toughness, ft-lb				
	Zone 1 Weld Metal	Zone 2 Weld Metal	HAZ 1	HAZ 2	Base Metal
ES 36-A1					
Top end	42	47	N. T.[1]	N. T.	50
Starting end	21	50	N. T.	167	51
ES 36-A2					
Top end	20	37	6	5	4
Starting end	16*	53	5	14	4
ES 36-B1					
Top end	N. P.[2]	42	57	140	47
Starting end	N. P.	22	N. T.	161	49
ES 36-B2					
Top end	N. P.	51	6	6	3
Starting end	N. P.	57	8	7	3

* An asterisk denotes that the set of specimens failed to meet the specified impact requirements.
[1] N. T. denotes that the zone was present but was not tested.
[2] N. P. denotes that the zone was not present in the weldment.

The zones tested in the electroslag weldments included the two weld metal zones (when present), the two heat-affected zones, and the unaffected base metal. The metallurgical structures present in these various zones were described in the previous section on weldment metallurgy. The results of these tests are presented in Tables 11 and 12 for welds made in A 588 and A 36 steels, respectively. Each value entered in the table represents either an average taken from a set of specimens as prescribed by the specification (1, 2) or an average of several such sets taken from one particular zone of the weldment. Figures 39 and 40 present cross-sectional drawings of four electroslag weldments showing numbers that correspond to the average impact strength measured at the points denoted by a cross. These figures illustrate the variations of impact toughness present in the various zones of the weldment. The results of the tests conducted on submerged arc weldments are presented in Tables 13 and 14 for A 588 and A 36 base plate, respectively. Figure 41 shows the variation in impact toughness that can occur in a typical submerged arc weldment.

Comparing the impact values representing the various electroslag weldment zones in Tables 11 and 12, we first note that the Zone 1 weld metal has a lower toughness than the Zone 2 weld metal. The only exception to this statement is weldment ES 588-B2a in Table 11, which had very low toughness in both weld metal zones. This result is in agreement with previously reported tests on electroslag weldments (10, 16) and is to be expected when consideration is given to the orientation of the grain structures with respect to the direction of crack propagation in the Charpy test specimen. The standard orientation for removing a Charpy specimen from the weld, directs the crack propagation parallel to the longitudinal axis of the crystals that comprise the Zone 1 weld metal and the failure that occurs is intergranular, i.e., the crystals separate along their grain boundaries. In Zone 2 weld metal the coarse columnar crystals are oriented at an angle varying approximately between 40 to 65 degrees with the direction of crack propagation, and the failure occurs in a transgranular mode, i.e., the crack propagates across the crystals. This can require more energy than crack propagation along the grain boundaries depending on the alloy composition of the weld. Some Zone 2 specimens do exhibit a partial intergranular type of fracture, but the plane of the crack is forced to deviate from its original plane to follow the grain boundaries. This results in a higher energy absorption than that required to propagate the crack parallel to the crystal axis. These statements will be further substantiated by the impact data from the anisotropic test series.

Next observe that the first heat-affected zone past the fusion line, HAZ 1, which is a zone of grain coarsening due to the overheating experienced, exhibits impact energy equal to or greater than the unaffected base metal.

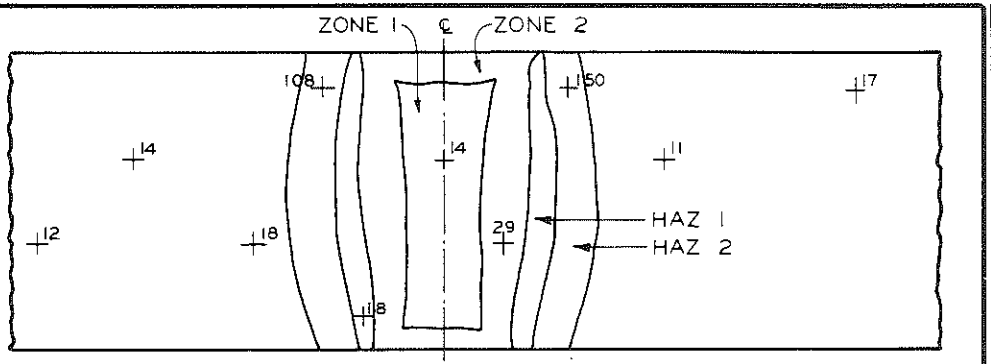

(A) Cooled shoe electroslag weldment in 3-in., A 588 plate (ES 588-A2).

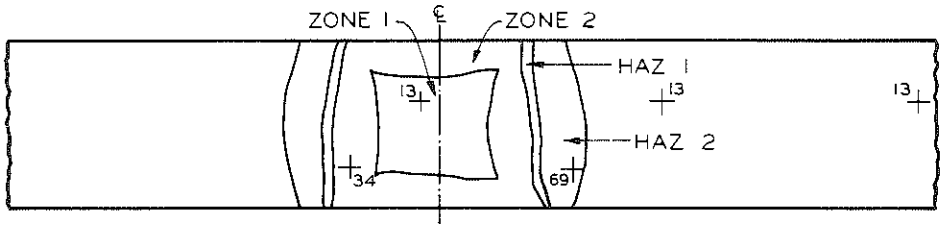

(B) Cooled shoe electroslag weldment in 1-3/4-in., A 588 plate (ES 588-A1).

Figure 39. Impact toughness (CVN) variation in electroslag weldments tested at 0 F. Each value shown represents a set of five Charpy specimens averaged as prescribed by the specification (2).

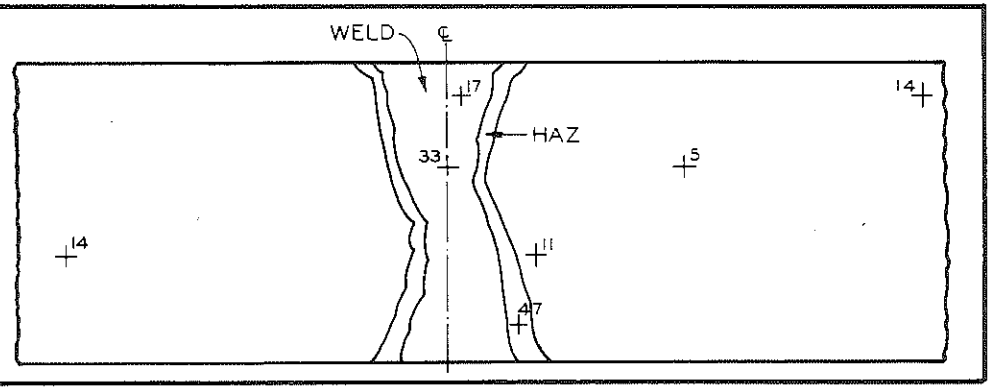

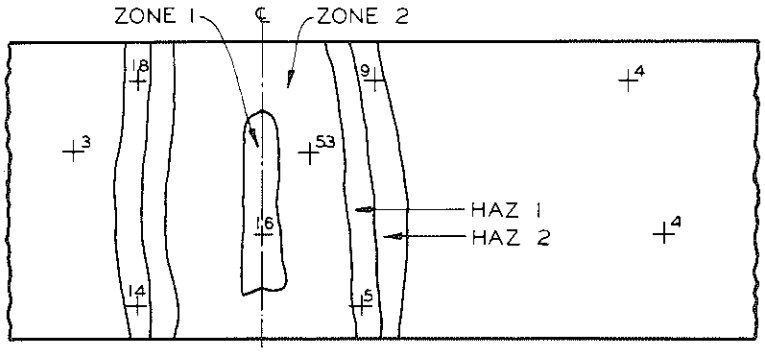

(A) Cooled shoe electroslag weldment in 3-in., A 36 plate (ES 36-A2).

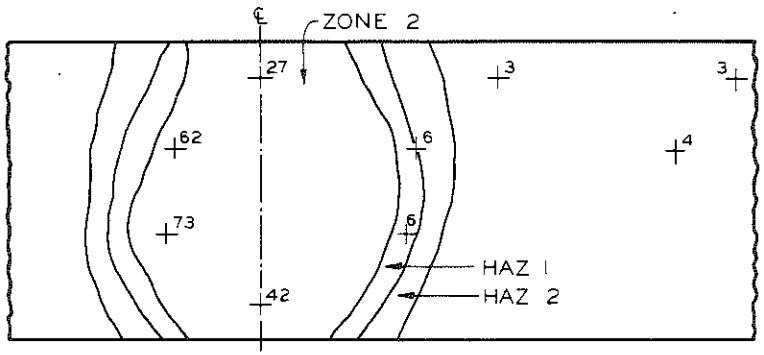

(B) Dry shoe electroslag weldment in 3-in., A 36 plate (ES 36-B2).

Figure 40. Impact toughness (CVN) variation in electroslag weldments tested at 0 F. Each value shown represents a set of five Charpy specimens averaged as prescribed by the specification (2).

Figure 41. Impact toughness (CVN) variation in a submerged arc weldment in 3-in. A 588 plate (SA 588-B2), tested at 0 F. Each value shown represents a set of five Charpy specimens averaged as prescribed by the specification (2).

TABLE 13
IMPACT TOUGHNESS (CVN) OF SUBMERGED ARC WELDMENTS IN A 588 STEEL
(Test Temperature 0 F)

Weldment Type (See Table 1)	Impact Toughness, ft-lb		
	Weld Metal	HAZ	Base Metal
SA 588-A1			
End 1	20*	104	22
End 2	25	88	17
SA 588-A2			
End 1	15*	45	15
End 2	25	60	16
SA 588-B1			
End 1	52	13	16
End 2	40	35	25
SA 588-B2			
End 1	13*, 30[1]	35	15
End 2	17*, 33	47	11

* An asterisk denotes that the set of specimens failed to meet the specified impact requirements.

[1] Two sets of specimens from the same weld section at different locations in the cross-section (see Fig. 41).

TABLE 14
IMPACT TOUGHNESS (CVN) OF SUBMERGED ARC WELDMENTS IN A 36 STEEL
(Test Temperature 0 F)

Weldment Type (See Table 1)	Impact Toughness, ft-lb		
	Weld Metal	HAZ	Base Metal
SA 36-A1			
End 1	18*	32	43
End 2	12*	129	51
SA 36-A2			
End 1	15*	32	4
End 2	19*	39	3
SA 36-B1			
End 1	61	28	3
End 2	59	6	3
SA 36-B2			
End 1	45	36	49
End 2	36	53	50

* An asterisk denotes that the set of specimens failed to meet the specified impact requirements.

This grain coarsening is known to be detrimental in other types of steel, especially high yield strength and quenched and tempered steels, but apparently causes no loss of toughness in the base metal for the ASTM A 588 and A 36 steels evaluated. This is the zone that requires careful evaluation if no previous data are available on the affect of such grain coarsening on a particular type of steel. The next heat-affected zone, HAZ 2, which was seen to be a zone of grain refinement, is greatly enhanced in impact strength. This type of fine grained structure, which is produced by the recrystallization effect of the heating and cooling cycle experienced during the welding, is expected to yield high impact strengths. The only exception to this high toughness in HAZ 2 is in weldments ES 36-A2 and ES 36-B2 where the base metal had extremely low toughness. In these two cases, the grain refinement present in HAZ 2 did more than double the low level of toughness present in the base plate, but these elevated values were still quite low.

The impact energies measured from specimens taken from the starting end of the weld were usually equal to or somewhat less than those measured from the top end of the weldment. The only exceptions to this are seen in Zone 2 weld metal in weld ES 588-B1 and in weld ES 36-A2. The higher impact energy measured in weldment ES 588-B1, in Zone 2 from the bottom of the weldment, was actually due to a change in the orientation of the large columnar crystals with respect to the axis of crack propagation, which resulted in a lower impact energy measured at the top of the weld. If the specimen sets had been positioned at the same point in the cross-section, this difference would not have occurred. In weldment ES 36-A2, the values at the starting end in Zone 2 do exceed those at the top end, with no apparent explanation except that both values are quite high. (The Zone 1 weld metal in this weldment does follow the trend of lower toughness on the starting end.) Thus, qualified by the two above exceptions and their explanation, it appears that the lowest toughness levels in the electroslag weldments tested (16 in. long) occur in the weld metal at the starting end of the weld. This would be an important fact to incorporate into specifications governing the acceptance testing of such welds. In fact since the impact toughness of the Zone 2 weld metal is so sensitive to the orientation of the large columnar crystals, which does vary throughout the weldment, it might be justified to conduct impact tests at both the start and the finish of the weld and at several positions within the cross-sections, or to selectively orient the specimens within the grain structure.

Impact specimens were taken from all the electroslag weldments from locations within 1 in. of the outside edge of HAZ 2 to determine if any alteration had occurred in the base metal, even though the microstructure

beyond HAZ 2 appears to be unaltered. No difference was recorded in this region in comparison to the outlying base metal; hence, only two heat-affected zones were produced in the steels welded. Some extremely low toughness values were measured in the base metal, especially in the 3-in. A 36 steel (Fig. 40). At the time these weldments were produced (1972) there were no toughness requirements on ASTM A 36 steel, and A 588 steel was required to produce 15 ft-lb at 40 F. Under the current specification by the American Association of State Highway and Transportation Officials, both A 36 and A 588 steels are required to meet a minimum toughness requirement in main members subject to tensile stress (13). Note in Figure 41 the large variation in the impact toughness measured at different locations in the base metal. Variations of this magnitude were recorded in both 1-3/4 and 3-in. thick plates of A 588 steel. It has long been recognized that the weld metal needs to possess a higher impact toughness than the base metal being welded. This is due to the severe service conditions placed on a weldment due to the presence of residual shrinkage stresses and fabrication flaws which do escape detection and repair. Such conditions often cause a weldment to fracture at a load much lower than would be theoretically predicted (3).

An interesting point noted from the data was that the variation of impact strength measured within a set of five specimens from any particular zone was in some cases considerable (a ratio of maximum to minimum of 2 or larger) in all the weld, heat-affected, and base metal zones. In other cases very little variation occurred within a set of five specimens. This variation occurred in spite of very careful control on specimen tolerances and notch tip acuity. Some of the variation within a weld metal zone could be attributed to a change in dendrite orientation with respect to the fracture path as evidenced by the broken specimens. In some cases, however, the fractured surfaces were essentially identical but energy absorption varied. It is not clear whether the variations occurring within a set of specimens from a particular zone point out the inherent, non-homogeneous nature of the metal or if such variability is due to the nature of the Charpy specimen itself. The average values obtained from any particular weldment zone, however, are representative of the impact toughness of the zone and do yield reproducible results. For comparison, the average of the five specimens from each set was computed as well as the average of the three specimens with the extreme high and low values discarded. These two averages were virtually identical, which indicates that the scheme specified by AWS (1, 2) does not account for the variation occurring in a set of specimens. What it does is allow the discarding of a low impact value from consideration. Such a specimen may, however, have a very important meaning in pointing out an unfavorable grain boundary orientation in a metal like electroslag

weld metal. This discussion also points out the danger involved in evaluating a weldment zone on the basis of only one specimen which may not be at all representative.

Comparing the results obtained for these electroslag weldments with the recommended AWS acceptance criterion of 15 ft-lb at 0 F, we see from Table 11 for A 588 steel that in all but one of the weldments, the Zone 1 weld metal fails to qualify. The exception is the dry shoe electroslag weldment made in a 1-3/4-in. A 588 plate. Next we note that the Zone 2 weld metal failed to qualify only in the two dry shoe electroslag welds made in 3-in. A 588 plate. Failure to meet the specified requirement may mean; a) does not exceed an average of 15 ft-lb, b) has more than one specimen of the three averaged below the minimum required average of 15 ft-lb, or c) the value for one of the specimens was below the minimum value permitted of 10 ft-lb (1, 2). In Table 12 for weldments made in A 36 steel we note that all zones passed with the exception of the Zone 1 weld metal at the starting end of the water cooled shoe electroslag weld made in the 3-in. plate. These observations point out two important facts. First is the need to carefully test the Zone 1 weld metal as well as the Zone 2 weld metal when evaluating the fracture toughness of the weldment. The procedure used in the AWS Specification (1, 2) for locating the specimens at the quarter thickness is not adequate for testing electroslag joints. This location will usually place the specimens in Zone 2 weld metal or in a combination of Zone 1 and Zone 2 weld metal, either of which will lead to a higher impact toughness than that measured in Zone 1. If only one set of specimens is tested, they should be located at the mid-thickness on the weld centerline at the starting end of the weld. This location will measure the lowest toughness value present in the weld metal. Even when Zone 1 is absent from the weld, the Zone 2, coarse columnar crystals will have their lowest impact toughness at the weld center because of the way the grain boundaries collimate at the center and the influence of the coarse secondary structure found in the center. The second fact that can be concluded from the data is that the electroslag weld metal structure is much more detrimental in the high strength, low alloy steel, A 588 than it is in the constructional grade of carbon steel, A 36. The complex alloy systems present in the various grades of A 588 steel result in a weld metal chemistry that is hard to control and unfavorable to the "as welded" crystal structures produced by electroslag welding. Without postweld heat treatment, it appears to be impossible to reliably weld A 588 steel by the electroslag process, using the present commercially available electrodes, if the impact toughness requirements are to be strictly adhered to.

The fractographs of typical fractured Charpy specimens in Figure 42 show the impact fracture appearances of the electroslag weldment zones.

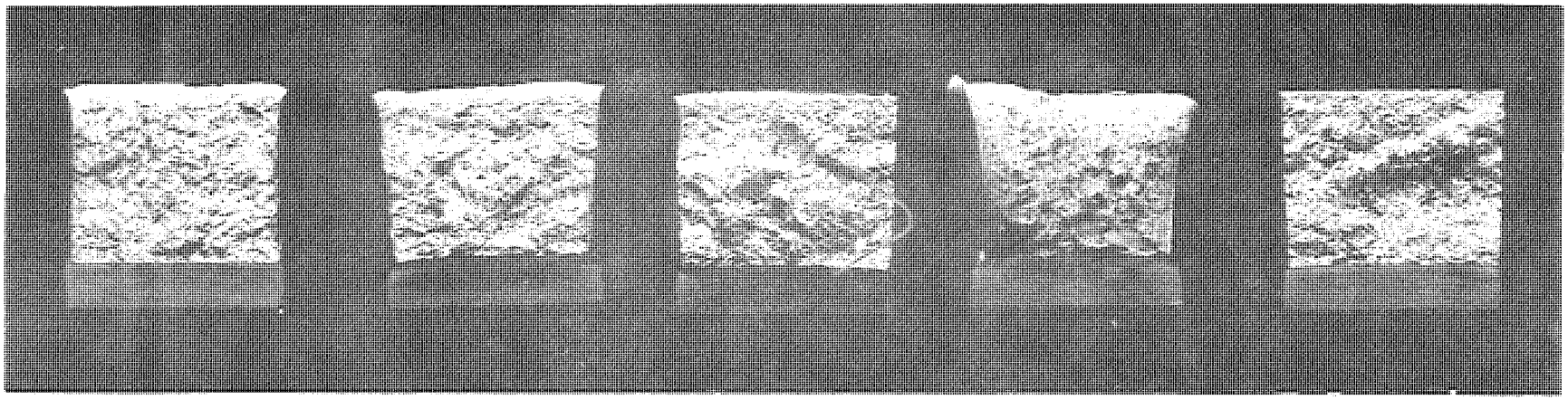

(A) Specimens from a cooled shoe electroslag weldment in A 588 steel (ES 588-A2). Left to right specimens are from Zone 1 weld metal, Zone 2 weld metal, HAZ 1, HAZ 2, and base metal.

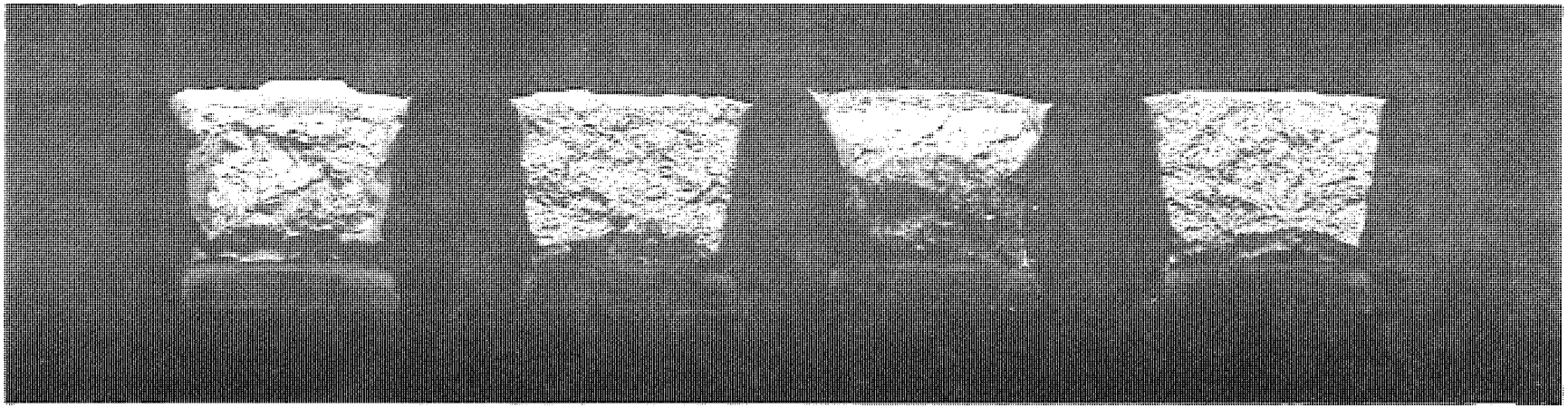

(B) Specimens from a dry shoe electroslag weldment in A 588 steel (ES 588-B2). Left to right specimens are from Zone 2 weld metal, HAZ 1, HAZ 2, and base metal.

Figure 42. Broken Charpy V-notch specimens showing the nature of the fractured surfaces through the various electroslag weldment zones (test temperature 0 F).

Note how the texture of the fractured surface correlates with the grain structure present in each zone. In Zone 1 weld metal, the fine columnar crystals are exposed since they were fractured parallel to the long axis of the crystals by intergranular separation. The Zone 2, coarse columnar crystals display a coarse, jagged fracture surface typical of the mixed transgranular-intergranular fracture through this zone. (Note that Zone 2 specimens do contain some smooth facets which show that some grain boundary separation has occurred.) The grain coarsening in HAZ 1 and the grain refinement in HAZ 2 are also evident in the fractured Charpy specimens. The lateral expansion seen on the back side of the specimens correlates directly with the amount of energy absorbed in the fracture. The large amount of expansion in the HAZ 2 specimen indicates the greatly elevated impact strength of the zone as compared to the base metal. It is difficult, however, to attempt to estimate the percent shear fracture on the specimens taken from the two weld metal zones because of the role of the crystal structures in the fracture. Thus it would not be reasonable to define a fracture appearance transition as defined in ASTM A 370, "Mechanical Testing of Steel Products."

Tables 13 and 14 present the results of the Charpy impact testing done on the submerged arc weldments in A 588 and A 36 steel, respectively. The weldments made by Fabricator A have poor impact properties in both steels. This result is most likely due to the fact that Fabricator A was quite inexperienced at submerged arc welding since they had used the electroslag process exclusively for butt joint welding for several years. The welding procedure they used led to an excessive deposition of weld metal and the interpass temperature ran quite high (800 F or higher). Grain coarsening was evident in the microstructures of Fabricator A's weldments which could account for their low toughness. In addition, the submerged arc weldments made by Fabricator A had a higher incidence of nonmetallic inclusions than those by Fabricator B, which also could lower the impact toughness. The chemical effects mentioned previously would likewise contribute to the low impact toughness. The weldments made by Fabricator B were very high in toughness and, with the exception of two locations in the weld placed in 3-in. A 588 steel, they greatly exceeded the required 20 ft-lb at 0 F. A cross-section of the weldment that had low toughness (SA 588-B2) shows the results obtained by testing the weld metal near the root of the joint and near the surface (Fig. 41). The location near the surface is where the impact toughness did not meet specifications. Again this is most likely attributed to the failure to control the maximum interpass temperature and as the weld deposition progressed, the excessive heat buildup degraded the toughness by coarsening the grain structure near the surface of the plate.

In all the submerged arc weldments made by both fabricators, the heat-affected zone produced impact strengths that were equal to or greatly improved over base metal. This is to be expected since the microstructure of the HAZ was seen to be a refinement on the grain structure of the base metal (Figs. 14 through 17).

The fractographs of typical fractured Charpy specimens in Figure 43 show the impact fracture appearances of the submerged arc weldment zones. The low toughness present in the Fabricator A weld metal is evident from the broken specimen, which lacks both lateral expansion and shear lip area. The Fabricator B weld metal, in contrast, exhibits a large amount of lateral expansion and shear lip, typical of a break in tough metal. Note the improved toughness exhibited by the HAZ in both weldments over that of the base metal. Different filler metals were used by the two fabricators in making these weldments (Table 1) which could also account for some of the difference in impact properties.

These results illustrate that it is possible to butt weld by submerged arc both A 36 and A 588 steel in thicknesses up to 3 in. and achieve the specified notch toughness in the "as welded" condition. They also point out that if improper procedures are used and if the maximum interpass temperature is not controlled, then submerged arc welding can also result in low toughness weld metal. It can also be concluded that the heat-affected zone present in a submerged arc weldment doesn't pose the potential problems present in the two heat-affected zones of electroslag welding. It should be noted, however, that if submerged arc welding is performed with an excessive heat input, the HAZ can contain a grain coarsening similar to that seen in HAZ 1 of electroslag weldments.

The comments made previously concerning the variation present in a set of five Charpy specimens from any particular electroslag weldment zone, likewise apply to the submerged arc weld metal. Thus the variations are not unique to the electroslag weld structure. Further study on the data for this project is planned to try to correlate variations in the impact strengths of a set of five specimens with some possible cause as evidenced in either the fractured surfaces or the microstructure.

Series II - Energy Transition-Temperature Testing

The Charpy impact test result is a function of the testing temperature of the specimen. Generally speaking, an increase in temperature will increase the energy absorbed by a specimen and a decrease in temperature will decrease the energy absorbed. Somewhere between +200 F and -40 F

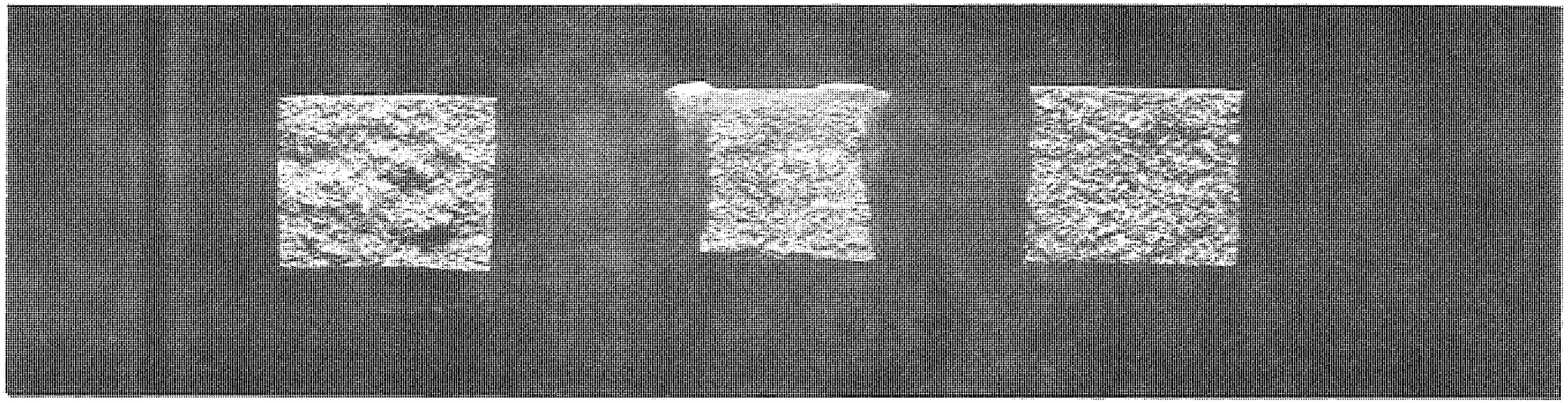

(A) Specimens from a submerged arc weldment in A 588 steel by Fabricator A (SA 588-A2). Left to right specimens are from weld metal, HAZ, and base metal.

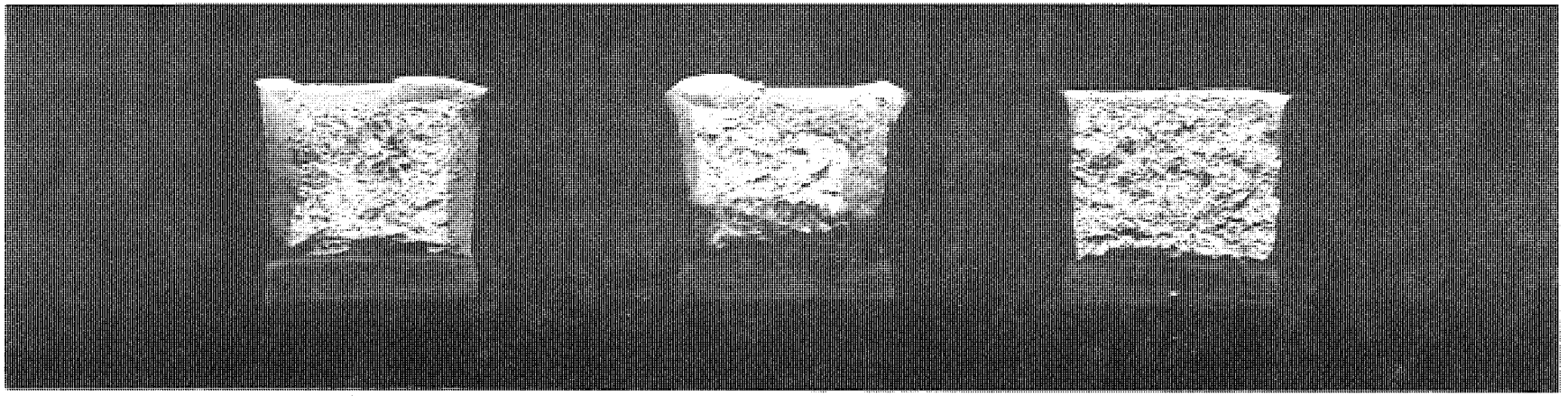

(B) Specimens from a submerged arc weldment in A 588 steel by Fabricator B (SA 588-B2). Left to right specimens are from weld metal, HAZ, and base metal.

Figure 43. Broken Charpy V-notch specimens showing the nature of the fractured surfaces through the various submerged arc weldment zones (test temperature 0 F).

most construction grade structural steels and weldments will undergo a temperature transition from a high, upper shelf energy level to a minimum, lower shelf energy level. The nature of this transition can be determined by conducting Charpy V-notch tests over the temperature range. The section of this transition-temperature curve of primary interest is the part that spans the range of service temperatures of the steel or weldment. Acceptance criteria often specify a minimum Charpy impact energy, such as 20 ft-lb, at some testing temperature, such as 0 F. The testing temperature, 0 F, is thus referred to as the 20 ft-lb transition temperature. This means that any testing on the steel above 0 F will yield energies above 20 ft-lb and any testing below 0 F will yield energies equal to or below 20 ft-lb. If, however, the service temperature of the steel (or weldment) goes significantly lower than 0 F, say -30 F for example, then the amount of decrease in energy below the 0 F level may be very important to the performance of the structure.

Electroslag and submerged arc weldments, similar to those tested at 0 F in the previous (Series I) acceptance testing, were tested over the temperature range of -40 to +40 F. These weldments were made in 3-in. thick by 16-in. wide plates. The weldments were sectioned into five blocks and Charpy specimens (in sets of five) were removed from all the various weld metal, heat-affected, and base metal zones in each block. Each weldment zone was then tested at the five temperatures -40, -20, 0, +20, and +40 F. The results of these tests are plotted as energy transition-temperature curves in Figures 44 through 47 for the electroslag weldments and in Figures 48 through 51 for the submerged arc weldments. The following discussion will attempt to draw out the pertinent findings displayed by these transition-temperature curves. It should be pointed out that in making comparisons between the cooled shoe and dry shoe electroslag weld metal zones, some of the differences seen could be partially due to the different welding wires used in the two methods. However, the alloy differences in the weldments tested are slight as is seen in Tables 5 and 6 and most of the trends can be reasonably attributed to the difference in the thermal cycles between the cooled and dry shoe electroslag welding techniques. Any trends in the transition-temperature curves that show an increase in the impact energy with a decrease in temperature are due to one of two reasons. First, all of the zones as defined are still somewhat non-homogeneous in themselves which leads to such variations. Second, due to the narrow width of some of the heat-affected zones, part of an adjoining zone sometimes was inadvertently included in the specimen and slightly biased the breaking energy.

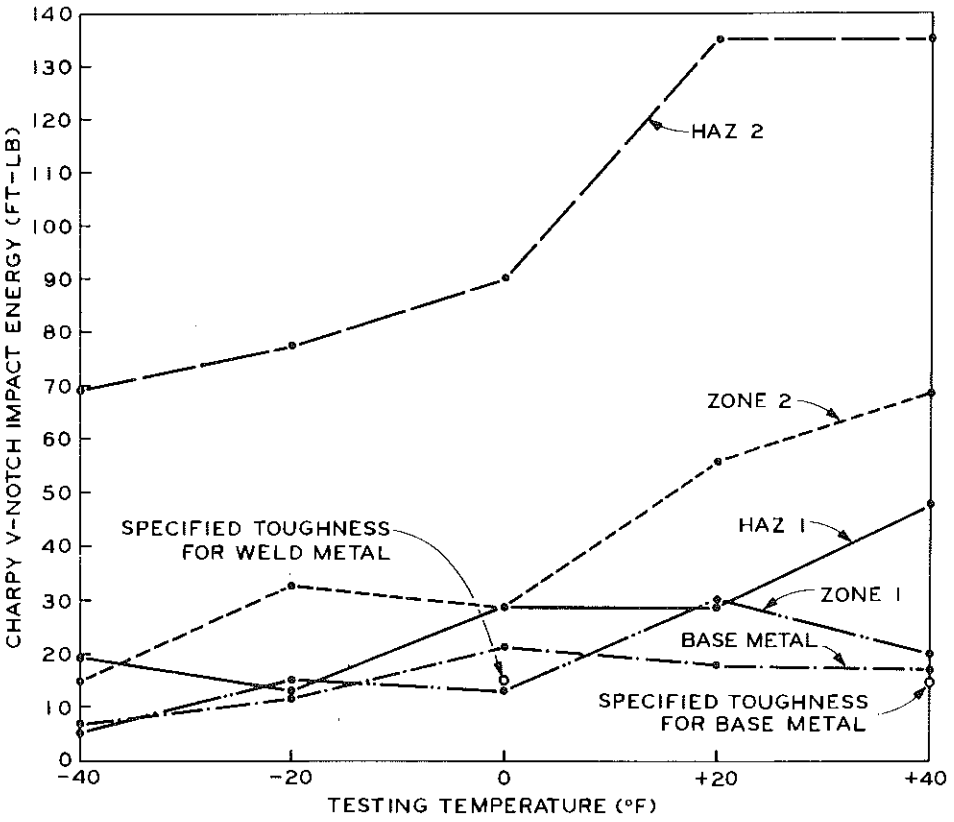

Figure 44. Energy transition-temperature curves for a cooled shoe electroslag weldment made in 3-in. A 588 steel (weldment ES 588-A2).

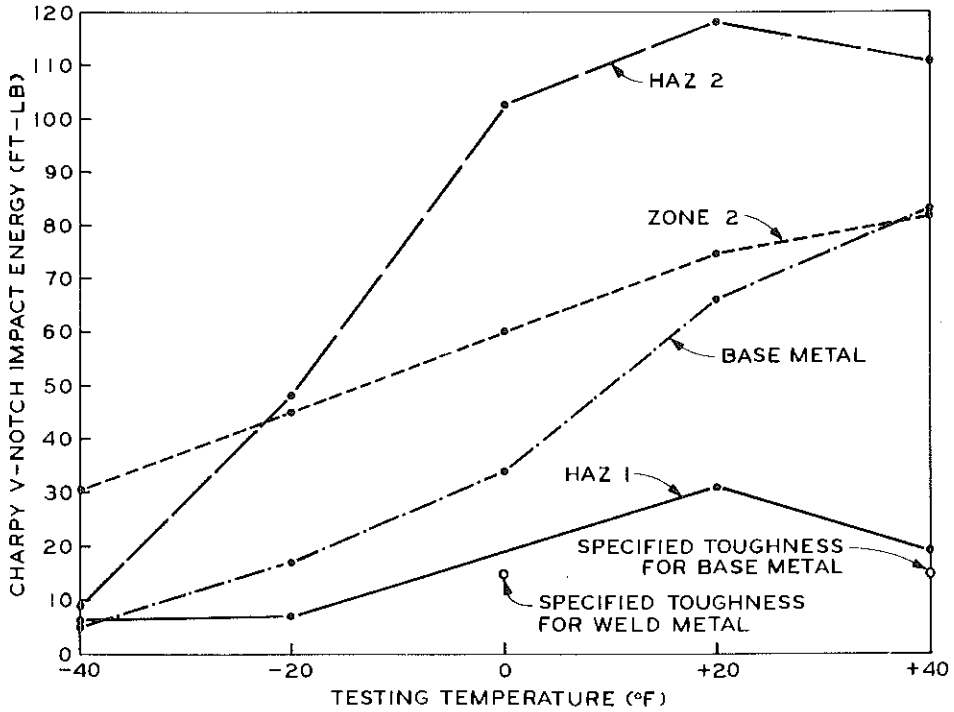

Figure 45. Energy transition-temperature curves for a dry shoe electroslag weldment made in 3-in. A 588 steel (weldment ES 588-B2).

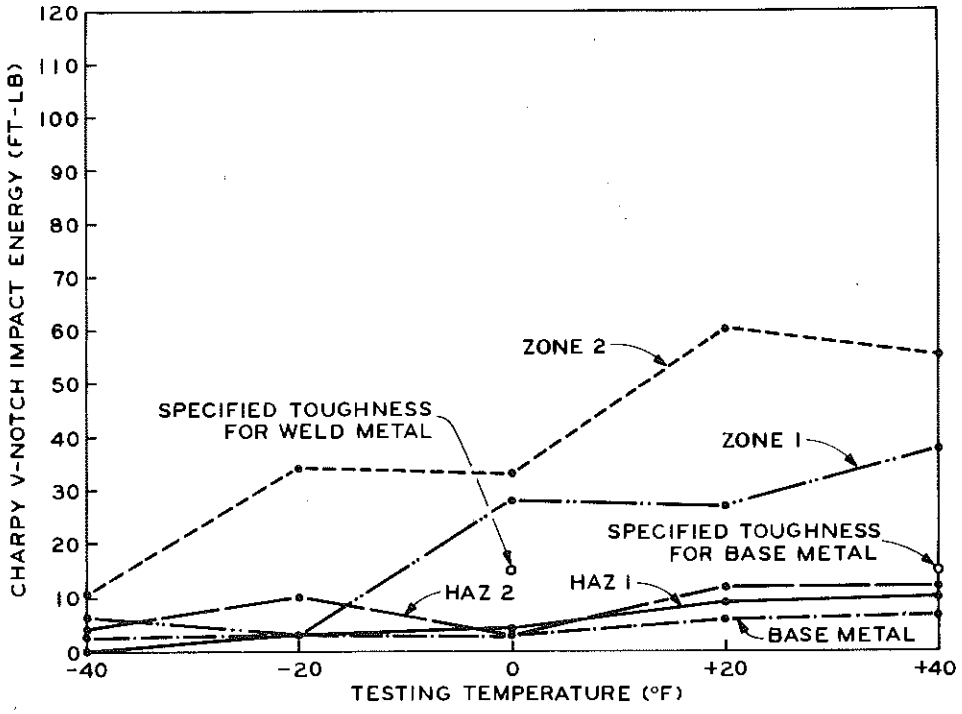

Figure 46. Energy transition-temperature curves for a cooled shoe electroslag weldment made in 3-in. A 36 steel (weldment ES 36-A2).

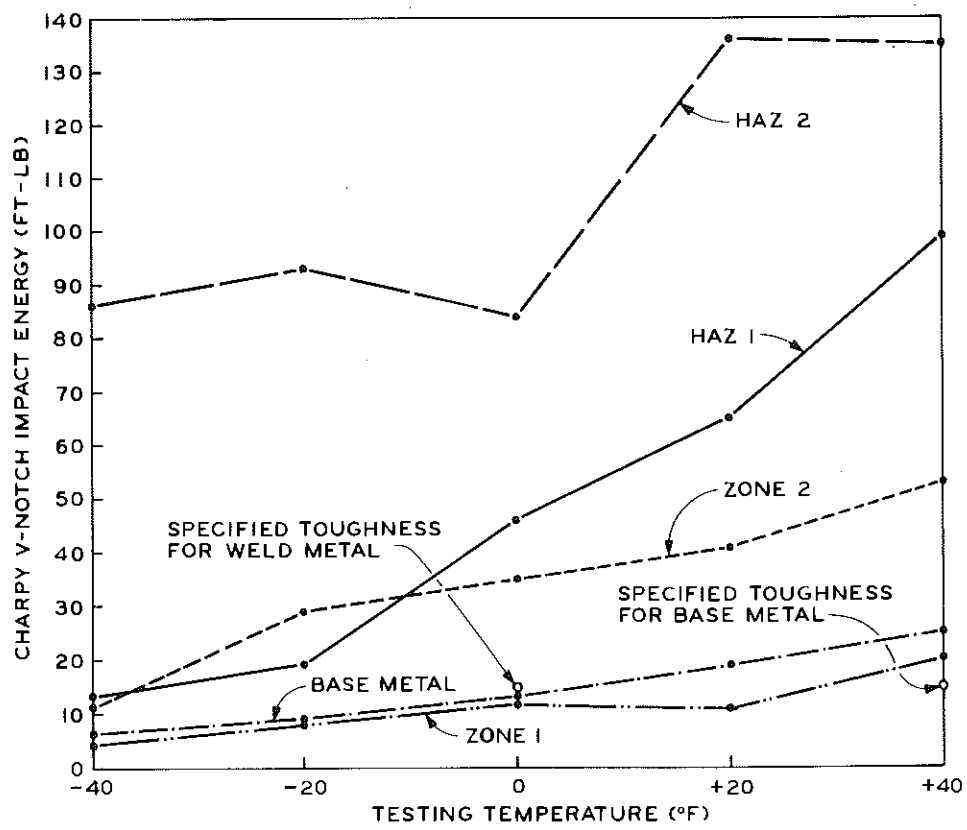

Figure 47. Energy transition-temperature curves for a dry shoe electroslag weldment made in 3-in. A 36 steel (weldment ES 36-B2).

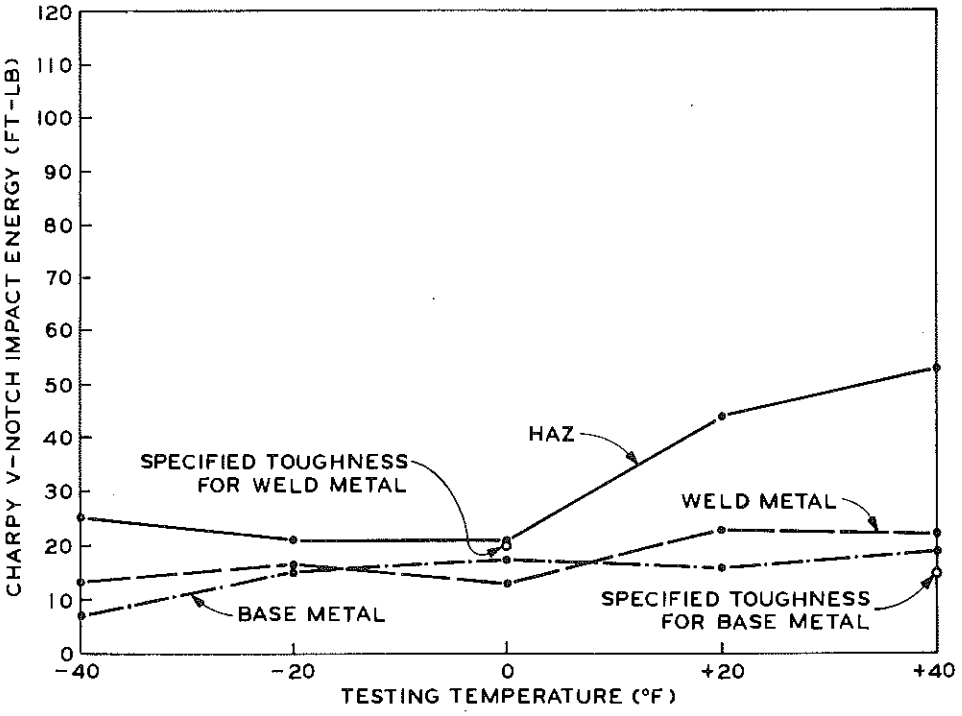

Figure 48. Energy transition-temperature curves for a submerged arc weldment by Fabricator A in 3-in. A 588 steel (weldment SA 588-A2).

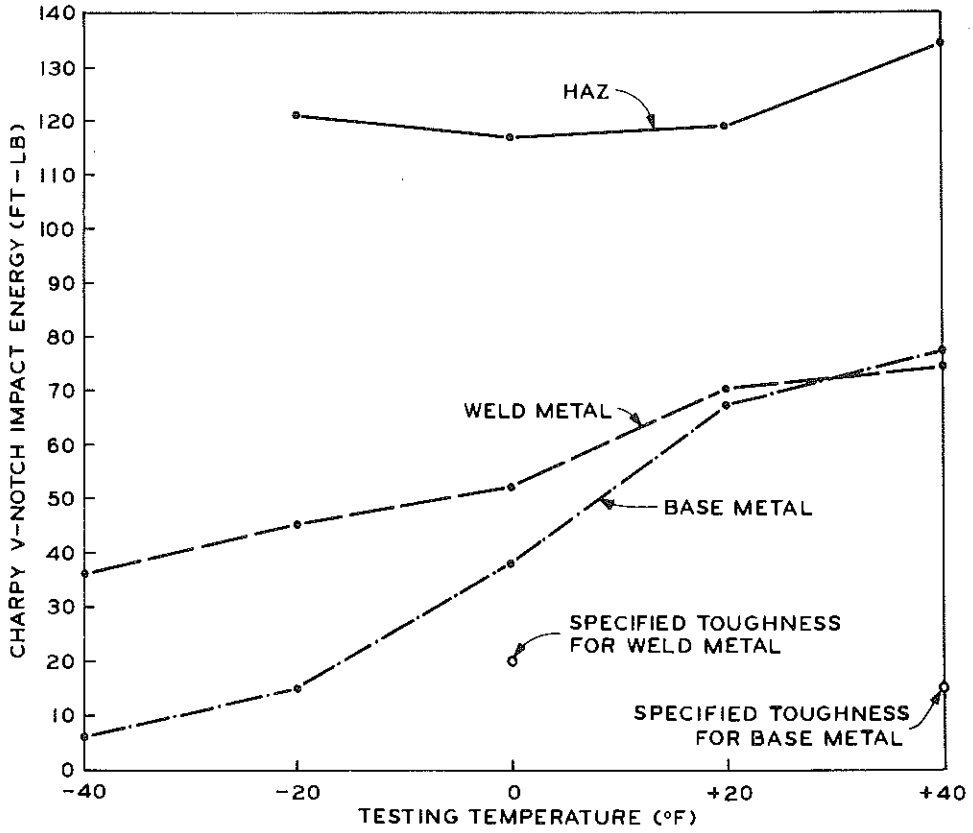

Figure 49. Energy transition-temperature curves for a submerged arc weldment by Fabricator B in 3-in. A 588 steel (weldment SA 588-B2).

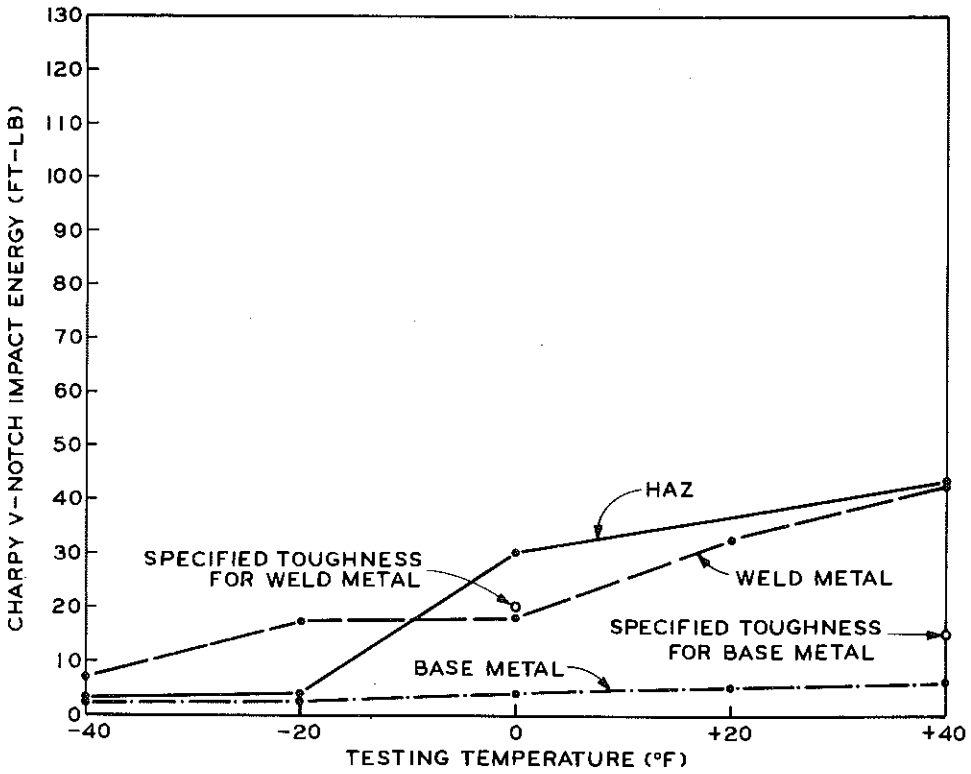

Figure 50. Energy transition-temperature curves for a submerged arc weldment by Fabricator A in 3-in. A 36 steel (weldment SA 36-A2).

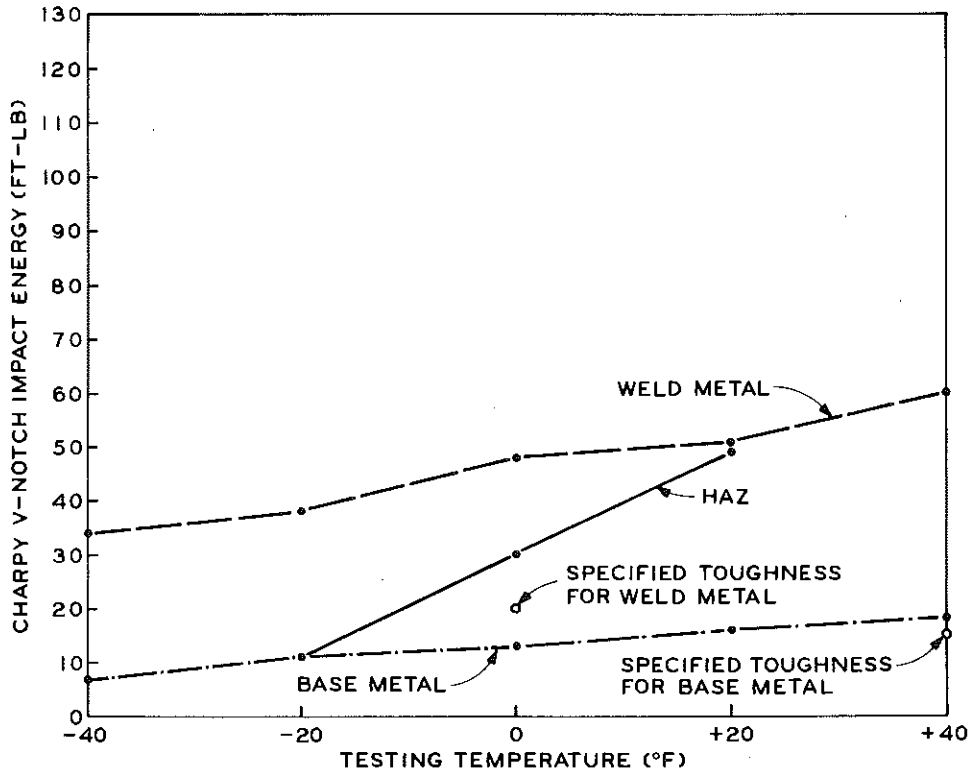

Figure 51. Energy transition-temperature curves for a submerged arc weldment by Fabricator B in 3-in. A 36 steel (weldment SA 36-B2).

The first discussion will be on the electroslag weldments in A 588 steel shown in Figure 44 for the cooled shoe method and Figure 45 for the dry shoe method. As seen in Figure 44, the Zone 1 weld metal (which consists of the thin columnar crystals that are oriented in the direction of welding), exhibits 20 ft-lb at +40 F and drops to 5 ft-lb at -40 F. Note that this Zone 1 falls short of the required 15 ft-lb at 0 F as was the case in the previous Series I on acceptance testing. The dry shoe weldment in Figure 45 had no Zone 1 weld metal. The Zone 2 weld metal (which consists of the coarse columnar crystals that are oriented at an acute angle with the direction of welding) exhibits very high toughness in both the cooled and dry shoe weldments. Even at -40 F, the absorbed energies are 15 and 30 ft-lb, respectively. The difference in impact strength exhibited by these two zones of weld metal is mainly due to the orientation of their long grain boundaries with respect to the direction of crack propagation in the Charpy test, as will be demonstrated in the anisotropic test series. In Figure 44 we see that the first heat-affected zone, HAZ 1 (which is a zone of grain coarsening due to overheating by the adjacent weld metal) exhibits higher toughness than the unaffected base metal at all temperatures. This can be explained by the fact that even though the primary structure of HAZ 1 is coarser than that of base metal, the secondary structure is much finer (Fig. 21) thus actually improving the impact toughness of the moderately tough base metal. On the other hand, in Figure 45 we see that HAZ 1 has the opposite effect on A 588 base metal with extremely high toughness. This illustrates that in a high toughness base metal, the grain coarsening present in the HAZ 1 primary structure can degrade the toughness. This points out the need to critically evaluate the effects of the heat-affected zones on the properties of the base metal when using electroslag welding. The effect of these heat-affected zones is always going to be relative to the initial properties of the base plate being welded. As would be expected by the grain refinement present in HAZ 2, its impact strength is greatly elevated over parent metal. The cooled shoe weld shows more increase in toughness of HAZ 2 than the dry shoe weld, possibly due to the initial difference in the base metal toughness as well as the finer structure present in the cooled shoe weld (compare Figs. 21(f) and 28(g)). It is interesting to note that the HAZ 2 in Figure 45 (dry shoe weldment) drops down to the base plate toughness at -40 F while the HAZ 2 in Figure 44 (cooled shoe weldment) remains at 70 ft-lb at -40 F. Comparing the transition curves for the base plate, we see that even though the plate in Figure 45 is extremely tough at temperatures above zero, the plates are almost equivalent at -20 F and below. This illustrates the fact that setting a certain toughness requirement on steel at some arbitrary temperature such as +40 F, doesn't necessarily guarantee adequate toughness over the whole range of service temperatures since toughness can decrease rapidly with temperature.

The next comparison to be made is for the electroslag weldments made in A 36 steel as shown in Figure 46 for the cooled shoe method and Figure 47 for the dry shoe. As seen in Figure 46, Zone 1 weld metal has high impact strength at 0 F and above but falls off rapidly to around 3 ft-lb at -20 F. Its resistance to brittle fracture at a service temperature of -20 F would most likely be low, even though the weld meets the requirement of 15 ft-lb at 0 F. Note that this Zone 1 weld metal tested considerably higher at 0 F than a similar weldment ES 36-A2, in Table 12. The Zone 1 weld metal in the dry shoe weldment exhibits low toughness as seen in Figure 47. It fails to meet the required 15 ft-lb at 0 F and remains inferior to base metal throughout the entire temperature range. The Zone 2 weld metal for both welding methods has very high toughness, not dropping below 30 ft-lb until tested below -20 F. Again it is the role of the orientation of the columnar crystals that causes the drastic difference in the impact strengths of the two weld metal zones. The effects of the heat-affected zones in A 36 steel is again dependent on the toughness of the base plate itself. In Figure 46 we see that both HAZ 1 and HAZ 2 have only a slight improvement over an extremely low toughness base plate. In Figure 47, however, where the base plate welded had a moderately high toughness, we see that HAZ 1 and HAZ 2 improve the toughness dramatically as was the case in the A 588 steel. We would further expect, as was shown in A 588 steel, that in an A 36 plate of very high toughness, the HAZ 1 would degrade the toughness due to its grain coarsening of the primary structure. The base metal itself, seen in Figure 46, represents low toughness A 36 steel that would possess little resistance to brittle fracture. In Figure 47, the base plate exceeds the required 15 ft-lb at 40 F and would be much more reliable in service. (Until recently there were no toughness requirements on A 36 steel and many structures are in service today with toughness curves similar to that shown in Figure 46.)

Figures 48 and 49 show the energy transition-temperature curves for the submerged arc weldments made in A 588 steel by Fabricators A and B, respectively. The weld metal in Figure 48 exhibits poor toughness, failing to meet the required 20 ft-lb at 0 F. The weld metal in Figure 49 exhibits very high toughness above 0 F and transitions between -20 and -40 F to 36 ft-lb, still a high level. As discussed before in the comparisons of the submerged arc welding of Fabricators A and B these energy curves show the difference between a poor weld resulting from an improper procedure and a good weld produced by using the proper procedure. Notice next the improvement over base plate toughness that is present in the HAZ. (The HAZ in a submerged arc weld is a zone of grain refinement of base metal. Grain coarsening can occur in the HAZ if interpass temperatures get too high, thus overheating the base metal adjacent to the weld.) Note also that the increase in toughness of the HAZ is a function of the initial base metal

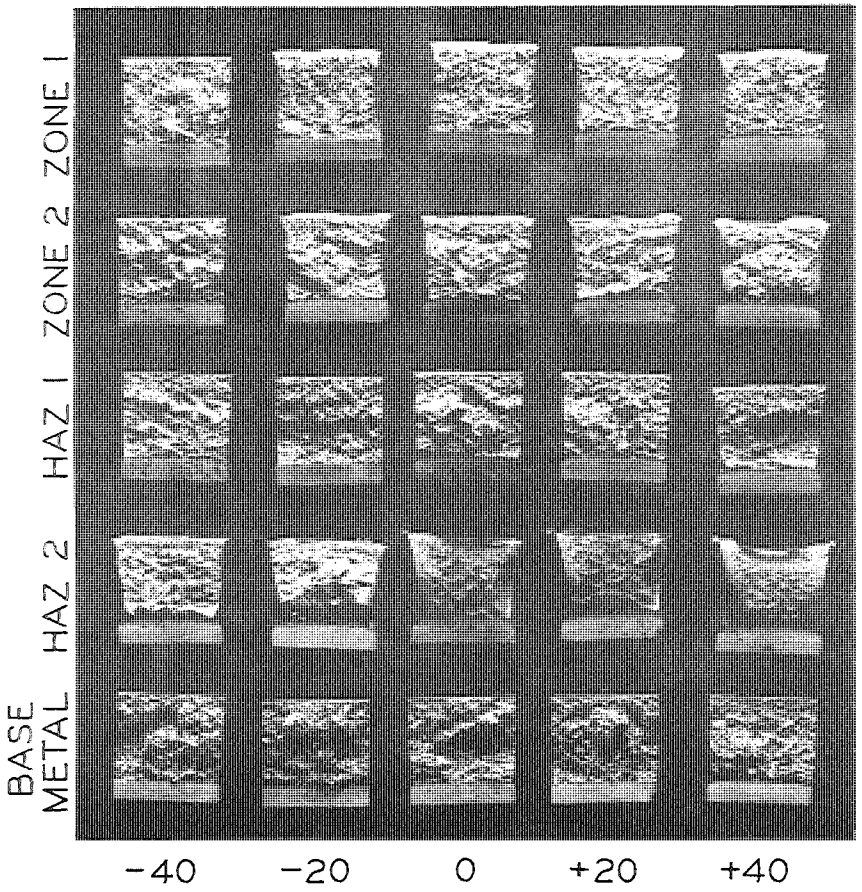

(A) Specimens from a cooled shoe electroslag weldment in A 588 steel (ES 588-A2). Top to bottom the rows are Zone 1 weld metal, Zone 2 weld metal, HAZ 1, HAZ 2, and base metal. (Taken from the tests reported in Fig. 44.)

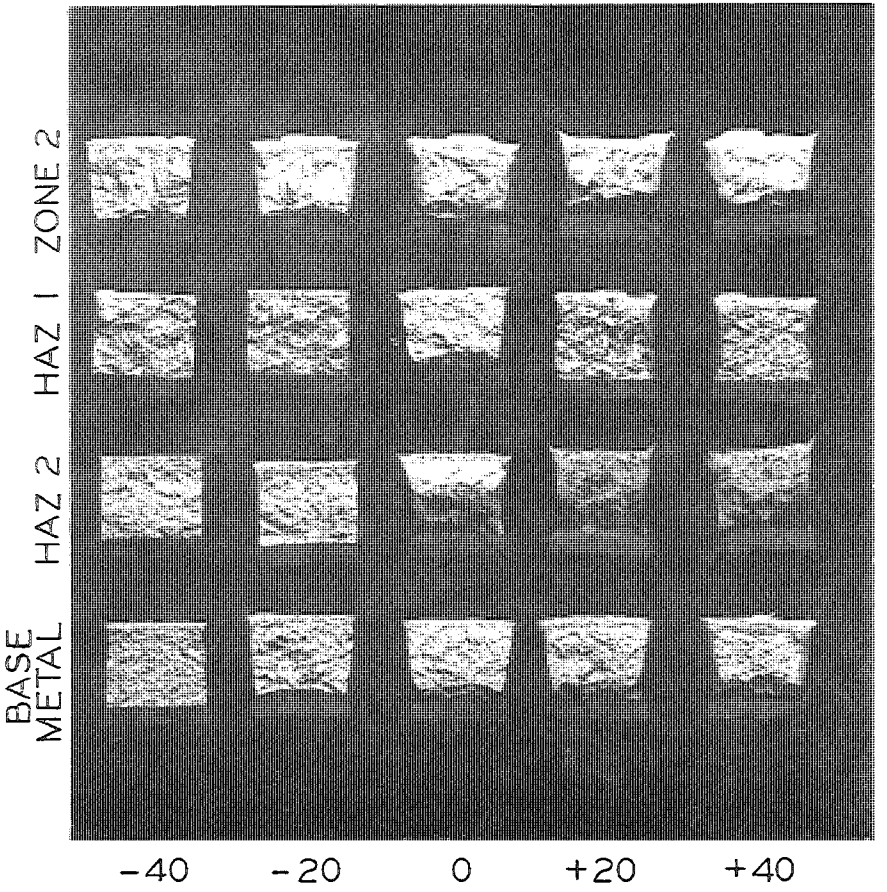

(B) Specimens from a dry shoe electroslag weldment in A 588 steel (ES 588-B2). Top to bottom, the rows are Zone 2 weld metal, HAZ 1, HAZ 2, and base metal. (Taken from the tests reported in Fig. 45.)

Figure 52. Broken Charpy V-notch specimens from the energy transition-temperature testing showing the nature of the fractures through the various electroslag weldment zones at the different testing temperatures. Left to right, the columns represent test temperatures of -40, -20, 0, +20, and +40 F.

toughness, as seen by the extreme improvement of the HAZ in Figure 49 where base metal toughness was high. Again it is interesting to note that the extreme toughness present in the base metal of Figure 49 decreases continuously at temperatures below 0 F.

Figures 50 and 51 show the test results for submerged arc weldments in A 36 steel by Fabricators A and B, respectively. The weld metal in Figure 50 shows good toughness at +40 F but transitions rapidly to below the required 20 ft-lb at 0 F. As before (Fig. 48) the problem with this weld metal stems from an improper procedure. The weld metal in Figure 51 exhibited very good toughness, even at -40 F. In both weldments we see that the heat-affected zone improves the toughness over base metal at temperatures above -20 F. It's interesting to note that in Figure 46, the two electroslag HAZs had no dramatic affect on the low toughness base metal but in Figure 50 the HAZ in the submerged arc weldment did. A misconception that is not uncommon is that a weldment placed in a low toughness steel with high weld/base metal dilution cannot be expected to be high in toughness. However, as shown in this example, the toughness of the steel itself can be greatly elevated by a heat treatment (such as that occurring in the weld HAZ). One of the major factors in the resulting weld metal toughness will thus be the thermal cycle involved, which can overcome many effects of base metal dilution (as long as the base metal has an acceptable alloy chemistry).

Presented in Figures 52 through 54 are arrays of broken Charpy specimens taken from the impact tests reported in Figures 44 through 51. These specimens are arranged in rows corresponding to the various weldment zones and columns corresponding to the testing temperatures covered from -40 to +40 F. These fractographs are included for completeness in presenting the results of the energy transition-temperature tests. Many fruitful observations can be made by retracing the discussions of the energy transition curves and noting how the various energy transitions are exhibited by changes in the fracture surfaces. In particular note how the lateral expansion and shear lip will increase with increasing toughness and how the two zones of electroslag weld metal maintain a fracture surface that reveals the primary microstructures present.

The pertinent question, concerning how much Charpy V-notch impact energy at what temperature will preclude the possibility of brittle fracture in a welded structure, is undergoing careful scrutiny at the present. One school of thought is that some minimum acceptable value, such as 20 ft-lb, should be provided by the material at its lowest service temperature. The less conservative point of view is usually employed in bridge construction that if we specify some toughness level, say 20 ft-lb, at a temperature such

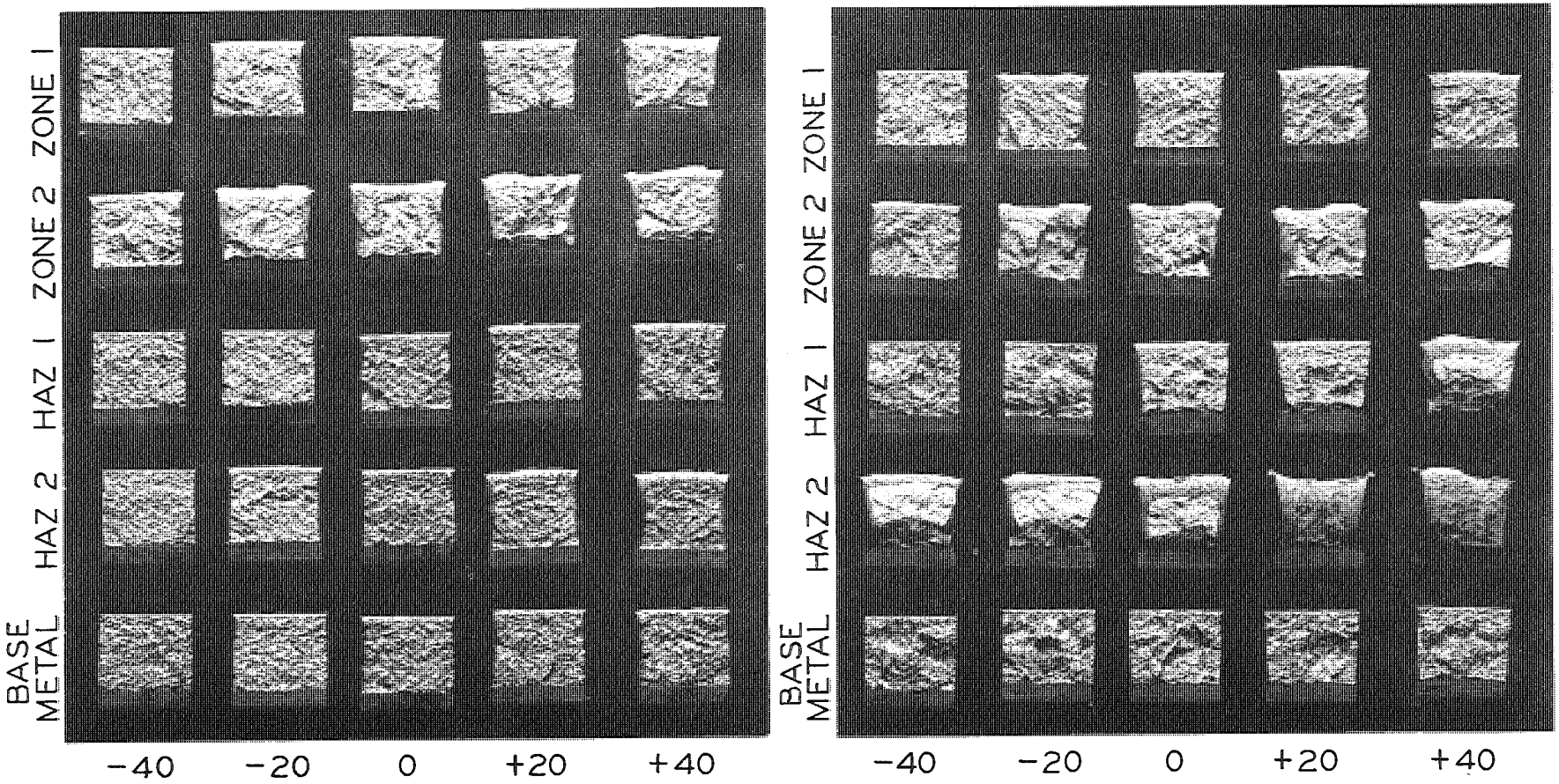

(A) Specimens from a cooled shoe electroslag weldment in A 36 steel (ES 36-A2). Top to bottom, the rows are Zone 1 weld metal, Zone 2 weld metal, HAZ 1, HAZ 2, and base metal. (Taken from the tests reported in Fig. 46.)

(B) Specimens from a dry shoe electroslag weldment in A 36 steel (ES 36-B2). Top to bottom, the rows are Zone 1 weld metal, Zone 2 weld metal, HAZ 1, HAZ 2, and base metal. (Taken from the tests reported in Fig. 47.)

Figure 53. Broken Charpy V-notch specimens from the energy transition-temperature testing showing the nature of the fractures through the various electroslag weldment zones at the different testing temperatures. Left to right, the columns represent test temperatures of -40, -20, 0, +20, and +40 F.

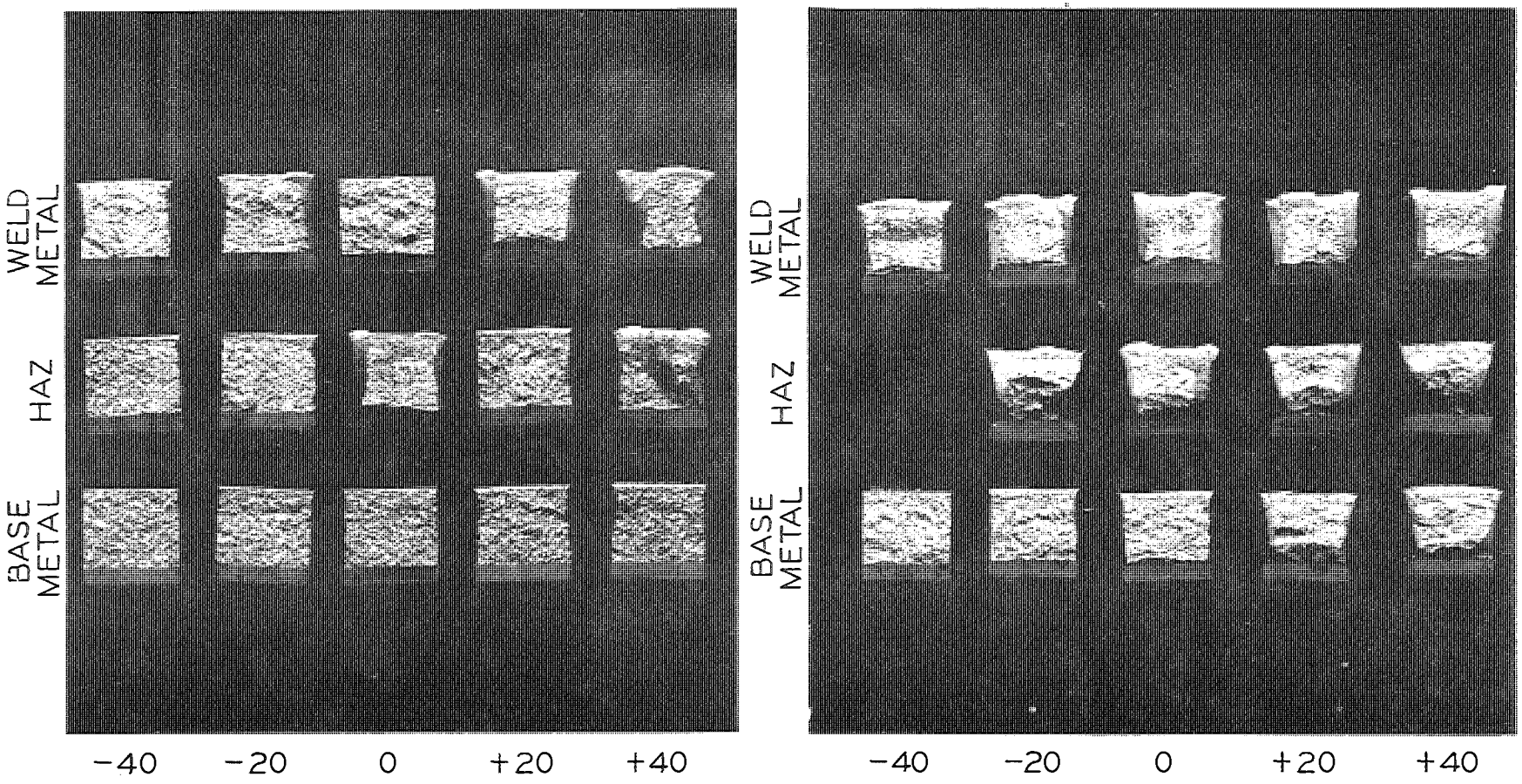

(A) Specimens from a submerged arc weldment in A 36 steel by Fabricator A (SA 36-A2). Top to bottom, the rows are weld metal, HAZ, and base metal. (Taken from the tests reported in Fig. 50.)

(B) Specimens from a submerged arc weldment in A 588 steel by Fabricator B (SA 588-B2). Top to bottom, the rows are weld metal, HAZ, and base metal. (Taken from the tests reported in Fig. 49.)

Figure 54. Broken Charpy V-notch specimens from the energy transition-temperature testing showing the nature of the fractures through the various submerged arc weldment zones at the different testing temperatures. Left to right, the columns represent test temperatures of -40, -20, 0, +20, and +40 F.

as 0 F, above the lowest service temperature, then we have "screened out" the brittle material and will get adequate toughness from the rest. The shortcoming of this approach is that one has no idea of how the energy transitions below the testing temperature, which can vary considerably as shown in the previous discussion. The most recent and promising approach to the problem is that proposed by Barsom (3, 8) who has established the validity of a relationship between the Charpy V-notch test and the plane strain fracture toughness, K_{IC}, as defined by ASTM E 399, for certain structural steels. This approach also takes account of the relationship between the strain rate experienced in service loading and that applied in testing. If these correlations prove valid for weld metal, toughness criteria can be based on the Charpy impact test and related to inherent weld metal toughness as measured by the K_{IC} test. This approach would allow the actual "design" against brittle failure occurring in a structure. Before such an approach can be assumed, however, much work needs to be done to establish the temperature-transition characteristics of weld metal toughness as measured by the Charpy V-notch specimen and the K_{IC} specimen and how they relate. Work to date has not been able to properly account for the role of the residual stress fields present in a weld (3).

Series III - Anisotropic Properties of Electroslag Weld Metal Impact Toughness

Grain structures such as those present in Zone 1 and Zone 2 electroslag weld metal are highly susceptible to anisotropies (or directional variations) in mechanical properties. Such directional variation is expected in the property of impact toughness since the large columnar grain boundaries may provide a path of low resistance to crack propagation. As mentioned in the section on tensile testing of electroslag weldments, these grain structures undoubtedly will likewise effect the tensile properties of yield point and ductility as measured by percent elongation or reduction in area, although no testing was done to quantify these effects.

Three types of electroslag weldments were tested for variations in Charpy impact toughness as the direction of crack propagation is varied with respect to the long axis of the columnar crystals of Zone 1 and Zone 2 weld metal. Figure 55 defines the specimen orientations used in assessing these directional variations. The angle θ is taken to be the angle between the direction of crack propagation in the Charpy specimen and the longitudinal axis of the weld. Theta = 0° is the standard orientation for impact testing of the weld metal. The angle ϕ is the angle between the long axis of the Zone 2 coarse columnar crystals and the longitudinal axis of the weld. Zone 1 weld metal was tested at the angle θ = 0°, which gives the crack a direction that is nearly parallel to the fine columnar crystals present in the

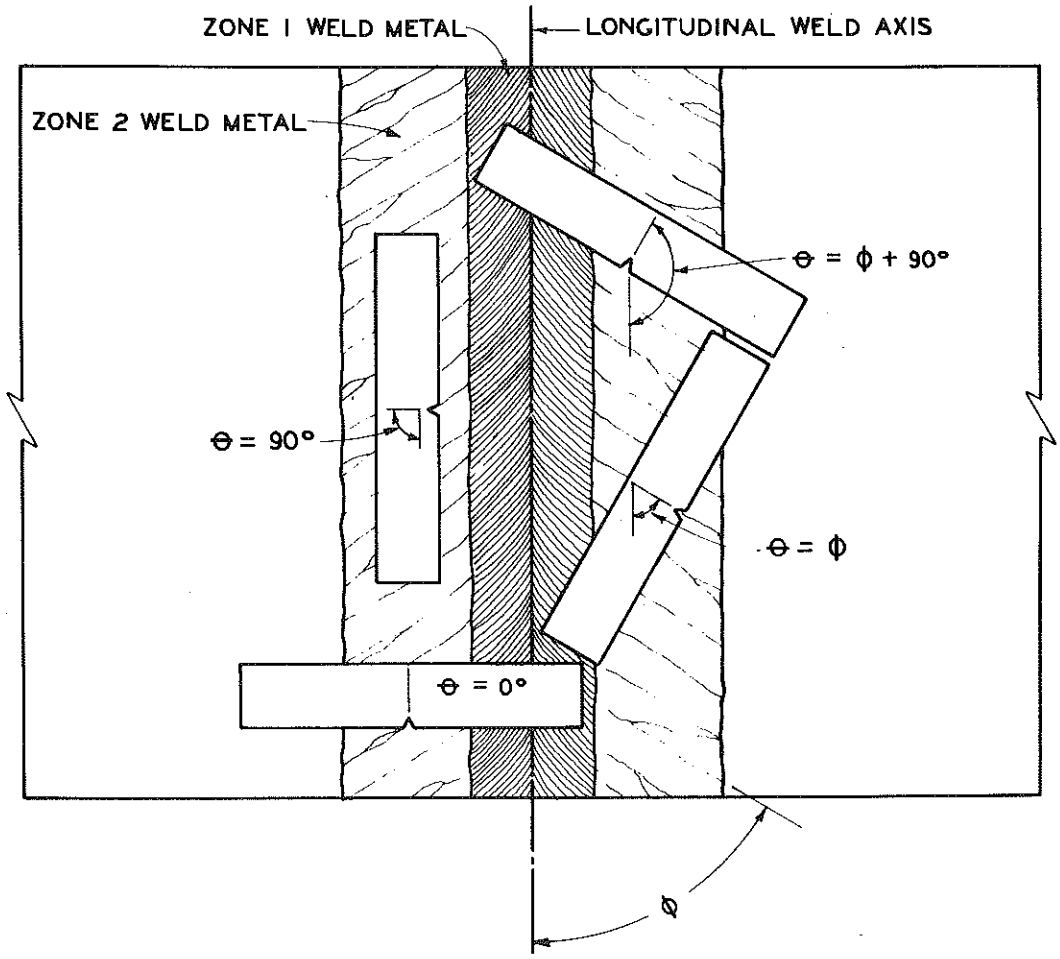

Figure 55. Specimen orientations used in testing the anisotropic nature of the Charpy impact toughness of electroslag weld metal. The angle θ is the angle between the direction of crack propagation in the Charpy specimen and the longitudinal axis of the weld. ($\theta = 0$ is the standard Charpy testing direction.) The angle ϕ is the angle between the long axis of the Zone 2 weld metal crystals and the longitudinal axis of the weld.

welds tested, and $\theta = 90°$ which causes fracture across the grains. Zone 2 weld metal was tested at the angles $\theta = 0°$, $90°$, $\Phi + 90°$, and Φ (Fig. 55). The results of these tests are shown in Table 15.

In the electroslag weldment made by the cooled shoe process in A 36 steel (ES 36-A2) we see that the Zone 1 weld metal tested in the standard testing direction, $\theta = 0°$, had a toughness of 10 ft-lb at 0 F. However, testing at $\theta = 90°$, the same Zone 1 weld metal had a toughness of 41 ft-lb at 0 F. Thus, in the A 36 alloy, the Zone 1 weld metal exhibited four times

greater toughness in a direction transverse to its columnar grain structure than it had in a direction nearly parallel to the long axis of the grains. In the similar electroslag weldment made in A 588 steel (ES 588-A2) the Zone 1 weld metal had a toughness of 22 ft-lb at the angle $\theta = 0°$ and 19 ft-lb at the angle $\theta = 90°$. Thus the alloy composition of A 588 steel seems to compensate for the anisotropic (i.e., directional) effects of the Zone 1 grain structure on the impact toughness. This is understandable since the amounts of nickel and chromium that are present in A 588 steel could strengthen the prior austenite grain boundaries enough to overcome their unfavorable orientation. Thus, we conclude that the Zone 1 weld metal is anisotropic in impact toughness in A 36 steel, but that the alloy composition of the A 588 steel seems to compensate for the anisotropy.

TABLE 15
ANISOTROPIC CHARPY IMPACT TEST RESULTS
ON ELECTROSLAG WELD METAL
(Test Temperature 0 F)

Weldment Type (See Table 2)	Impact Toughness (ft-lb) in the Θ Direction[1]			
	$\Theta = 0°$	$\Theta = 90°$	$\Theta = \Phi + 90°$	$\Theta = \Phi$
ES 36-A2				
Zone 1 Weld Metal	10(3)[2]	41(2)		
Zone 2 Weld Metal	51(3)	52(1)	54(3)	25(3)
ES 36-B2				
Zone 1 Weld Metal	N. T.[3]	N. T.		
Zone 2 Weld Metal	69(3)	N. T.	64(3)	33(2)
ES 588-A2				
Zone 1 Weld Metal	22(3)	19(2)		
Zone 2 Weld Metal	33(3)	32(5)	34(3)	23(3)

[1] Θ is the angle between the direction of cracking in the Charpy specimen and the longitudinal axis of the weld. Φ is the angle between the long axis of the Zone 2 weld metal crystals and the longitudinal axis of the weld (see Fig. 55).
[2] Number in brackets is the number of specimens tested to give the average value shown.
[3] N. T. denotes not tested.

A similar trend is seen in the Zone 2 weld metal. In weldments ES 36-A2 and ES 36-B2, electroslag welds in A 36 steel produced by the cooled shoe and dry shoe methods, respectively, the lowest toughness is obtained by propagating the Charpy test crack in the direction $\theta = \Phi$, which is parallel to the long axis of the grains and forces the fracture along the grain boundaries. In weldment ES 36-A2, the directions $\theta = 0°$, 90° and $\Phi + 90°$

are all transgranular types of fracture and produce twice the impact toughness of that measured at $\theta = \phi$. In weldment ES 36-B2 the test directions $\theta = 0°$ and $\phi + 90°$ produce approximately three times the toughness of the direction $\theta = \phi$. In weldment ES 588-A2, a cooled shoe weld in A 588 steel, the directions $\theta = 0°$, 90°, and $\phi + 90°$ give approximately a 40 percent increase in the impact toughness as compared to that measured in the direction $\theta = \phi$. The alloy strengthening of the grain boundaries in A 588 steel is still present but not as effective as it was in the Zone 1 weld metal. We conclude, then, that the large grain structure present in the Zone 2 weld metal produces a significant reduction in the impact toughness in the direction parallel to the long axis of the grains but is partially compensated for in A 588 steel by the alloying effects in the grain boundaries.

The fractographs in Figures 56 through 58 reveal the nature of the crack propagation path in the Charpy specimens oriented at the various test angles. In all cases the fracture path was predominately intergranular (i.e., along grain boundaries) when the crack propagation direction was initiated parallel to the columnar grain's long axis and transgranular (i.e., across the grains) when the crack direction was at an angle to this grain axis. The effect is much more pronounced in the A 36 steel than in A 588. Zone 1 weld metal showed no anisotropy of impact properties in the A 588 steel. However, the Zone 2 weld metal in A 588 did show a reduction of about 45 percent in toughness in the direction parallel to the grains.

When an electroslag butt joint weldment is loaded in uniaxial tension, such as in a bridge beam, the anisotropies that have been shown to exist are not too serious. The Zone 1 weld metal has a severe weakening of impact properties along the main axis of the weld ($\theta = 0°$) but fortunately this is the direction of crack propagation in the standard acceptance testing. The problem that does exist is that most specifications don't require testing of the Zone 1 weld metal at all. An additional problem is the probable anisotropic nature of the Zone 1 weld metal ductility that was mentioned previously in the section on tensile properties. The plane of minimum toughness in the Zone 2 weld metal will usually lie between 50° to 65° (i.e., $\theta = \phi$) from the longitudinal axis of the weld. Under the normal uniaxial loading condition, the toughness measured at $\theta = 0°$ corresponds to the applied loading. However, if an electroslag weldment is put into a highly restrained joint or a state of biaxial loading, the low toughness measured along the axis of the columnar crystals could become very critical. Very careful analysis and testing should be carried out if such an application were to arise in an electroslag welded joint. To be safe, fracture toughness testing should be carried out in all of the various directions whenever "as welded" electroslag joints are subjected to a biaxial or triaxial stress con-

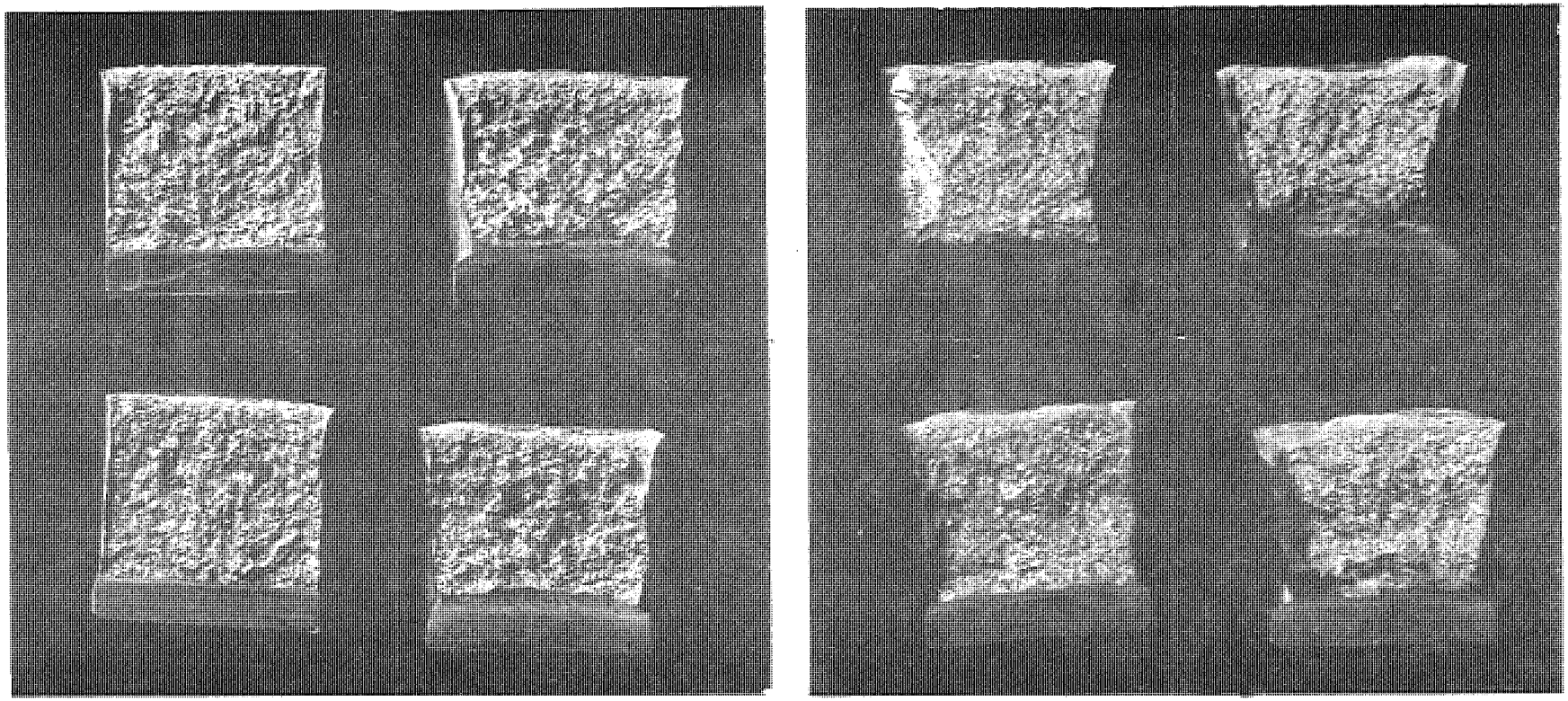

(A) Specimens from Zone 1 weld metal. Surfaces shown on the left are from a $\theta = 0$ degree specimen, note the fine columnar crystal structure revealed. Surfaces shown on the right are from a $\theta = 90$ degree specimen that had four times more toughness.

(B) Specimens from Zone 2 weld metal. Surfaces on left are from a $\theta = \phi$ specimen, note the grain boundary facet exposed. Surfaces on the right are from a $\theta = 0$ degree specimen that had twice the toughness, note the increase in lateral expansion and shear lip.

Figure 56. Fractographs of broken Charpy specimens taken from the anisotropic test series on a cooled shoe electroslag weld in A 36 steel (ES 36-A2) (test temperature 0 F).

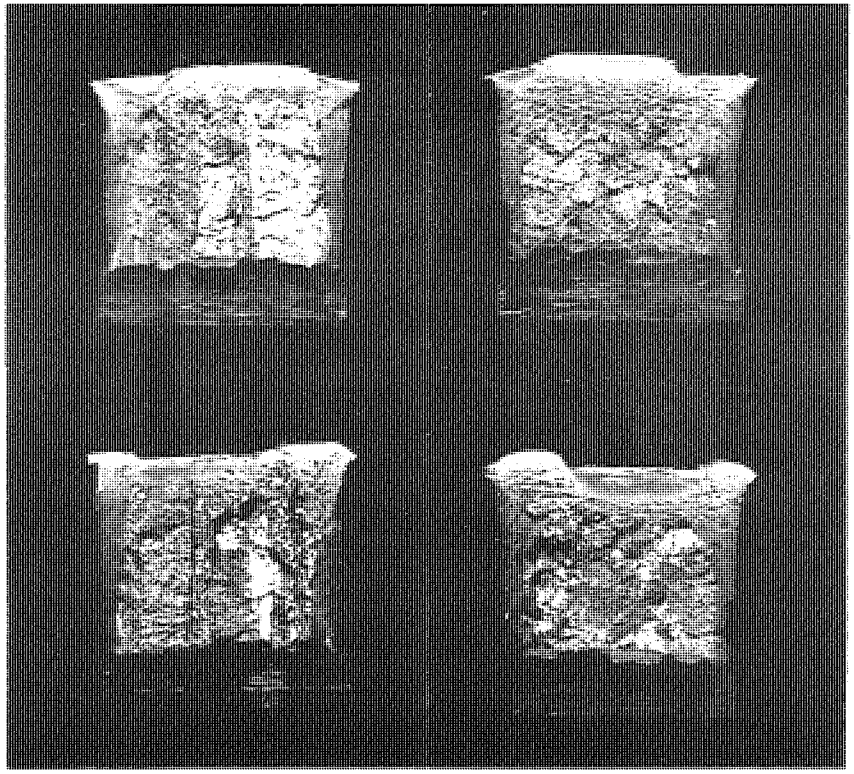

(A) Specimens from Zone 2 weld metal. Surfaces on the left are from a $\theta = \phi$ specimen, note the facets showing the grain boundary fracture path. Surfaces on the right are from a $\theta = 0$ degree specimen with three times the toughness, note the change in fracture mode to transgranular.

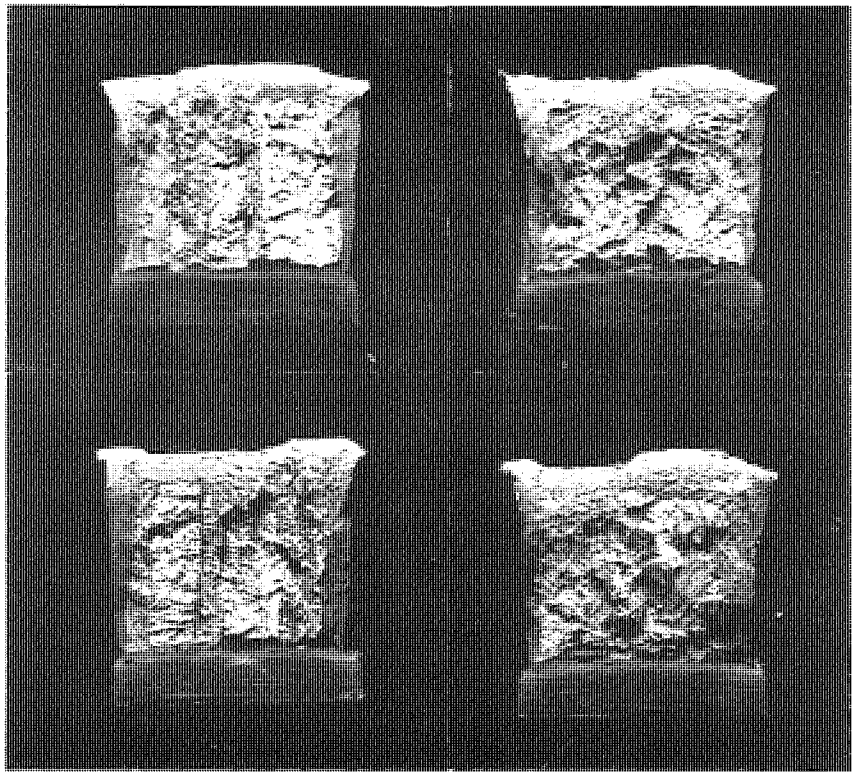

(B) Specimens from Zone 2 weld metal showing same surface on left as in (A). Surfaces on the right are from a $\theta = \phi + 90$ degree specimen with three times the toughness, again showing a transgranular type of fracture.

Figure 57. Fractographs of broken Charpy specimens taken from the anisotropic test series on a dry shoe electroslag weld in A 36 steel (ES 36-B2) (test temperature 0 F).

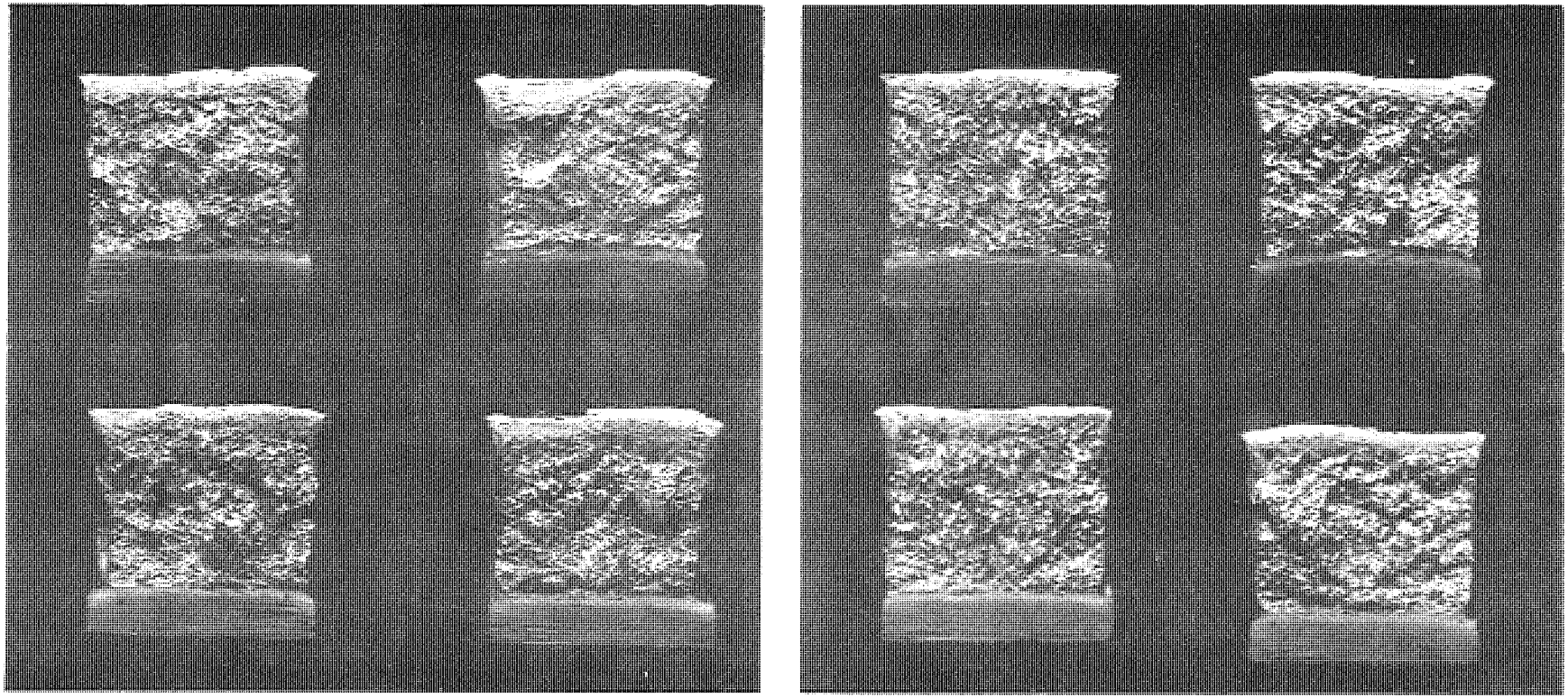

(A) Specimens from Zone 1 weld metal. Surfaces on the left are from a $\Theta = 0$ degree specimen and those on the right are from a $\Theta = 90$ degree specimen. Fracture surfaces reveal intergranular and transgranular cracking, respectively, but the toughness was equivalent.

(B) Specimens from Zone 2 weld metal. Surfaces on the left are from a $\Theta = \phi$ specimen and those on the right are from a $\Theta = 0$ degree specimen. The toughness in the ϕ direction was about 45 percent lower than in the $\Theta = 0$ degree direction. Grain boundary cleavage is not as evident as in the A 36 weldments.

Figure 58. Fractographs of broken Charpy specimens taken from the anisotropic test series on a cooled shoe electroslag weld in A 588 steel (ES 588-A2) (test temperature 0 F).

dition. The point that needs to be made is that the anisotropic nature of electroslag weld metal properties is dependent on the alloy composition. No generalization can be made to predict the direction of minimum strength (impact or tensile) with respect to the grain structures present. Only by testing in the various directions can this be determined. An additional problem arising in the use of "as welded" electroslag butt joints is the variation that occurs along the length of the weld in the angle ϕ (the angle between the Zone 2 columnar crystals and the weld axis). A slight shift in ϕ could significantly alter the state of stress in the plane of the columnar grain boundaries. Such fluctuations in the state of stress along the ϕ direction would have to be accounted for in the original design to preclude the possibility of exceeding a failure condition along this plane (especially in biaxial or triaxial stress conditions). The primary lesson to be learned here is that the coarse grain structure resulting from this type of welding, can significantly alter the properties of the metal, depending upon the location and orientation of the applied stress or strain. This could have serious consequences, especially in highly restrained weldments subjected to biaxial or triaxial states of stress.

Fatigue-Notch Sensitivity Evaluation

A program of constant amplitude, axial fatigue testing of notched tensile specimens was conducted to determine the qualitative effects of the various metallurgical zones present in electroslag and submerged arc weldments on fatigue crack initiation from a pre-existing flaw or discontinuity. It has been established that in fatigue failures of bridge beams, the fatigue cracks invariably originate at some fabrication flaw or geometric discontinuity and that the major part of the life of a beam is consumed in the initiation of a fatigue crack from the flaw or discontinuity (4). The type of testing needed to properly evaluate the fatigue properties of an electroslag welded plate girder is full-scale beam testing, such as that conducted on submerged arc welded girders in Ref. (4). Not having the facilities to do this full-scale testing, we decided that the notched specimen testing would at least give a qualitative comparison between the various electroslag and submerged arc weldment zones. Full-scale beam testing of electroslag weldments is scheduled as part of the current NCHRP Project 10-10 "Acceptance Criteria for Electroslag Weldments in Bridges," being conducted by the U. S. Steel Corporation (12). Hopefully, completion of this full-scale testing will give a quantitative comparison of electroslag butt weldments, with the known properties (4) of submerged arc butt weldments.

The notched-specimen fatigue work was designed and conducted in accordance with ASTM E 466, "Constant Amplitude Axial Fatigue Tests of Metallic Materials," (17). The objective of this evaluation was in accord-

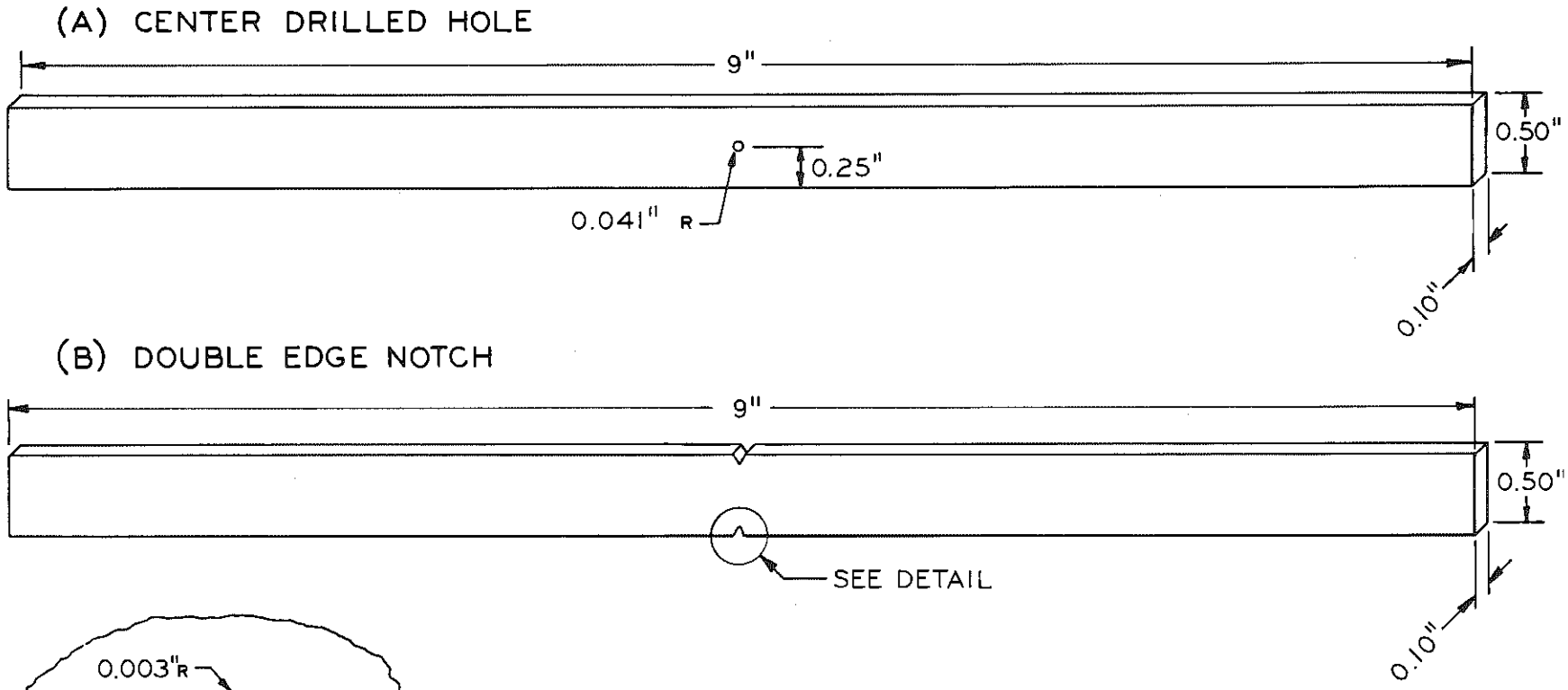

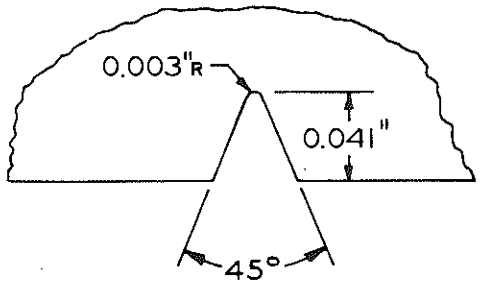

Figure 59. Details of notched-fatigue tensile specimens.

(A) Specimen with center hole crack starter ($K_t = 2.6$).

(B) Specimen with double edge notch crack starter ($K_t = 28$).

ance with the stated "significance" of ASTM E 466 that such tests "...may be used as a guide to the selection of metallic materials for service under conditions of repeated direct stress." In other words, this type of test is recognized as a qualitative method of ranking various metals as to their fatigue properties. The objective was to rank the various metallurgical zones in the weldments with respect to their resistance to crack initiation in the presence of a controlled notch condition. These results cannot be directly applied to design conditions in a girder because the conditions of service loading are not exactly paralleled in the test. However, the results can reveal any significant differences in the fatigue susceptibility of the various weldment zones.

The specimens used in the notched-fatigue tests were tensile plate specimens with details as shown in Figure 59. Two series of tests were run, the first using the relatively mild crack starter shown in Figure 59a, a center drilled hole of radius 0.041 in., and the second using a severe crack starter with the double edge notch having a terminal radius of 0.003 in. The theoretical elastic stress concentration factors, K_t, for the two notch conditions and the geometry shown are 2.6 and 28, respectively (18). (The maximum theoretical elastic stress occurs at the notch tip and is equal to K_t times the nominal stress based on the net section area.) The specimens were finished (longitudinally) smooth on the surfaces with a surface grinder and very close tolerances were maintained on all dimensions and notch conditions. In each test the nominal stress applied was based on the actual net section of each specimen which was measured on an optical comparator at 40x magnification. A cyclic tensile stress range was applied to the specimens using electro-hydraulic testing equipment with closed-loop control. Self-aligning grips that pivot on spherical seats were used for gripping the specimen. These grips eliminated possible bending effects on the specimens, that could arise from misalignment. The stress ranges applied maintained tension on the specimen and used a sinusoidal forcing function with the frequency between 20 and 40 cps. Steel is insensitive to frequency effects at such low frequencies. The failure criterion applied to the specimen was complete separation of the specimen by cracking. Observation of specimen failures established that nearly 100 percent of the cycle life of a specimen was consumed before the fatigue crack became visible. Once visible, the specimen would fail in a few additional cycles. With the small size of specimen used, the fatigue test was entirely a measure of the load cycles required to initiate a fatigue crack at the tip of a pre-existing flaw. No information was derived on fatigue crack propagation rates through the various weldment zones.

The specimens were removed from the weldments with their long axis transverse to the weld (i.e., in the direction across the weld, the direction

of applied stress in service loading) and their 0.50-in. face located in the transverse cross-section through the thickness of the weldment. Before the specimens were notched they were macroetched to define the exact location of the weld metal and heat-affected zones. The locations of the notches were carefully marked in the various zones to be tested and then machined. After machining, all notch parameters were verified on an optical comparator at 40x magnification to establish conformance with the specified condition. Three replications were made in each zone of each weldment tested. Additional replications would have been more desirable for statistical validity, but time and available funds limited the number of tests that could be run. Also, three was the number of specimens tested previously in a similar type of study on submerged arc weld metal (4).

The weldments tested include cooled shoe (Fabricator A) and dry shoe (Fabricator B) electroslag in 1-3/4 and 3-in. plates in both A 588 and A 36 steels; and submerged arc weldments made by both fabricators in the same thicknesses and steels. Two series of tests were conducted, the first using the center hole crack starter and the second using the double edge notch crack starter. These two conditions were selected as representative of a relatively mild type of flaw (center hole) such as might arise from an inclusion or porosity bubble, and a relatively severe type of flaw (double edge notch) such as that formed by a weld crack or lack of fusion defect. Much sharper flaw tips can occur in a weld than that of the 0.003 in. radius, but this was the sharpest that could be machined with repeatability. The stress ranges applied to the various specimens, and results of the test series are summarized in the following discussions.

Series I - Fatigue Tests with Center Hole Crack Starter

It has been well established that the governing variable in the cyclic fatigue life of a steel specimen or beam is the applied stress range, the maximum and minimum stress having no measurable influence as long as they are within the elastic range. The stress ranges applied in these tests were selected somewhat emperically, using the criterion that failure should occur in less than 1,000,000 (or 10^6) cycles. The only control set on maximum and minimum stress levels was to keep the maximum stress below the minimum actual yield point of the particular steel tested and the minimum stress above zero. The stress ranges thus selected were 42,500 psi (5,000 min to 47,500 max) for the A 588 steel and 38,000 psi (2,000 min to 40,000 max) for the A 36 steel. With these stress ranges applied, the number of cycles to failure were recorded for each test and any specimens exceeding 1.5×10^6 cycles (run-out point) were terminated without failure. Although these stress ranges are much higher than any experienced in actual service loading on bridge beams (19) they are equivalent to those used

by Fisher (4) in studying the fatigue behavior of notched submerged arc groove welds. Increasing the sharpness of the notch in a specimen will decrease the stress range that can be sustained for a given number of cycles. This trend will be seen in the double edge notch test series where the stress ranges are greatly reduced to 21,000 psi for the A 588 steel and 28,000 psi for the A 36 steel with cycle life increasing only slightly in the presence of the sharper edge notch condition. Thus the stress ranges used are valid within the scope of the objective of the notched-fatigue test, which is to rate the relative sensitivity of the various weldment zones to fatigue crack initiation at the tip of a flaw. (These tests will not determine if a minimum stress range exists for each zone, below which a sharp flaw will not initiate a fatigue crack.)

Tests were run on specimens with a center hole located in the various weldment zones present, including the unaffected base metal. In addition to this, it was possible to place the hole crack-starter directly on the fusion line to test it for any possible weakening. Table 16 lists the results of the fatigue tests on the electroslag weldments made in A 588 steel. The numbers recorded in the columns give the average cycles to failure, the number of specimens represented by the average, and the standard deviation of the mean expressed as a percent of the mean, which gives a statistical measure of the scatter in the data. The results shown in Table 16 are summarized in the following comparisons. The cycle life of Zone 1 weld metal is either less than or (approximately) equal to the cycle life of Zone 2 weld metal. The cycle life of both weld metal zones from the 3-in. joints (ES 588-A2 and ES 588-B2) are less than those from the 1-3/4-in. joints (ES 588-A1 and ES 588-B1). In the Zone 2 weld metal the cycle life of a cooled shoe weld is lower than the cycle life of the dry shoe weld of the same plate thickness. The cycle lives of Zone 1 and Zone 2 weld metal are less than those for both of the heat-affected zones and the base metal. Weldment ES 588-B1 shows the cycle life of HAZ 1 as less than HAZ 2, which is less than base metal. The other weldments show HAZ 1 having a greater life than HAZ 2 and in two cases greater than the base metal. HAZ 2 has a lower cycle life than the base metal in all cases. The interesting thing to note is that HAZ 2, which was greatly improved in impact energy, appears to be more susceptible to fatigue crack initiation than base metal or HAZ 1 in most cases. Crack initiation in the fusion line specimens yielded cycle lives equivalent to either the Zone 2 weld metal or HAZ 1, showing no weakening at the bond line. A high standard deviation occurred in most of the base metal sets which apparently attests to the non-homogeneous nature of the base metal in response to this test.

Table 17 presents the results of the fatigue tests on the submerged arc weldments in A 588 steel with the same hole crack starter and stress range

TABLE 16

NOTCHED-FATIGUE TEST RESULTS FOR ELECTROSLAG WELDMENTS IN A 588 STEEL

High Stress Range (42.5 ksi) With Center Hole Crack Starter (K_t = 2.6)

Weldment Type (See Table 2)	Weldment Zones Tested					
	Zone 1 Weld Metal	Zone 2 Weld Metal	Fusion Line	HAZ 1	HAZ 2	Base Metal
(1-3/4-in.)						
ES 588-A1						
N[1] (thousands)	197	257	293(1 o-)[2]	548	326	459
X	3	3	2	2	3	6
s	9%	20%	16%	20%	10%	37%
(3-in.)						
ES 588-A2						
N (thousands)	154	140	394	315	220	399
X	3	3	3	3	3	6
s	14%	7%	27%	14%	12%	47%
(1-3/4-in.)						
ES 588-B1						
N (thousands)	None	302	400	399	456	519
X		3	3	3	3	6
s		31%	23%	18%	24%	35%
(3-in.)						
ES 588-B2						
N (thousands)	134	194	356	267	204	220
X	3	3	1	3	3	5
s	12%	10%	---	2%	15%	9%

[1] N = mean number of cycles to failure.
X = number of samples averaged in the mean.
s = standard deviation of the mean expressed as a percent of the mean.
[2] (Y o-) denotes that Y specimens exceeded 1.5 x 10^6 cycles without failure.

TABLE 17

NOTCHED-FATIGUE TEST RESULTS FOR SUBMERGED ARC WELDMENTS IN A 588 STEEL

High Stress Range (42.5 ksi) With Center Hole Crack Starter (K_t = 2.6)

Weldment Type (See Table 1)	Weldment Zones Tested			
	Weld Metal	Fusion Line	HAZ	Base Metal
(1-3/4-in.)				
SA 588-A1				
N[1] (thousands)	402(3 o-)[2]	302	533(1 o-)	468
X	3	3	2	6
s	52%	26%	2%	42%
(3-in.)				
SA 588-A2				
N (thousands)	227	334(2 o-)	(3 o-)	389
X	3	1	-----	6
s	11%	---	-----	44%
(1-3/4-in.)				
SA 588-B1				
N (thousands)	(3 o-)	342	303	282
X	-----	3	3	6
s	-----	63%	1%	33%
(3-in.)				
SA 588-B2				
N (thousands)	390(1 o-)	273	294	236
X	5	3	3	6
s	39%	44%	45%	13%

[1] N = mean number of cycles to failure.
X = number of samples averaged in the mean.
s = standard deviation of the mean expressed as a percent of the mean.
[2] (Y o-) denotes that Y specimens exceeded 1.5 x 10^6 cycles without failure.

as that of Table 16. Only one zone of weld metal was defined for submerged arc weldments, but this zone does contain the non-homogeneous effects of one pass refining the structure of a previous pass. (These areas are very small in size, while the zones identified in electroslag welds cover considerable portions of the cross-sections.) This microstructural variation is apparently reflected in the fatigue test results. The weldments in Table 17 represent those comparable to the electroslag welds in Table 16, but made by the submerged arc process. The results in the column under weld metal show the above mentioned non-homogeneous effects where several samples exceeded the run-out point without failure while other specimens failed before the run-out point. The submerged arc weldments made by Fabricator A are seen to be lower in cycle life than both the HAZ and the base metal (except for the run-out specimens that contained the refined structure). These same welds were lower in impact toughness and ductility as well. The poor quality weld that resulted from the welding procedure of Fabricator A is thus manifested in the fatigue test as well as the impact and tensile tests. The submerged arc weldments of Fabricator B are seen to exceed the cycle lives of both the HAZ and the base metal. As in the electroslag weldments, the 3-in. welds show lower lives than the corresponding 1-3/4-in. welds. It is interesting to note that in all the submerged arc weldments, the HAZ has a higher life than the base metal. This effect is most pronounced in the welds of Fabricator A, probably due to the heat treatment resulting from the greater amount of heat input to the joint. The fusion line failures in weldment SA 588-A1 were lower than either the weld metal or the HAZ.

Contrasting the results of Table 16 with those of Table 17 we see that the electroslag weld metal zones have a significantly lower cycle life than the weld metal from a similar joint made by the submerged arc process. The electroslag weld metal was consistently lower in cycle life than the base metal while the submerged arc weld metal was higher, except for the poor quality welds of Fabricator A. The HAZ of the submerged arc welding and, with one exception, the HAZ 1 of the electroslag weldments improved the cycle life of the base metal. HAZ 2 of the electroslag weldments degraded the cycle life of the base metal. One problem with the tendency of HAZ 2 to lower the crack initiation life of the base plate is that the fabrication flaws that are introduced by the removal of run-off tabs and starting sumps occur in this area. Thus, a "pre-existing flaw" condition can easily occur in the HAZ 2 region.

Table 18 presents the results of the fatigue tests on electroslag weldments in A 36 steel with the center hole specimens subjected to a stress range of 38 ksi. Again we note that Zone 1 weld metal has a cycle life less than or equal to Zone 2 weld metal. However, both weld metal zones are

TABLE 18
NOTCH-FATIGUE TEST RESULTS FOR ELECTROSLAG WELDMENTS IN A 36 STEEL
High Stress Range (38 ksi) With
Center Hole Crack Starter (K_t = 2.6)

Weldment Type (See Table 2)	Weldment Zones Tested					
	Zone 1 Weld Metal	Zone 2 Weld Metal	Fusion Line	HAZ 1	HAZ 2	Base Metal
(1-3/4-in.)						
ES 36-A1						
N[1] (thousands)	394	399(1 o-) [2]	821	597	478	200
X	3	2	2	3	3	6
s	33%	26%	21%	41%	15%	28%
(3-in.)						
ES 36-A2						
N (thousands)	238	337	340	312	270	172
X	2	2	3	3	3	5
s	5%	15%	27%	8%	16%	24%
(1-3/4-in.)						
ES 36-B1						
N (thousands)	None	559	311	376	593	182
X		3	3	3	3	6
s		68%	10%	26%	26%	41%
(3-in.)						
ES 36-B2						
N (thousands)	195	363	353	233	389	122
X	3	3	3	3	3	6
s	13%	33%	51%	7%	32%	12%

[1] N = mean number of cycles to failure.
X = number of samples averaged in the mean.
s = standard deviation of the mean expressed as a percent of the mean.
[2] (Y o-) denotes that Y specimens exceeded 1.5 x 10^6 cycles without failure.

TABLE 19
NOTCHED-FATIGUE TEST RESULTS FOR SUBMERGED ARC WELDMENTS IN A 36 STEEL
High Stress Range (38 ksi) With
Center Hole Crack Starter (K_t = 2.6)

Weldment Type (See Table 1)	Weldment Zones Tested			
	Weld Metal	Fusion Line	HAZ	Base Metal
(1-3/4-in.)				
SA 36-A1				
N[1] (thousands)	560(2 o-) [2]	520	344(1 o-)	340
X	1	3	2	6
s	---	19%	7%	15%
(3-in.)				
SA 36-A2				
N (thousands)	629(4 o-)	684	311(1 o-)	252
X	1	3	2	5
s	---	39%	3%	22%
(1-3/4-in.)				
SA 36-B1				
N (thousands)	492(1 o-)	217(2 o-)	470	298
X	2	1	3	6
s	20%	---	47%	26%
(3-in.)				
SA 36-B2				
N (thousands)	570(1 o-)	362	471(1 o-)	103
X	5	3	2	3
s	25%	3%	9%	5%

[1] N = mean number of cycles to failure.
X = number of samples averaged in the mean.
s = standard deviation of the mean expressed as a percent of the mean.
[2] (Y o-) denotes that Y specimens exceeded 1.5 x 10^6 cycles without failure.

higher in cycle life than the base metal in all the weldments. It is interesting to note this reversal in trend over that occurring in A 588 steel, which is apparently due to the difference in the alloy systems involved. As before, we note that the weld metal zones in the 3-in. joint have lower cycle lives than the corresponding zones in the 1-3/4-in. joints. The differences between the cooled shoe and dry shoe weld metal zones show no well defined trend as they did in the A 588 steel. In all the weldments of Table 18, the HAZs have a greater cycle life than the base metal. For the cooled shoe process, HAZ 1 is greater than HAZ 2, but for the dry shoe process HAZ 2 is greater than HAZ 1. This reversal in the trend is most likely due to the A 36 alloy system as affected by the different thermal cycles involved in the cooled shoe and dry shoe weldments. (In the A 588 alloy, HAZ 1 was always greater than HAZ 2.) The Zone 1 weld metal is in all cases lower than the HAZs but the Zone 2 weld metal relationship varies. The cycle life on the fusion line follows the trends of either the Zone 2 weld metal or the HAZ 1 except for weldment ES 36-B1 where it is seen to be slightly lower than either zone.

Table 19 presents the results of the fatigue tests on the submerged arc weldments in A 36 steel with the same notch and stress conditions as those of Table 18. The weldments of Table 19 are the submerged arc counterparts of the electroslag weldments of Table 18. The cycle life of the weld metal is in all cases much higher than the cycle life of the base metal and higher than that of the HAZ. Note that the Fabricator A weldments that had a lower weld metal life than the base metal in the A 588 alloy have a higher life in A 36. The A 588 steel chemistry apparently produces an adverse reaction to the overheating that was involved in Fabricator A's submerged arc welding procedure that does not occur in the A 36 chemistry weldments. The occurrence of areas of refined microstructure in the submerged arc weld metal leads to specimens that run-out (exceed 1.5×10^6 cycles) without failure. The weld metal in the 3-in. joints is higher in cycle life than that in the 1-3/4-in. joints. This trend is opposite that which occurred in the A 588 weldments and can also be related to the effects on the A 588 steel of increased heat input. The HAZ on all the submerged arc weldments has a higher cycle life than base metal. The fusion line specimens show that the Fabricator B weldments have some low cycle lives as compared to the adjoining zones. No problem seems to exist in the Fabricator A fusion line tests.

Contrasting the results of Tables 18 and 19 we conclude that the electroslag weld metal zones have a lower cycle life than the corresponding submerged arc weld metal (A 36 steel). The one exception is in weldment ES 36-B1 where the cycle life was comparable to the submerged arc weld metal, but the standard deviation of this zone was high which cast doubt on

TABLE 20

NOTCHED-FATIGUE TEST RESULTS FOR ELECTROSLAG WELDMENTS IN A 588 STEEL

Low Stress Range (21 ksi) With

Double Edge Notch Crack Starter (K_t = 28)

Weldment Type (See Table 2)	Weldment Zones Tested				
	Zone 1 Weld Metal	Zone 2 Weld Metal	HAZ 1	HAZ 2	Base Metal
(1-3/4-in.)					
ES 588-A1					
N[1] (thousands)	753(1 o-) [2]	792(1 o-)	828(1 o-)	640	813(1 o-)
X	2	1	2	3	2
s	3%	---	23%	10%	20%
(1-3/4-in.)					
ES 588-B1					
N (thousands)	None	(3 o-)	706(2 o-)	1,032	977(1 o-)
X		-----	1	3	2
s		-----	---	28%	28%
(3-in.)					
ES 588-B2					
N (thousands)	1,466	755(1 o-)	1,073(1 o-)	936	583
X	3	2	2	3	3
s	37%	23%	28%	12%	13%

[1] N = mean number of cycles to failure.
X = number of specimens averaged in the mean.
x = standard deviation of the mean expressed as a percent of the mean.
[2] (Y o-) denotes that Y specimens exceeded 2 x 10^6 cycles without failure.

TABLE 21

NOTCHED-FATIGUE TEST RESULTS FOR SUBMERGED ARC WELDMENTS IN A 588 STEEL

Low Stress Range (21 ksi) With

Double Edge Notch Crack Starter (K_t = 28)

Weldment Type (See Table 1)	Weldment Zones Tested		
	Weld Metal	HAZ	Base Metal
(3-in.)			
SA 588-A2			
N[1] (thousands)	1,138(1 o-) [2]	(3 o-)	931(2 o-)
X	2	-----	1
s	10%	-----	---
(3-in.)			
SA 588-B2			
N (thousands)	(3 o-)	1,121(1 o-)	1,499
X	-----	2	3
s	-----	22%	45%

[1] N = mean number of cycles to failure.
X = number of specimens averaged in the mean.
s = standard deviation of the mean expressed as a percent of the mean.
[2] (Y o-) denotes that Y specimens exceeded 2 x 10^6 cycles without failure.

the validity of the average (out of the three specimens tested, one specimen went nearly 10^6 cycles and the other two only about 340,000). Both welding processes produced weld metal that exceeded the cycle life of base metal, but the submerged arc was much higher than the electroslag. All HAZs produced by the two welding processes had higher lives than the base metal, so no potential degradation, such as occurred in HAZ 2 in A 588 steel, was present in the A 36 weldment.

Due to the small cross-section of the specimens used in these tests, not much was revealed by the appearance of the fractured surfaces. The general grain size present in the zones was apparent in the fracture and the Zone 2 electroslag weld metal specimens appeared to crack along the prior austenite grain boundaries that traversed the specimen. Sometimes the fatigue crack would deviate out of the transverse plane to follow such a boundary line.

Series II - Fatigue Tests with Double Edge Notch Crack Starter

This series of fatigue tests was run on specimens from the identical weldments tested in Series I with a reduced stress range and a more severe crack starter condition. The stress range applied to the A 588 weldments was 21,000 psi and that applied to the A 36 weldments was 28,000 psi. These stress ranges were selected because they would produce fatigue crack initiation in most of the weldment zones in less than 2×10^6 cycles (note that the run-out point has been redefined as 2,000,000 cycles.) This greatly reduced stress range produces failures in the specimens within cycle lives comparable to those determined in the Series I tests. This result illustrates the interaction between notch severity and stress range. As the sharpness of the notch continues to increase, the stress range necessary for failure at any given cycle life will decrease. The amount of elastic constraint at the notch tip may also influence the stress range that can be sustained for a given number of cycles. Elastic constraint in the specimens being tested (Fig. 59) is minimal, the specimen being practically in a plane stress condition.

Table 20 lists the results of the fatigue tests on electroslag weldments in A 588 steel with the double edge notch crack starter and an applied stress range of 21 ksi. Using the double edge notch it was not possible to test the fusion line as before because of its curvature. In these double edge notch tests the stress range has been reduced by 50 percent and the severity of the crack starter flaw has been greatly increased. The notch used is still not as severe as that which can occur in a fabrication flaw. The results reported here do, however, substantiate the trend that increasing the flaw

sharpness (i.e., raising the theoretical elastic stress concentration factor, K_t) will decrease the stress range required for failure at a given cycle life. Data for the 3-in. electroslag weldment made by the cooled shoe process were not obtained for this stress range and flaw condition. The results for the 1-3/4-in. cooled shoe weld (ES 588-A1) show that the Zone 1 weld metal has a slightly lower life than the Zone 2 weld metal. The fatigue lives of Zone 2 weld metal, HAZ 1, and base metal are all approximately equivalent (Zone 1 being slightly lower). As was the case in the circular notch tests (Table 16), HAZ 2 shows a lower fatigue life than the A 588 base metal. In the dry shoe electroslag weldments, we see that the Zone 1 and Zone 2 weld metal have a higher fatigue life than the base metal. The Zone 2 weld metal in the 1-3/4-in. weld had a very high resistance to crack initiation as seen by the three run-out specimens. The 3-in. weld specimens had a Zone 1 life that exceeded that of the Zone 2 weld metal. The 3-in. weldment also shows a lower weld metal life than the 1-3/4-in. weldment. In the dry shoe weldments, both HAZs are either approximately equivalent to or greater than the base metal in cycle life.

Table 21 presents the results of fatigue tests run on submerged arc weldments in 3-in. thick plates of A 588 steel with the double edge notch and a stress range of 21 ksi. In weldment SA 588-A2, which was made by Fabricator A using the procedure which led to overheating of the weld and HAZ, we see that the weld metal is only slightly higher than the base metal in cycle life. The HAZ has been greatly increased in life due to the overheating affect on the A 588 steel. The weldment SA 588-B2 by Fabricator B shows a very high cycle life in the weld metal and a slightly lower life in the HAZ as compared to base metal.

Comparing the results from Tables 20 and 21 we see that the submerged arc weld metal is again higher in cycle life than the electroslag weld metal zones. The electroslag weld metal at this stress range (21 ksi) and flaw condition does, however, equal or exceed the cycle life of the base metal (with one exception). This is the opposite of the effect that was seen in Table 15 where the electroslag weld metal under a stress range of 42.5 ksi and a circular crack starter, gave a cycle life that was significantly lower than base metal. Thus, we can conclude that at high stress ranges (in excess of the 21 ksi) the electroslag weld metal becomes increasingly more sensitive to fatigue crack initiation than the A 588 base metal. At this lower stress range of 21 ksi the cycle life of the electroslag weld metal is still lower than that of submerged arc weld metal (e.g., weldment SA 588-B2 compared to ES 588-B2). Hence the submerged arc weld metal would be expected to be more resistant to the initiation of a fatigue crack from a flaw than would electroslag weld metal. This can only be substantiated by large scale beam testing but the trend predicted by these tests

should be valid since fatigue crack initiation at a "flaw tip" is a localized phenomenon. The critical question to be answered is at what minimum stress range does such fatigue crack initiation become possible?

Table 22 presents the fatigue results for double edge notch specimens from the A 36 electroslag weldments with a stress range of 28 ksi applied. The first two weldments shown were made by the cooled shoe process and have a Zone 1 weld metal life approximately equal to, or lower than the Zone 2 weld metal. Both weldments have a lower cycle life in the weld metal than in the base plate. In the 1-3/4-in. weldment, HAZ 1 is higher and HAZ 2 is lower in cycle life than the base metal. In the 3-in. weldment, both HAZ 1 and HAZ 2 have lower lives than the base metal; however, the base plate tests were quite high in this weldment. The second two weldments in the table were dry shoe electroslag weldments and no Zone 1 specimens were available for testing in weldment ES 36-B2 (no Zone 1 existed in ES 36-B1). The Zone 2 weld metal had a cycle life equivalent to the base metal in both thicknesses. HAZ 1 was equal to or greater than base metal and HAZ 2 was lower than base metal in the two weldments. Comparing these results with those in Table 18 on A 36 steel weldments with the circular crack starter and 28 ksi stress range we see a reversal in trends. At the high stress range of Table 18, the weld metal and HAZs had higher cycle lives than the base metal. At the lower stress range of Table 22 with a sharp crack starter, the weld metal and HAZ 2 from the electroslag weldments have cycle lives less than or equal to the A 36 base metal. Also in comparing the results in Tables 18 and 22 we see that the cycle life of the A 36 base plate has actually increased at the lower stress range. The cycle life of the electroslag weld metal zones, however, has decreased at the lower stress range. Thus, the trends seen here are apparently due to the electroslag microstructure and not the A 36 steel chemistry. (This is just opposite the effect that was observed in the A 588 alloy weldments.)

Table 23 presents the results of fatigue tests run on the submerged arc weldments in A 36 steel by Fabricator B. The same edge notch condition and stress range (28 ksi) was applied as in Table 22. The weld metal is seen to be greater than or equal to base metal in fatigue life. (Note the base metal results listed are the same as those listed in Table 21 for ES 36-B1 and ES 36-B2 since the weldments were made in the same corresponding plates.) The HAZ tested shows an improved cycle life over base metal. The 1-3/4-in. submerged arc weldment has a higher cycle life in the weld metal zone than the electroslag weld metal zones from Table 22 (except for the high life recorded for Zone 2 of weldment ES 36-A2). The 3-in. submerged arc weldment is slightly greater in cycle life than the comparable electroslag weldment ES 36-B2. The standard deviation of the SA

TABLE 22
NOTCHED-FATIGUE TEST RESULTS FOR ELECTROSLAG WELDMENTS IN A 36 STEEL
Low Stress Range (28 ksi) With
Double Edge Notch Crack Starter (K_t = 28)

Weldment Type (See Table 2)	Weldmeut Zones Tested				
	Zone 1 Weld Metal	Zone 2 Weld Metal	HAZ 1	HAZ 2	Base Metal
(1-3/4-in.)					
ES 36-A1					
N[1] (thousands)	226	213	293	172	244
X	3	3	3	3	3
s	19%	31%	27%	4%	54%
(3-in.)					
ES 36-A2					
N (thousands)	296	879	380(1O→)[2]	544	1,348
X	3	4	2	2	2
s	40%	47%	16%	27%	16%
(1-3/4-in.)					
ES 36-B1					
N (thousands)	None	226	326	183	236
X		3	3	3	3
s		11%	46%	24%	23%
(3-in.)					
ES 36-B2					
N (thousands)	---	198	200	184	219
X		4	3	2	2
s		20%	27%	41%	5%

[1] N = mean number of cycles to failure.
X = number of specimens averaged in the mean.
s = standard deviation of the mean expressed as a percentage of the mean.
[2] (YO→) denotes that Y specimens exceeded 2 x 10^3 cycles without failure.

TABLE 23
NOTCHED-FATIGUE TEST RESULTS FOR SUBMERGED ARC WELDMENTS IN A 36 STEEL
Low Stress Range (28 ksi) With
Double Edge Notch Crack Starter (K_t = 28)

Weldment Type (See Table 1)	Weldment Zones Tested		
	Weld Metal	HAZ	Base Metal
(1-3/4-in.)			
SA 36-B1			
N[1] (thousands)	587	---	236
X	3		3
s	60%		23%
(3-in.)			
SA 36-B2			
N (thousands)	219	268	219
X	3	3	2
s	12%	9%	5%

[1] N = mean number of cycles to failure.
X = number of specimens averaged in the mean.
s = standard deviation of the mean expressed as a percentage of the mean.

36-B1 weld metal is high but all the specimens averaged were higher in cycle life than the electroslag weld zones. Based on these limited number of submerged arc tests, it is concluded that the cycle life of the submerged arc weld metal is equal to or greater than the corresponding electroslag weld metal under this stress range and flaw condition.

Summary of Notched Fatigue Tests

A 588 Steel

The following conclusions summarize the trends observed in the notched fatigue crack initiation tests on A 588 electroslag and submerged arc weldments.

1) Tests using the center hole crack starter and a stress range of 42.5 ksi on A 588 electroslag weldments (Table 16) show that Zone 1 weld metal has a lower fatigue life than Zone 2 weld metal, both zones are lower than the base metal and HAZ 2 has a lower fatigue life than the base metal. (In one case HAZ 1 was also lower than base metal.) No plane-of-weakness was detected from the specimens tested with the crack starter located on the fusion line.

2) Tests using the center hole crack starter and a stress range of 42.5 ksi on A 588 submerged arc weldments (Table 17) show that both the weld metal (with one exception) and the HAZ exceed the fatigue life of the base metal. In one weldment produced by Fabricator A, the fusion line samples had a lower fatigue life than either adjacent zone.

3) At the 42.5 ksi stress range with the circular crack starter the submerged arc weld metal had a significantly higher fatigue life than the corresponding electroslag weld metal (factor of 2 or more). Thus, under this high stress range, the submerged arc weld metal would be more resistant to fatigue crack initiation in the presence of a flaw than the electroslag weld metal. No fatigue problems would be predicted in the HAZ of a submerged arc weldment but the HAZ 2 of an electroslag weldment offers a potential for reduced fatigue resistance. It is in the location of this HAZ 2 where flaws due to removal of the starting sump and run-off blocks occur in fabrication.

4) Tests using the double edge notch crack starter and a stress range of 21 ksi on A 588 electroslag weldments (Table 20) show that the weld metal zones are equal to or greater than the base metal in fatigue life. The HAZs are also equal to or greater than base metal in fatigue life except for one case where HAZ 2 was lower.

5) Tests using the double edge notch crack starter and a stress range of 21 ksi on A 588 submerged arc weldments (Table 21) show that both the weld metal and the HAZ are greater than or equal to the base metal in fatigue life.

6) At the 21 ksi stress range with the double edge notch crack starter the submerged arc weld metal had a significantly higher fatigue life than the corresponding electroslag weld metal. Thus, submerged arc weld metal is superior to the electroslag weld metal in resisting fatigue crack initiation at the tip of a flaw at this stress range.

7) In all the fatigue test series on the electroslag and submerged arc weldments on A 588 steel the weldments in the 3-in. plate had lower fatigue lives than the corresponding weldments placed in 1-3/4-in. plates. This difference is attributed to the adverse effects of the additional heat input to the 3-in. weldments on the subsequent metallurgical structure.

A 36 Steel

The following conclusions summarize the trends observed in the notched fatigue crack initiation tests on A 36 electroslag and submerged arc weldments.

1) Tests using a center hole crack starter and a stress range of 38 ksi on A 36 electroslag weldments (Table 18) show that Zone 1 weld metal has a fatigue life less than or equal to Zone 2 weld metal. Both weld metal zones and both HAZs exceed the fatigue life of the base metal. In one case the specimens with the crack starter located on the fusion line had a cycle life slightly lower than either adjacent zone.

2) Tests using a center hole crack starter and a stress range of 38 ksi on A 36 submerged arc weldments (Table 19) show that the weld metal and the HAZ exceed the fatigue life of the base metal. The specimens with the crack starter located on the fusion line revealed a significant reduction in the fatigue life in the two weldments made by Fabricator B.

3) At the 38 ksi stress range with a circular crack starter the submerged arc weld metal had a significantly higher fatigue life than the weld metal zones of the corresponding electroslag weldments. The weld metal zones and HAZs of both types of weldments exceeded the fatigue life of the base metal. As was the case in the A 588 steel weldments, the submerged arc weld metal should be more resistant to fatigue crack initiation at a flaw than the electroslag weld metal at this stress range. Some reduction in the fatigue life was observed at the fusion line in both the submerged arc and the electroslag weldments.

4) Tests using a double edge notch crack starter and a stress range of 28 ksi on A 36 electroslag weldments (Table 22) show that both weld metal zones have fatigue lives less than or equal to the fatigue life of the base metal. HAZ 2 is lower in fatigue life than the base metal. The severity of the notch apparently has an adverse effect on the electroslag weld metal in A 36 steel (opposite the trend noted in A 588 steel).

5) Tests using a double edge notch crack starter and a stress range of 28 ksi on A 36 submerged arc weldments (Table 23) show that the weld metal is greater than or equal to the base metal in fatigue life. The HAZ tested also had a fatigue life greater than the base metal.

6) At the 28 ksi stress range with a double edge notch crack starter the A 36 submerged arc weld metal had a significantly higher fatigue life than the corresponding electroslag weld metal in the 1-3/4-in. weldment, and slightly higher in the 3-in. weldment. Both types of weldments were effected adversely by increasing the severity of the notch. The electroslag weldments had a lower fatigue life in HAZ 2 than in the base metal.

7) With the exception of weldment ES 36-A2, the 3-in. joints had a lower fatigue life in the various zones than the corresponding 1-3/4-in. joints in both the submerged arc and electroslag processes.

It is concluded that the results of these notched fatigue tests do give a valid qualitative appraisal of the various weldment zones tested. The objective of the tests was to determine any difference in fatigue crack initiation life under cyclic tensile loading in the presence of an initial "flaw" condition. This was accomplished within the guidelines of ASTM E 466, "Constant Amplitude Axial Fatigue Tests of Metallic Materials." Such differences do exist between the submerged arc and the electroslag weldments as stated in the above conclusions. However, the limitations of the results of these tests should be carefully noted. No direct predictions can be made concerning the fatigue crack initiation life in the various weldment zones in a welded beam under service loading. The testing conditions do not parallel the service conditions on the weldments. The geometry of the test specimens, the notch conditions, and the stress ranges are different than service conditions. It can be stated that an increase in notch sharpness will give a corresponding decrease in the stress range required for fatigue crack initiation in a given number of cycles in any of the weldment zones. The question that remains unanswered is; given the sharpest notch condition that can occur from a fabrication flaw, is there a minimum stress range, below which a fatigue crack will not initiate at the flaw? If the answer to this is yes, the next question that needs to be answered is; are the stress ranges applied to such weldments in service below this critical stress level

and consequently is fatigue crack initiation an impossibility in the weldments? Past experience with submerged arc weldments has shown that such fatigue damage is rarely encountered, but it does occur. Service experience with electroslag weldments in highway bridge loading is very limited when compared to submerged arc weldments, and the possibility of such failures has not been precluded. The only way to safely evaluate the true fatigue characteristics of electroslag welded butt joints is full-scale beam testing. This hopefully will be accomplished by the NCHRP Project 10-10 on electroslag welding that was mentioned previously (12).

IMPLEMENTATION OF RESEARCH

Because of the preliminary results of this research, the Michigan Department of State Highways and Transportation called for requalification of the electroslag process. The use of electroslag butt welding was terminated in June of 1974 because of the inability of any of the users of the process to qualify in accordance with the AWS Specifications that were in effect (1). Further action was taken in the Michigan Specification (13) to prohibit the use of electroslag welding on bridge girders in areas of tension or stress reversals. The qualification procedure specification was changed to modify the inadequacies of the existing specifications that are cited in this report. The following is from the Michigan Supplemental Specification for Welding Structural Steel as it relates to electroslag welding.

1) For exposed, bare unpainted applications of ASTM A 588, the weld metal shall meet the chemical composition requirements of Table 4.14, AWS D1.1-Rev. 74. This will be verified in the weld metal taken from the procedure qualification test plate.

2) Sufficient all-weld-metal tension specimens will be removed from the weldment to test all the weld zones present.

3) The Appendix C requirements of AWS D1.1-Rev. 74 are mandatory and are modified as follows:

Appendix C, Paragraph C2.1 - Paragraph C2.1 shall be deleted.

Appendix C, Paragraph C2.2 - The present Paragraph C2.2 shall be replaced with a new paragraph as follows: "For material of any thickness specimens shall be tested at 0 F for notched bar impact properties of the weld metal. The impact values shall not be less than those in the following table."

Size of Specimen	Minimum impact value required for average of five specimens, ft-lb	Minimum impact value permitted on one specimen only in a set of five specimens, ft-lb
10.0 mm x 10.0 mm	15.0	10.0
10.0 mm x 7.5 mm	12.5	8.5
10.0 mm x 5.0 mm	10.0	7.0
10.0 mm x 2.5 mm	5.0	3.5

Appendix C, Paragraph C2.3 - Paragraph C2.3 shall be revised as follows: "If the value for more than one of the five specimens is below the minimum average requirement, or if the value for one of the five specimens is below the minimum value permitted on one specimen, a retest shall be made, and the value of all of the five specimens must equal or exceed the specified minimum average value. Such a retest shall be permitted only when the average value of the five specimens equals or exceeds the minimum value permitted on one specimen."

Appendix C, Paragraph C2.4 - A new Paragraph C2.4 shall be added as follows: "All heat-affected zones adjacent to the weld fusion line shall be defined by etching the weld cross section and shall be tested for notched bar impact properties. The impact values determined shall not be less than the values required on the base metal being welded (see Supplemental Specification for Structural Steel Bridges, 8.06 (Ref. 13)). When computing the average value of the impact properties of the heat-affected zones, the extreme lowest and extreme highest value obtained with the five specimens shall be disregarded."

Appendix C, Paragraph C3.1 - The present Paragraph C3.1 shall be replaced with a new paragraph as follows: "Five Charpy V-notch impact test specimens shall be machined from each weld metal zone (usually two present) and from each heat-affected zone (usually two present) from the same test weld assembly (AWS Fig. 5.10.1.3c) made to determine weld joint properties. All zones present in the weldment will be defined by etching prior to the layout or removal of any test specimens."

Appendix C, Paragraph C3.3 - The first sentence of Paragraph C3.3 shall be replaced with the following: "The longitudinal centerline of the specimens shall be transverse to the weld axis, and shall be located in the weldment cross section at any location necessary to include the weld zone or heat-affected zone being tested."

Subsequent to this research the Michigan Supplemental Specification for Welding Structural Steel has undergone several revisions to place better control on the procedure specifications used in butt welding. Poor quality submerged arc butt welding, such as that produced by Fabricator A in this study, has been eliminated by modifying and requalifying the welding procedures currently in use. Tighter control of the weld metal chemistry is also being implemented to assure conformance to the specified range required by the welding application.

Further implementation of these results has involved the Department in the new Research Project 75 F-144, "Bridge Girder Butt Welds--Resistance to Brittle Fracture, Fatigue and Corrosion." In this project a "Linear Elastic Fracture Mechanics" approach will be used to evaluate fracture toughness and fatigue properties of the weldments. This approach will avoid the limitations of specimen size that were present in the Charpy impact and fatigue-notch evaluations of this project. Corrosion studies will be directed at evaluation of the corrosion resistance of the weld metal zones with chemistry that conforms to the AWS specified range and with chemistry that does not conform, similar to those documented in this study and known to be in service.

REFERENCES

1. Specifications for Welded Highway and Railway Bridges, AWS D2.0-69, American Welding Society, 1969.

2. AWS Structural Welding Code, AWS D1.1-Rev. 74, American Welding Society, 1974.

3. Barsom, J. M., "The Development of AASHTO Fracture-Toughness Requirements for Bridge Steels," Presented at the U. S.-Japan Co-operative Science Seminar held at Tokoku University, Sendai, Japan, August 1974.

4. Fisher, J. W., et al, "Effect of Weldments on the Fatigue Strength of Steel Beams," NCHRP Report No. 102, National Cooperative Highway Research Program, Washington, D. C., 1970.

5. Terms and Definitions, AWS A3.0-69, American Welding Society, 1969.

6. Welding Handbook, 6th edition, Chapter 48, American Welding Society, 1970.

7. Scrawley, J. E., and Brown, W. F., Jr., "Fracture Toughness Testing Methods," Proceedings of the Symposium on Fracture Toughness Testing and Its Applications, ASTM STP 381, pp 133-198, 1964.

8. Barsom, J. M., and Rolfe, S. T., "Correlations Between K_{IC} and Charpy V-notch Test Results in the Transition Temperature Range," Impact Testing of Metals, ASTM STP 466, pp 281-302, 1970.

9. Campbell, H. C., "Electroslag, Electrogas, and Related Welding Processes," Welding Research Council, Bulletin No. 154, p 14, September 1970.

10. Paton, B. E., Electroslag Welding, American Welding Society, 2nd edition, New York, 1962.

11. Kunihiro, T., and Nakajima, H., "Micro-Cracking in Consumable-Nozzle Electroslag Weld Metal," Proceedings of the Japan-U. S. Seminar, Significance of Defects in Welded Structures, University of Tokyo Press, pp 105-109, 1974.

12. Private communications with W. P. Benter, Jr., principal investigator NCHRP Project 10-10, "Acceptance Criteria for Electroslag Weldments in Bridges," NCHRP, Washington, D. C., May 1, 1974.

13. The 1973 edition, Standard Specifications for Highway Construction, and the associated Supplemental Specifications for Welding Structural Steel, and Supplemental Specifications for Structural Steel for Bridges, Michigan Department of State Highways and Transportation, Lansing, Michigan.

14. Linnert, G. E., Welding Metallurgy, American Welding Society, 3rd edition, Vol. II, pp 66-72, 1965.

15. Slimmon, P. R., "Arc Welding of Weathering Steels," Welding Journal, December 1968.

16. Paton, B. E., "Electroslag Welding of Very Thick Materials," Welding Journal, pp 1115-1122, December 1962.

17. Metals - Physical, Mechanical, Corrosion Testing, Part 10, ASTM Annual Standards, E 466-72T, "Constant Amplitude Axial Fatigue Tests of Metallic Materials," American Society for Testing and Materials, Philadelphia, PA, pp 592-596, 1975.

18. Black, Paul H., Machine Design, McGraw-Hill, pp 33, 396, 1955.

19. Cudney, G. R., "Stress Histories of Highway Bridges," J. Struc. Division, ASCE, Vol. 94, ST 12, December 1968.